The role of BH3-only proteins in haematopoietic stem and progenitor cells

Dissertation

zur Erlangung der Doktorwürde der Fakultät für Biologie
der Albert-Ludwigs-Universität Freiburg im Breisgau

Vorgelegt von
Daniela Bertele

März 2013

Dekan der Fakultät für Biologie: Prof. Dr. Ad Aertsen
Promotionsvorsitzender: Prof. Dr. Stefan Rotter

Betreuerin der Arbeit: Dr. Miriam Erlacher
Betreuer seitens der Fakultät: Prof. Dr. Christoph Borner

Ko-Referentin: Prof. Dr. Heike L. Pahl
Drittprüfer: Dr. Tilman Brummer

Tag der Verkündigung des Prüfungsergebnisses: 10.05.2013

Abstract

Haematopoietic stem cell transplantation (HSCT) is the only curative treatment for many haematological, immunological or malignant diseases. Therapy is still associated with the risk of graft failure or delayed engraftment resulting in increased infection-related mortality. We hypothesized that cell death occurring during transplantation might reduce the numbers of functional donor stem cells, and that apoptosis inhibition thereby might improve HSCT efficiency. During transplantation, haematopoietic stem and progenitor cells (HSPCs) lack survival signals (i.e. cytokines) which are normally provided by the stem cell niche. It is well known that loss of cytokines triggers the intrinsic apoptosis pathway which is controlled by the Bcl-2 family. While anti-apoptotic Bcl-2 family members have been described earlier to regulate HSPC survival, the role of their counterparts, the pro-apoptotic BH3-only proteins has still to be elucidated.

We identified two BH3-only proteins, Bim and Bmf, as critical regulators of HSPC survival. Both *bim*$^{-/-}$ and *bmf*$^{-/-}$ murine HSPCs (LSK cells) performed significantly better than wildtype LSK cells during early and long-term reconstitution of the haematopoietic system of lethally irradiated mice. In addition, less *bim*$^{-/-}$ than wt BM cells were required for successful host reconstitution. By excluding a role of Bim for other cellular pathways (i.e. homing, proliferation and differentiation of HSPCs) we could demonstrate that the increased transplantation efficiency observed in *bim*$^{-/-}$ LSK cells can be ascribed exclusively to apoptosis inhibition. These results urged us to investigate the role of BIM and BMF in the regulation of transplantation-associated cell death in human HSPCs (CD34^{+} cells). In line with our mouse experiments, CD34^{+} cells with reduced levels of BIM or BMF performed better in reconstituting the haematopoietic system of newborn *rag2*$^{-/-}\gamma c^{-/-}$ mice. In order to mimic the clinical procedure of HSCT more precisely, we furthermore injected CD34^{+} cells intravenously into 7 week old *rag2*$^{-/-}\gamma c^{-/-}$ mice. Again, CD34^{+} cells expressing BIM shRNA showed an engraftment advantage compared to cells expressing a control shRNA (Luciferase shRNA).

Together, our findings identify Bim and Bmf as major limiting factors during HSCT. We therefore suggest that their therapeutic inhibition could increase HSPC survival and thereby promote and accelerate haematopoietic regeneration after HSCT. Since permanent apoptosis inhibition in HSPCs might promote lymphomagenesis, inhibition of Bim and Bmf must be transient to enable translation into a clinical setting. Although transiently acting adenoviral vectors turned out to be unsuitable for efficient gene transfer and expression, promising new technologies might soon enable translation of our results into clinical application.

Zusammenfassung

Die hämatopoetische Stammzelltransplantation (HSCT) ist die einzige kurative Behandlung für viele hämatologische, immunologische oder maligne Erkrankungen. Diese Therapie ist jedoch immer noch mit dem Risiko von Transplantatversagen, verzögertem Engraftment und dadurch erhöhter infektionsbedingter Mortalität verbunden. Wir gehen davon aus, dass während der Transplantation ein signifikanter Anteil der transplantierten Spender-Stammzellen abstirbt und dass Zelltod-Hemmung somit die HSCT-Effizienz verbessern könnte. Im Verlauf einer Transplantation fehlen hämatopoetischen Stamm- und Vorläuferzellen (HSPCs) nämlich wichtige Überlebenssignale (z.B. Zytokine), die normalerweise von der Stammzellnische bereitgestellt werden. Es ist bekannt, dass ein Verlust von Zytokinen den intrinsischen Apoptose-Signalweg auslöst, der von der Bcl-2-Familie reguliert wird. Obwohl bereits gezeigt wurde, dass anti-apoptotische Bcl-2-Proteine (z.B. Bcl-2 selbst, Bcl-x_L und Mcl-1) das Überleben von HSPCs regulieren, ist die Rolle ihrer Gegenspieler, der pro-apoptotischen BH3-only-Proteine bisher unbekannt.

In diesem Projekt identifizierten wir zwei BH3-only Proteine, Bim und Bmf, als wichtige Regulatoren für das Überleben von HSPCs. Sowohl *bim*$^{-/-}$ als auch *bmf*$^{-/-}$ HSPCs der Maus (LSK-Zellen) zeigten im Vergleich zu Wildtyp-LSK-Zellen eine deutlich bessere frühe sowie langfristige Rekonstitution des blutbildenden Systems von letal bestrahlten Mäusen. Darüber hinaus waren weniger *bim*$^{-/-}$ als Wildtyp-Knochenmarkszellen für eine erfolgreiche Rekonstitution des Empfängers erforderlich. Weiterhin konnten wir eine Rolle von Bim für andere zelluläre Signalwege (Homing, Proliferation und Differenzierung von HSPCs) ausschließen und damit zeigen, dass die erhöhte Transplantations-Effizienz von *bim*$^{-/-}$ LSK-Zellen allein auf Apoptose-Hemmung zurückzuführen ist. Diese Ergebnisse veranlassten uns, die Rolle von BIM und BMF für die Regulierung des Transplantations-assoziierten Zelltodes auch in humanen HSPCs (CD34$^+$-Zellen) zu untersuchen. Dafür entwickelten wir zwei unterschiedliche Xenograft-Modelle. Ähnlich wie in den Maus-Transplantations-Experimenten rekonstitutierten CD34$^+$ Zellen das hämatopoeti-

sche System von neugeborenen *rag2*$^{-/-}\gamma c^{-/-}$ Mäusen dann besser, wenn die Expression von BIM und BMF durch die RNA-Interferenz-Methode gehemmt wurde.

Zusammenfassend konnten wir mit dieser Studie zeigen, dass Bim und Bmf wichtige limitierende Faktoren bei der HSCT sind, und dass durch ihre Hemmung das Überleben von HSPCs erhöht wird. Da dies zu einer beschleunigten hämatopoetischen Regeneration nach der HSCT führte und die Anzahl benötigter Stammzellen deutlich reduzierte, bietet es sich an, unsere Ergebnisse therapeutisch zu nutzen und Apoptose in Spenderzellen während der Transplantation zu hemmen. Da jedoch eine permanente Apoptose-Hemmung in HSPCs die Entstehung von Lymphomen und Leukämien sowie Autoimmunerkrankungen fördern könnte, darf die Hemmung von Bim und Bmf für die klinische Anwendung nur kurzzeitig sein. Erste Ergebnisse zeigten, dass ein transienter adenoviraler Gentransfer leider keine effiziente Genexpression vermittelt. Neue und vielversprechende Technologien könnten jedoch voraussichtlich bald eine Weiterentwicklung und schlussendlich klinische Anwendung unserer Ergebnisse ermöglichen.

Danksagung

In erster Linie möchte ich mich bei Miriam Erlacher (MD/PhD) für das interessante Projekt, die vielen hilfreichen Diskussionen, Ideen und Ratschläge und natürlich für die finanzielle Unterstützung bedanken.

Ein großes Dankeschön auch an Herrn Prof. Dr. Christoph Borner für die vielen hilfreichen Diskussionen, die wissenschaftlichen Ratschläge und für die Begutachtung meiner Arbeit. Mein besonderer Dank gilt auch Frau Prof. Dr. Charlotte Niemeyer für die finanzielle Unterstützung und die Ermöglichung meiner Teilnahme an dem Intensivkurs über Stammzellen in Oxford.

Außerdem möchte ich mich bei meinen Kolleginnen und Kollegen für die tolle Zeit im Labor, für die angenehme Arbeitsatmosphäre und für die große Hilfsbereitschaft bedanken. Ein besonderer Dank gebührt dabei Nora Fischer und Christine Silberer insbesondere für die HSPC-Isolation während der letzten zwei Jahre.

Des Weiteren bedanke ich mich bei unseren Kooperationspartnern für die große Unterstützung. Danke an: Prof. Dr. Andreas Villunger vom Biozentrum der Medizinischen Universität Innsbruck, für die Bereitstellung der Knockout-Mäuse und die Möglichkeit zur Durchführung einiger Maus-Experimente in seinem Labor; Verena Labi, Claudia Wöss und Denise Tischner für die Unterstützung bei der Durchführung einiger Experimente; Prof. Dr. Heike L. Pahl vom Zentrum für Klinische Forschung des Universitätsklinikums Freiburg, für die Möglichkeit der lentiviralen Vektor-Konstruktion in ihrem Labor und Dr. Sven Schwemmers für seine Hilfe bei der Vektor-Klonierung; Prof. Dr. Christoph Borner und Nina Raulf vom Institut für Molekulare Medizin und Zellforschung der Universität Freiburg für die Überlassung der BCL-2 und BCL-XL cDNA und Dr. Ulrich Maurer und Silke Lindner für die hilfreichen Diskussionen während meiner Arbeit; Prof. Dr. Stephan Geley aus dem Biozentrum der Medizinische Universität Innsbruck für seine Unterstützung bei der adenoviralen Vektor-Konstruktion; Xiaolong Fan von der Universität Lund in Schweden

für den Ad5/F35-vector; Dr. Mirjam Kunze und dem gesamten geburtshilflichen Team vom Universitätsklinikum Freiburg für die Bereitstellung von Nabelschnurblut und für die Einholung der Zustimmung der Eltern.

Abschließend danke ich meiner Familie und meinem Freund Michael Karg ganz herzlich für ihre große Unterstützung in jeder Hinsicht.

Contents

List of Figures

List of Tables

Abbreviations

7-AAD	7-Amino-Actinomycin D
E.coli	Escherichia coli
Ad5	Adenovirus serotype 5
AhR	Aryl hydrocarbon receptor
AIDS	Acquired immunodeficiency syndrome
AIF	Apoptosis-inducing factor
Amp	AmpR
AmpR	Ampicillin resistance gene
Apaf1	Apoptosis protease-activating factor-1
APC	Allophycocyanin
APS	Ammonium persulfate
ATP	Adenosine triphosphate
B2m	Beta-2-microglobulin
Bad	Bcl-2 antagonist of cell death
Bak	Bcl-2 antagonistic killer
Bax	Bcl-2 associated X protein
Bcl-2	B cell lymphoma-2 protein
Bcl-G	Apoptosis facilitator Bcl-2-like protein 14
BCL-RA.	BCL-RAMBO = Bcl-2-like protein 13
Bcl-w	Bcl-2-like 2
Bcl-xL	Bcl-extra long
BE	BoosterExpress™ reagent
BH	Bcl-2 homology
Bid	Bcl-2 interacting domain death agonist
Bik	Bcl-2 interacting killer
Bim	Bcl-2 interacting mediator of cell death
BimEL	Bim-extra long
BimL	Bim-long
BimS	Bim-short
BM	Bone marrow
Bmf	Bcl-2 modifying factor
BmfS	Bmf-short
Bmi1	B lymphoma Mo-MLV insertion region 1 homolog
BNIP-3L	BCL2/adenovirus E1B 19 kDa protein-interacting protein 3-like
Bok	Bcl-2 related ovarian killer
bp	Base pair
BSA	Bovine serum albumin
C/EBP	CCAAT-enhancer binding protein
CAR	Coxsackie and adenovirus receptor
CAR cells	CXCL12-abundant reticular cells
CARD	Caspase recruitment domain
CB	Cord blood
CD	Cluster of Differentiation
CD95-L	CD95-ligand
CDK5	Cyclin-dependent kinase 5
cDNA	Copy DNA
CFU	Colony Forming Unit
CHOP	C/EBP homologous protein
cIAP	Cellular inhibitor of apoptosis protein
CIP	Calf Intestinal Alkaline Phosphatase
CLP	Common-lymphoid progenitor
CMP	Common myeloid progenitor
CMV	Cytomegalovirus
cPPT	Central polypurine tract
CSF	Colony-stimulating factor
CTLA1	Cytotoxic T-lymphocyte-associated serine esterase 1
CXCL12	Chemokine (C-X-C motif) ligand 12
CXCR4	C-X-C chemokine receptor type 4
d	Day
DAPI	4',6-diamidino-2-phenylindole
dATP	Deoxyadenosine triphosphate
DD	Death domain

DED	Death effector domain
DEPC	Diethyl Pyrocarbonate
DISC	Death inducing signaling complex
DLC1	Dynein light chain 1
DMEM	Dulbeccos modified eagle medium
DMSO	Dimethyl sulfoxide
DNA	Deoxyribonucleic acid
DPBS	Dulbeccos Phosphate Buffered Saline
DPPIV	Dipeptidylpeptidase IV
DR	Death receptor
DTT	1,4-Dithiothreitol
E	Erythroid
EDTA	Ethylene-diamine-tetraacetic acid
eGFP	Enhanced green fluorescent protein
ER	Endoplasmic reticulum
ERK	Extracellular signal-regulated kinase
FACS	Fluorescence-activated cell sorting
FADD	Fas associated death domain protein
FAM	Carboxyfluorescein
FBS	Fetal bovine serum
FCS	Fetal calf serum
FITC	Fluorescein isothiocyanate
FLIP	Flice-inhibitory protein
Flt3L	Fms-related tyrosine kinase 3 ligand
FOXO3A	Forkhead transcription factor 3A
G-CSF	Granulocyte colony-stimulating factor
GEMM	Granulocyte, Erythrocyte, Macrophage, Megakaryocyte
Gent	GentaR
GentaR	Gentamicin resistance gene
GFP	Green fluorescent protein
GM	Granulocyte, Macrophage
GM-CSF	Granulocyte-macrophage colony-stimulating factor
GMP	Granulocyte-monocyte progenitor
GUSB	Glucuronidase, beta
GvHD	Graft-versus-host disease
GvL	Graft-versus-leukemia
Gy	Gray
h	Hour
HEK	Human embryonic kidney
HeLa	Henrietta Lacks
HEPES	4-(2-hydroxyethyl)-1-piperazineethanesulfonic acid
HLA	Human leukocyte antigen
HR	Homologous recombination
Hrk	Harakiri
HRP	Horseradish peroxidase
HSCs	Haematopoietic stem cells
HSCT	Haematopoietic stem cell transplantation
HSPCs	Haematopoietic stem and progenitor cells
hU6	Human U6
i.v.	intravenous
ICAD	Inhibitor of caspase-activated DNase
IL	Interleukin
IMDM	Iscoves Modified Dulbeccos Medium
IMS	Intermembrane space
IRES	Internal ribosome entry site
IT-HSCs	Intermediate HSCs
ITR	Inverted terminal repeat
IU	Infectious units
JNK	Jun N-terminal kinase
Kan	KanR
KanR	Kanamycin resistance gene
L-ITR	Left-hand ITR
LeGO	Lentiviral gene ontology
LMPP	Lymphoid-primed multipotent progenitor
LSK	$Lineage^{-}sca1^{+}c\text{-}kit^{+}$
LT-HSCs	Long-term HSCs
Luci	Luciferase
M	Molar
Mcl-1	Myeloid cell leukemia factor-1

MEP	Megakaryocyte-erythrocyte progenitor
MHSC	Mobilized haematopoietic stem cells
min	Minute
MLP	Multi-lymphoid progenitor
MLV	Murine leukemia virus
Moap1	Modulator of apoptosis 1
MOI	Multiplicity of infection
MOMP	Mitochondrial outer membrane permeabilization
MPP	Multipotent progenitor
MRF	Membrane-remodeling factors
mRNA	Messenger RNA
NAIP	NLR family, apoptosis inhibitory protein
NK	Natural killer
NOD	Non-obese diabetic
OD	Optical density
P/S	Penicillin/Streptomycin
p21	Cyclin-dependent kinase inhibitor 1
PAGE	Polyacrylamide gel electrophoresis
Pak2	p21-activated kinase 2
PARN	Poly(A)-specific ribonuclease
PB	Peripheral blood
PCR	Polymerase chain reaction
PE/Cy7	Phycoerythrin/Cyanine dye 7
pGhU6	pLeGO-hU6
PGK	Phosphoglycerate kinase 1 promoter
pH	Potentia hydrogenii
PI3K	Phosphoinositide 3-kinase
piG	pLeGO-iG
PIPES	Piperazin-N,N'-bis-(2-ethansulfonsure)
PMSF	Phenylmethylsulfonyl fluoride
PRE	Post-transcriptional regulatory element
Prkdc	Protein kinase, DNA activated, catalytic polypeptide
PS	Phosphatidylserine
Puma	p53 upregulated modulator of apoptosis
qRT-PCR	Quantitative reverse transcription polymerase chain reaction
R-ITR	Right-hand ITR
rh	Recombinant human
RIP1	receptor-interacting protein 1
rm	Recombinant murine
RNA	Ribonucleic acid
RNAi	RNA interference
rpm	Rounds per minute
RPMI	Roswell Park Memorial Institute
RRE	Rev responsive element
rRNA	Ribosomal RNA
RT	Room temperature
RT-MLPA	Reverse transcriptase multiplex ligation-dependent probe amplification
s	Second
SCF	Stem cell factor
scid	Severe combined immunodeficiency
SD	Standard deviation
SDF-1	Stromal cell-derived factor I; alternative name CXCL12
SDS	Sodium dodecyl sulfate
SEM	Standard error of the mean
SERP.-B	SERPIN-B
SFFV	Spleen focus-forming virus
SFM	Serum-free medium
shRNA	Short-hairpin RNA
SIN-LTR	Self-inactivating-long-terminal repeat
SIRPa	Signal regulatory protein alpha
SIV	Simian immunodeficiency virus
SLAM	Signaling lymphocyte activation molecule
Smac	Second mitochondrial activator of caspase
SOB	Super Optimal Broth
SOC	Super Optimal Broth with Catabolite repression
SR1	StemReginin 1
ST-HSCs	Short-term HSCs

TAE	Tris-Acetate
Tak1	TGF-β-activated kinase-1
tBid	Truncated Bid
TEMED	N,N,N',N'-tetramethylethane-1,2-diamine
TEPA	Tetraethylenepentamine
tg	Transgenic
THT	Tetracycline-sensitive RNAse P H1 promoter
TM	Transmembrane
TNF	Tumor necrosis factor
TPO	Thrombopoietin
TRAIL	TNF-related apoptosis-inducing ligand
treosulfan	L-threitol 1,4-bismethanesulphonate, Ovastat
tx	Transplantation
UBA	Ubiquitin-associated domain
UCB	Umbilical cord blood
UCBT	UCB transplantation
UV	Ultraviolet
vsv	Vesicular stomatitis virus
WAS	Wiskott-Aldrich syndrom
WPRE	Woodchuck hepatitis virus post-trancriptional regulatory element
wt	Wild type
WWE	Trp-Trp-Glu interaction module
XIAP	X-linked inhibitor of apoptosis protein
ZFN	Zink-finger nuclease

1

Introduction

1.1 Haematopoietic stem and progenitor cells

Haematopoietic stem cells (HSCs) give rise to all mature blood cells and maintain haematopoietic homeostasis. The life-long regeneration of haematopoietic cells (haematopoiesis) depends on cell fate decisions of HSCs to undergo self-renewal, differentiation or programmed cell death (Figure 1.1) and of their progenitor cells capable to undergo lineage commitment, proliferation, terminal differentiation or programmed cell death (Blank *et al.*, 2008). Self-renewal, a unique property of stem cells, is often achieved in adult stem cells by asymmetric division. Asymmetric division generates two non-identical daughter cells, one maintaining stem cell identity (self-renewal) and another one committed to specialized functions (differentiation) (Till *et al.*, 1964). Besides self-renewal the quiescent state (G_0 phase of the cell cycle) of HSCs is critical for HSC maintenance (Yoshihara *et al.*, 2007). Additionally to these unique stem cell properties, programmed cell death plays an important role for the regulation of the HSC pool size (Domen *et al.*, 2000).

These different cell fates are presumed to be regulated by several intrinsic and extrinsic factors. Intrinsic factors that have been shown to preserve HSC stemness include Bmi1, contributing to HSC self-renewal likely via repression of p16 and p19 to permit proliferation and inhibit p53-mediated apoptosis, respectively (Park *et al.*, 2003). On the other hand, HSC proliferation, growth and survival are controlled by the PI3K signaling pathway in response to growth factors, nutrients and oxygen status, with pathway hyperactivation decreasing HSC quiescence and hypoactivation reducing HSC proliferation/differentation (Warr *et al.*, 2011). Extrinsic factors supporting HSC activity are provided by multiple subsets of osteoblasts (Calvi *et al.*, 2003; Zhang *et al.*, 2003), mesenchymal progenitor cells (Nakamura *et al.*, 2010), endothelial cells (Kiel *et al.*, 2005) as well as CXCL12-abundant reticular (CAR) cells (Sugiyama *et al.*, 2006),

building up a special microenvironment within the bone marrow also called ”stem cell niche”. While the hypoxic osteoblastic niche (located at the endosteal bone surface) is thought to maintain the quiescent state of HSCs, the oxygenic vascular niche (located in the microvasculature sinusoidal endothelium) may support proliferation, differentiation and mobilization of HSCs (Yin *et al.*, 2006). Cytokines (interleukin-3 (IL3), fms-related tyrosine kinase 3 ligand (Flt3L), stem cell factor (SCF)), chemokines (CXCL12) as well as growth factors (angiopoietin-1, granulocyte-CSF, granulocyte-macrophage-CSF) were reported to be major extrinsic factors required for HSC homeostasis (Warr *et al.*, 2011). Moreover, it has been shown that Wnt (Fleming *et al.*, 2008), Hedgehog (Zhao *et al.*, 2009) and Notch (Stier *et al.*, 2002) signaling pathways are important for HSC self-renewal.

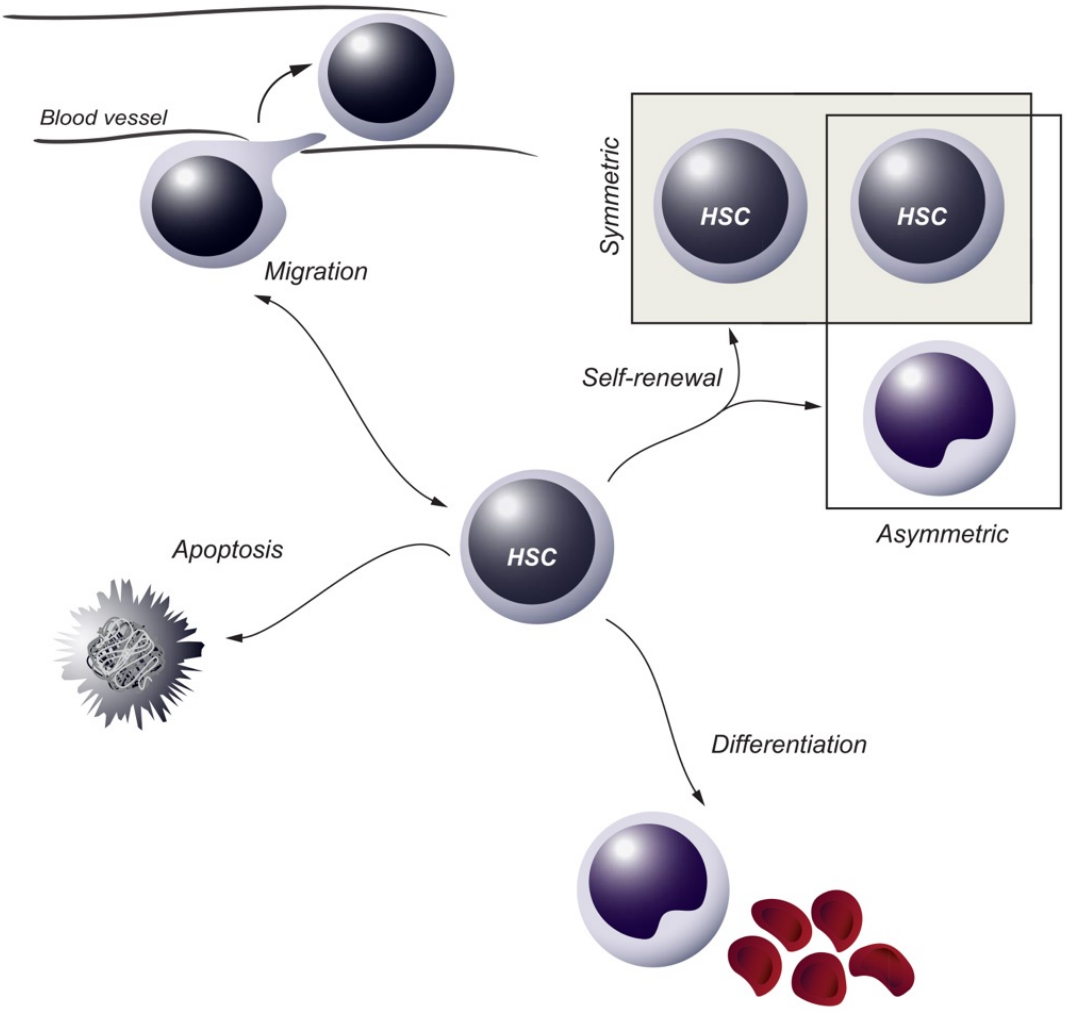

Figure 1.1: Cell fate choices of haematopoietic stem cells (HSC) - HSCs are able to self-renew in a symmetric or asymmetric fashion, differentiate into a lineage committed progenitor, undergo apoptosis or migrate between organs via the bloodstream (Blank *et al.*, 2008).

Primitive human haematopoietic stem cells are extremely rare, and only 1 in $9.3x10^5$ cord blood (CB) cells, 1 in $3x10^6$ adult bone marrow (BM) cells or 1 in $6x10^6$ mobilized peripheral blood (PB) cells is able to engraft the BM of severe combined immunodeficient (SCID) mice (Wang *et al.*, 1997). However, HSCs can be enriched based on a variety of cell surface markers (Figure 1.2).

In mice, cells negative for all lineage markers (a combination of cell surface markers identifying different terminally differentiated blood cells) but positive for Sca1 and c-Kit are named LSK cells (lineage$^-$sca1$^+$c-kit$^+$)(Ikuta & Weissman, 1992; Spangrude *et al.*, 1988). The LSK-fraction, a functionally heterogenous population, is capable to reconstitute the haematopoietic system and consists of HSCs (Lin$^-$Kit$^+$Sca1$^+$CD34$^-$) and multipotent progenitors (MPPs; Lin$^-$Kit$^+$Sca1$^+$ CD34$^+$) (Osawa *et al.*, 1996). Additionally, the signaling lymphocyte activation molecule (SLAM) family receptors CD150, CD244 and CD48 define HSCs (CD150$^+$CD244$^-$CD48$^-$) and MPPs (CD244$^+$ CD150$^-$CD48$^-$) within the LSK-fraction of the BM (Kiel *et al.*, 2005). HSCs can be further divided into long-term (LT)-HSCs (bona fide HSCs), defined by their ability to reconstitute the haematopoietic system of lethally irradiated recipients several times, intermediate (IT)-HSCs with prolonged but time-limited reconstitution potential and short-term (ST)-HSCs contributing only transiently to the repopulation (approximately 12 weeks) (Benveniste *et al.*, 2010; Christensen & Weissman, 2001). This separation is based on the expression of Flk2/FLt3 by ST-HSCs, CD49b^{hi} by IT-HSCs and CD49b^{lo} by LT-HSCs (Adolfsson *et al.*, 2001; Benveniste *et al.*, 2010).

Human cells capable to reconstitute the haematopoietic system upon transplantation in conditioned humans or immunodeficient mice are expressing the cell surface marker CD34. Within the highly heterogenous CD34$^+$ cell population, rare HSCs can be separated from lineage-restricted progenitors based on the cell surface markers CD45RA (Mayani *et al.*, 1993), CD90 (Baum *et al.*, 1992) and CD38 (Hao *et al.*, 1995) as shown in Figure 1.2. Additional expression of CD49f determines HSCs with the ability to generate long-term multilineage grafts (Notta *et al.*, 2011).

Differentiation of HSCs gives rise to MPPs with an incomplete self-renewal capacity and the ability to undergo specification by further differentiation (Kiel *et al.*, 2005; Majeti *et al.*, 2007). Downstream of the MPP the common myeloid progenitor (CMP) gives rise to the granulocyte-monocyte progenitor (GMP) restricted to granulocyte and macrophage development and the megakaryocyte-erythrocyte progenitor (MEP) restricted to megakaryocytes and erythrocytes

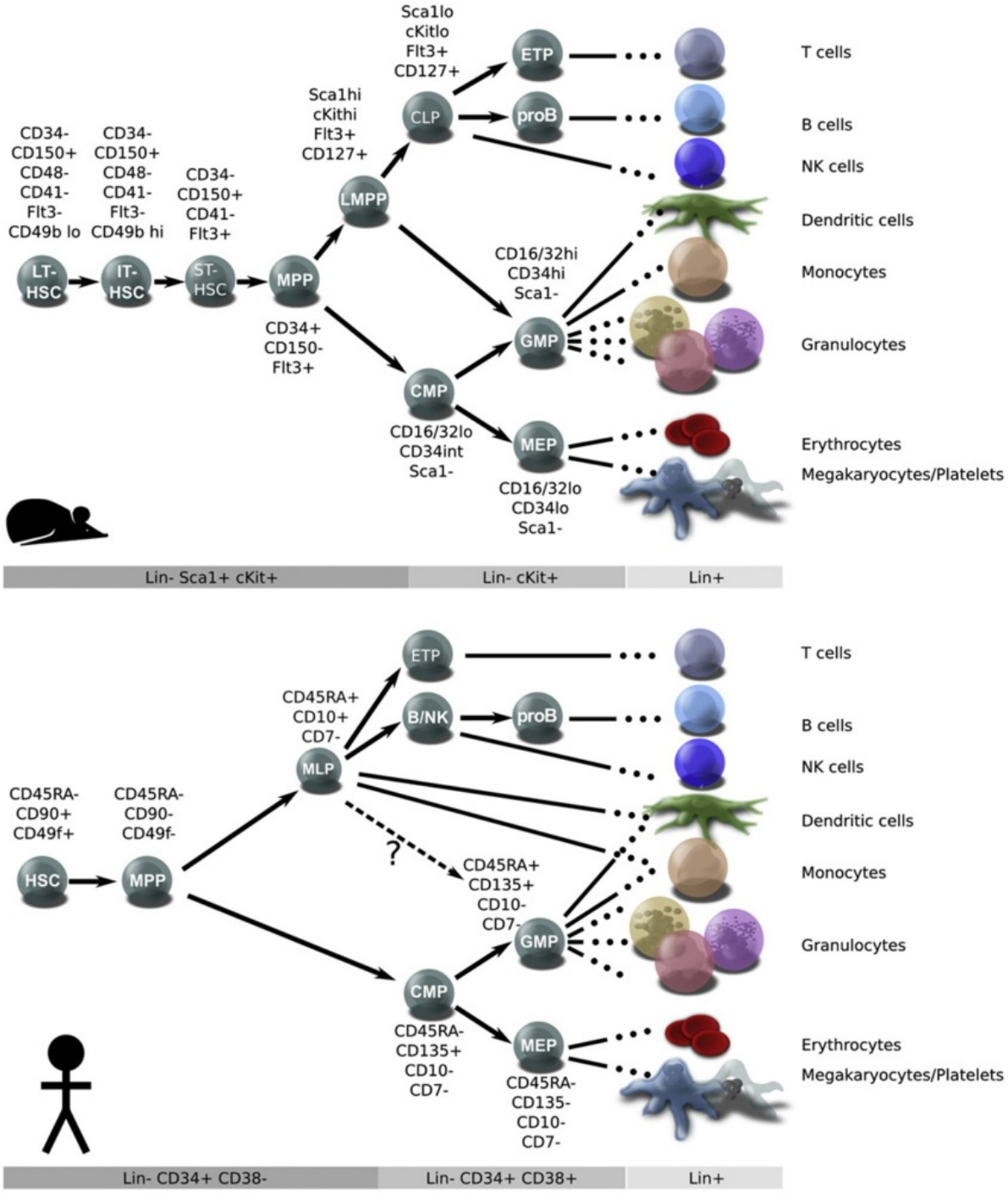

Figure 1.2: Current model of the haematopoietic hierarchy in mice and humans - HSPCs are defined by the indicated cell surface phenotypes. Mouse HSCs can be distinguished based on their repopulation duration in long-term (LT), intermediate-term (IT) and short-term (ST) HSCs. Within the $Lin^{-}CD34^{+}CD38^{-}$ cell population human HSCs can be defined by the expression of CD49f and CD90. Further downstream multipotent progenitors (MPP) give rise to lymphoid-primed multipotent progenitors (LMPP) in mice and multi-lymphoid progenitors (MLP) in humans that can further differentiate into all lymphoid and some myeloid cell types. MPPs can also differentiate into common myeloid progenitors (CMP) that give rise to megakaryocyte-erythrocyte progenitors (MEP) and granulocyte-macrophage progenitors (GMP) in mice as well as in humans (Doulatov *et al.*, 2012).

(Akashi *et al.*, 2000). While myeloid/megakaryocyte/erythrocyte specification seems to be similar in humans and mice, different progenitors have been described for lymphoid specification. In mice, the lymphoid-primed multipotent progenitors (LMPP) sustaining lymphoid, granulocyte and macrophage differentiation potential but lacking erytro-megakaryocyte potential have been identified upstream of the common-lymphoid progenitor (CLP) (Adolfsson *et al.*, 2005; Kondo *et al.*, 1997). In humans, only the multi-lymphoid progenitor (MLP), capable of differentiating into all lymphoid cell types, monocytes, macrophages and dendritic cells, has been described (Doulatov *et al.*, 2010). Thus, both mouse and human haematopoiesis is not strictly separated in myeloid and lymphoid differentation.

1.2 Haematopoietic stem cell transplantation

1.2.1 Therapeutic application of HSPCs and their limitations

Transplantation of autologous or allogeneic haematopoietic stem and progenitor cells (HSPCs), collected from BM, mobilized peripheral blood (PB) or umbilical cord blood (UCB) is often performed to reestablish haematopoietic function in patients suffering from blood diseases, immunodeficiencies and cancer (Samavedi *et al.*, 2009). PB can be enriched for $CD34^+$ cells by G-CSF mediated stem cell mobilization. G-CSF frees $CD34^+$ cells from the BM by causing secretion of neutrophil elastases, which degrade BM stromal cell-derived factor I (SDF-1) that anchors $CD34^+$ cells via their CXCR4 receptor to the BM (Petit *et al.*, 2002).

Therapy of relapsed or high risk haematological malignancies is primarily based on allogeneic haematopoietic stem cell transplantation (HSCT) owing an immune-mediated graft-versus-leukemia (GvL) effect (Kolb, 2008). This GvL effect is mediated by residual $CD4^+$ and $CD8^+$ T cells in stem and progenitor cell populations isolated from BM or mobilized PB of the donor. However, besides the beneficial GvL effect donor T cells also attack host tissue leading to graft-versus-host disease (GvHD) with increased incidence upon mismatch of donor-recipient human leukocyte antigen (HLA) (Morishima *et al.*, 2002). UCB, leading to milder GvHD has emerged as an alternative allogeneic HSCT source for patients lacking a suitable donor (Wagner *et al.*, 1996). The milder GvHD observed after HSCT might be due to the presence of predominantly naïve and immature T cells and immunosuppressive regulatory T cells in UCB (Godfrey *et al.*, 2005; Han *et al.*, 2008). Worldwide banking of CB grafts dramatically reduces delays associated with the search for a matched donor and is especially beneficial for patients with fast progressing disease. However, a remaining limitation of CB transplantation in comparison to PB or BM HSCT is the enhanced infection related mortality as a consequence

of delayed engraftment and immune reconstitution (Rubinstein *et al.*, 1998). The delayed engraftment might be due to the low number of HSPCs collected from a single CB together with the limited number of accessory cells supporting engraftment like lymphocytes. Moreover, immaturity and/or a decreased homing capacity of the CB collected cells might explain this phenomenon (Rocha & Broxmeyer, 2010). Due to the relatively low numbers of $CD34^+$ cells present within a CB unit, UCB transplantation (UCBT) is mainly used for small children. In order to overcome the clinical limitations still associated with UCBT several approaches have been investigated (described in 1.2.3). Experimental model systems used to investigate such novel therapeutic approaches are based on immunodeficient mouse strains allowing the engraftment of human HSPCs.

1.2.2 Mouse models of HSCT

Human biology research is restricted largely to *in vitro* studies since *in vivo* studies are limited due to ethical and/or technical constraints. However, *in vitro* assays lack complexity and crucial components which are normally provided by an organism. To overcome these limitations, different animal models have been established.

Competitive transplantation models are often used to compare the reconstitution ability of murine haematopoietic stem cells derived from two donors with diverse genotypes. Donor cells can be distinguished with the help of the Ly5/CD45 panhaematopoietic surface marker, which exists in two allotypes, Ly5.1 and Ly5.2 (Komuro *et al.*, 1974). Moreover, stem cell frequency within a haematopoieitc population can be determined using limiting dilution transplantation assays (Sieburg *et al.*, 2002).

This is, however, not sufficient to analyze the *in vivo* behavior of human HSCs. Therefore, xenotransplantation models for human haematopoiesis have been developed. In most cases immunodeficient mouse strains allowing the engraftment of human cells, are used. Mouse xenotransplantation models provide an important research tool to study human biological processes like the ability of human HSCs to reconstitute the haematopoietic system, the development and function of the immune system, human specific infectious diseases, autoimmunity, human cancer as well as utilization of human stem cells for regenerative medicine (Shultz *et al.*, 2012). Engraftment of human haematopoietic cells was first described in CB17 mice suffering from a severe combined immunodeficiency (scid) mutation in the protein kinase, DNA activated, catalytic polypeptide (Prkdc) resulting in lack of mature mouse T and B cells (Bosma *et al.*, 1983).

High levels of innate immunity and natural killer (NK)-cell activity however decreased human cell engraftment in CB17-*scid* mice. In order to overcome this limitation, mice were crossed onto the non-obese diabetic (NOD) strain background (Shultz *et al.*, 1995). NOD-*scid* mice have no mature T and B cells and no functional NK cells. Similarly, *rag2*$^{-/-}$ mice lack mature T and B cells, since the recombination activating genes Rag1 and Rag2 activate V(D)J recombination, a genomic rearrangement process that is involved in generation of immunoglobulines and T cell receptors (Oettinger *et al.*, 1990). Another further step was very important for the development of immunodeficient recipient mice: the deletion of the common gamma-chain on a NOD-*scid* or BALB/c-*rag2*$^{-/-}$ background (Ito *et al.*, 2002; Traggiai *et al.*, 2004). This common gamma-chain is part of many cytokine receptors regulating lymphoid homeostasis, such as IL-2R, IL-4R and IL-7R and its deletion results in the complete loss of B,T and NK cells (Nakajima *et al.*, 1997; Sugamura *et al.*, 1996). Immunodeficient mice bearing the common gamma-chain mutation are routinely irradiated prior to transplantaion with human HSCs to enhance SCF expression, which supports HSC engraftment, proliferation and survival and to dampen innate immunity of recipient mice (Broudy, 1997; Limanni *et al.*, 1995).

Human HSC engraftment is not only affected by the immunodeficient mouse strain used (McDermott *et al.*, 2010) but also by the route of transplantation and the source of human HSCs (Lepus *et al.*, 2009). Optimal conditions have not yet been identified and further comparative analyses are required. Injection routes of HSCs include intravenous injection into irradiated newborn or adult recipient mice, or intrahepatic injection into newborn mice to directly place HSCs into their supportive microenvironment (niche) and thereby circumvent homing requirements. As described by Traggiai, intrahepatic injection of human CB derived CD34^{+} cells into irradiated newborn *rag2*$^{-/-}\gamma c^{-/-}$ mice leads to the development of a human adaptive immune system involving *de novo* development of B, T and dendritic cells as well as the formation of structured primary and secondary lymphoid organs (Traggiai *et al.*, 2004).

Although the absence of the common gamma-chain has greatly improved the engraftment of human HSCs in immunodeficient mice, a proper haematopoietic and immune system development is still restricted due to species-specificity of human haematopoietic cytokines, MHC molecules, homing molecules and residual host immune function against human cells (Shultz *et al.*, 2007). Many of these limitations were recently addressed by the delivery of human species-specific factors into mice supporting haematopoietic cell development and maintenance as well as by targeted inactivation of genes responsible for the innate mouse immune system. One approach for the creation of ”next-generation” immunodeficient mice was the

transgenic expression of the human signal regulatory protein alpha (SIRPa) in *rag2*$^{-/-}\gamma c^{-/-}$ mice or accordingly by transducing mouse CD47 into human progenitor cells to enable an interaction between SIRPa and CD47, which negatively regulates phagocytosis of haematopoietic cells (Legrand *et al.*, 2011; Strowig *et al.*, 2011). Furthermore, the gene replacement of mouse TPO by the gene encoding for human TPO efficiently increased human HSC self-renewal capacity and human myelopoiesis (Rongvaux *et al.*, 2011). Transgenic expression of membrane-bound human SCF greatly supported engraftment of human HSC into non-irradiated newborn NOD-*scid IL2r*γ^{null} mice (Brehm *et al.*, 2012). In summary, genetic modifications highly improved the development and function of the human haematopoietic and immune system in humanized mice, and these have now become indispensable for translational biomedical research.

1.2.3 Current approaches to increase efficacy of HSCT

Efficiency of UCBT is mainly limited by the low number of HSPCs present in a single CB unit, restricting the use of UCB grafts to small children.

So far, the most successful approach to circumvent the limited cell dose of a single CB graft is the double-unit CB transplantation increasing the use of CB for HSCT in adults (Barker *et al.*, 2005). However, usually only one of the two transplanted CB units contributes to the sustained recovery of the haematopoietic and immune system in the patient (Barker *et al.*, 2005). The reason for this phenomenon is still unclear. One possible explanation was the order of infusion, with the first infused CB being superior over time (Ballen *et al.*, 2007). Furthermore, the CB unit with higher numbers and viability of $CD34^+$ cells seems to predominate in a double CB transplantation setting (Haspel *et al.*, 2007). Most interestingly, effector $CD8^+$ T cells arising from the engrafting unit mediate early immune rejection against the non-engrafting unit (Gutman *et al.*, 2010). Although the transplantation of two CB units leads to increased GvHD it seems to lower transplantation related mortality (MacMillan *et al.*, 2009).

Moreover, infusion of a CB unit together with T cell depleted mobilized haematopoietic stem cells (MHSC) from a third party donor was reported to reduce post-transplant neutropenia due to early engraftment of the MHSCs. Thus, the incidence of neutropenia-related infections was lower (Bautista *et al.*, 2008). Interestingly, the combination of G-SCF with plerixafor has been shown to enhance mobilization of HSCs to the PB. Plerixafor is a small-molecule inhibitor of the CXCR4 receptor, which is expressed on $CD34^+$ cells and anchors them to the BM (Brave *et al.*, 2010).

The efficacy of UCBT can also be increased by *ex vivo* expansion of HSPCs. Cultivation of cord blood progenitor cells with low amounts of Notch ligand Delta1 enhanced early human haematopoietic reconstitution in NOD-*scid* mice (Delaney *et al.*, 2005). In a phase I/II clinical trial half of a CB unit was cultured for 21 days with an early acting cytokine cocktail (TPO, IL6, Flt3L and SCF) supplemented with the high-affinity copper chelator tetraethylenepentamine (TEPA), which was shown to decrease $CD34^+$ cell differentiation and enhance their capability to engraft in SCID mice (De Lima *et al.*, 2008; Peled *et al.*, 2005). Infusion of the unmanipulated together with the *ex vivo* expanded CB fraction was well tolerated by patients (De Lima *et al.*, 2008). In another recently initiated clinical trial, HSPCs are expanded by using an aryl hydrocarbon receptor antagonist, which was described to efficiently expand HSPCs *in vitro* (Boitano *et al.*, 2010).

In addition, a promising strategy to enhance CB transplantation efficiency is the improvement of *in vivo* homing of CB HSPCs through inhibition of the CD26/dipeptidylpeptidase IV (DPPIV) with Diprotin A (Campbell *et al.*, 2007). CD26/DPPIV, expressed by a subpopulation of CB derived $CD34^+$ cells, cleaves and thereby inactivates the stromal cell-derived factor-1/CXCL12, which plays an important role in HSPC homing and engraftment due to its interaction with the CXCR4-receptor of HSPCs (Broxmeyer *et al.*, 2003; Christopherson II *et al.*, 2002). Direct intra-bone injection (phase I/II clinical trial) of CB cells seems to increase homing capacity of these cells, accompanied by a reduced incidence of acute GvHD (Frassoni *et al.*, 2008). Interestingly, recently published data indicate that DPPIV also cleaves and thereby decreases the activity of GM-CSF, G-CSF, IL3 and erythropoietin (Broxmeyer *et al.*, 2012). Moreover, Broxmeyer and colleagues observed an increased recovery of haematopoiesis after stress *in vivo* upon deficiency or inhibition of DPPIV.

1.3 Apoptosis and other cell death pathways

Apoptosis is a cell death program that is critically involved in the regulation of physiological processes such as embryonic development and the maintenance of tissue homeostasis in adult organisms (Ulukaya *et al.*, 2011). The term ”apoptosis” originates from the Greek language and describes a process like ”falling of” leaves from trees (Kerr *et al.*, 1972). Homeostasis within tissues strongly depends on the balance between cell proliferation and apoptosis, and disruption of this balance by dysfunction of apoptosis can contribute to the pathogenesis of various human diseases. While cancer or autoimmunity are caused by decreased apoptosis rates, neurodegenerative disorders or acquired immunodeficiency syndrome (AIDS) are characterized by excessive apoptosis (Ulukaya *et al.*, 2011). Typical morphological changes during apoptosis, as described by Kerr et al., include chromatin condensation, nuclear fragmentation, cell shrinkage, plasma membrane blebbing and the formation of small vesicles named ”apoptotic bodies”, which are rapidly removed by phagocytosis without induction of inflammation (Kerr *et al.*, 1972).

Aside from apoptosis (type I), cell death can occur via autophagy (type II) or necrosis (type III) (Lockshin & Zakeri, 2004). Autophagy is a ”self-eating” process mediated by lysosomal degradation and is characterized by extensive accumulation of vesicles (Yuan & Kroemer, 2010). Autophagy is normally used for degradation of long-lived proteins and organelles but can also serve to recycle cellular material during starvation (Levine *et al.*, 2005). Therefore, autophagy is primarily important to keep cells alive during starvation. Only prolonged autophagy leads to cell death (Levine *et al.*, 2005). Necrotic cell death is characterized by cell and organelle swelling, plasma membrane rupture and cell content release accompanied by inflammation. Recently, a programmed form of necrosis has been described. This so called ”necroptosis” is executed through so called receptor-interacting protein kinases RIP1 and RIP3 (Degterev *et al.*, 2005; Yuan & Kroemer, 2010).

1.3.1 Apoptosis signaling

Apoptosis can be initiated by death receptors on the cell surface (extrinsic pathway) or by mitochondria (intrinsic pathway) as shown in Figure 1.3. Both pathways require activation of caspases (Cys Asp acid proteases). These enzymes are characterized by a cysteine residue in their active site and their highly specific cleavage of substrates after an aspartate residue within tetrapeptide sequences (Tait & Green, 2010). Caspases involved in apoptosis can be divided into initiator caspases (such as caspase-8 and caspase-9) and executioner caspases (caspase-3,-6,-7) (Li & Yuan, 2008). Other caspases such as caspase-1 are not involved in cell

death signaling but rather in inflammatory processes (Sansonetti *et al.*, 2000). Caspases are synthesized as inactive zymogens consisting of either a long prodomain (initiator caspases), containing a caspase recruitment domain (CARD) or a death effector domain (DED), or a short prodomain (executioner caspases), together with a large subunit (20 kDa) bearing the catalytic dyad residues and a small subunit (10 kDa) (Li & Yuan, 2008). Proteolytic cleavage of the inactive zymogens removes prodomains and separates the large and small subunit (Li & Yuan, 2008). As soon as initiator caspases are activated, they proteolytically cleave and activate executioner caspases (Tait & Green, 2010). These, in turn, cleave several cellular substrates like the inhibitor of caspase-activated DNase (ICAD), thereby releasing the active nuclease CAD, which subsequently leads to DNA fragmentation (Enari *et al.*, 1998).

The extrinsic apoptosis pathway is initiated upon binding of death ligands of the tumor necrosis factor (TNF) family like CD95-ligand (CD95-L or Fas-L) or TNF-related apoptosis-inducing ligand (TRAIL) to their cognate death receptors (DR) of the TNF receptor family such as CD95 (Fas/APO-1) (Oehm *et al.*, 1992), TRAIL-receptor-1 (DR4) (Pan *et al.*, 1997) or TRAIL-receptor-2 (DR5) (Chaudhary *et al.*, 1997). TNF family-ligands and receptors tend to form trimers (Locksley *et al.*, 2001). After death ligand binding, conformational changes of the death receptor lead to the recruitment of adapter proteins such as Fas associated death domain protein (FADD) (Chinnaiyan *et al.*, 1995). FADD contains two domains, a death domain (DD), which enables binding to the intracellular DD of the receptor and a DED for the interaction with procaspase-8 (Muzio *et al.*, 1996). Formation of this so called death inducing signaling complex (DISC) mediates autocatalytic cleavage of procaspase-8 (Lavrik *et al.*, 2003). Activated caspase-8 is released into the cytoplasm and activates executioner caspases thereby triggering the apoptotic cascade. In type I cells DISC mediated caspase-8 activation is sufficient to fully activate caspase-3 and execute apoptosis. In contrast, type II cells require additional activation of the mitochondrial pathway via cleavage and activation of Bid (tBid = truncated, active form) by caspase-8 (Li *et al.*, 1998; Scaffidi *et al.*, 1998). The DISC-mediated activation of caspase-8 can be regulated by the cellular Flice-inhibitory protein (FLIP) (Irmler *et al.*, 1997). The short isoforms of cFLIP can prevent caspase-8 activation and processing after recruitment to the DISC by competing with caspase-8 for FADD binding (Golks *et al.*, 2005; Krueger *et al.*, 2001).

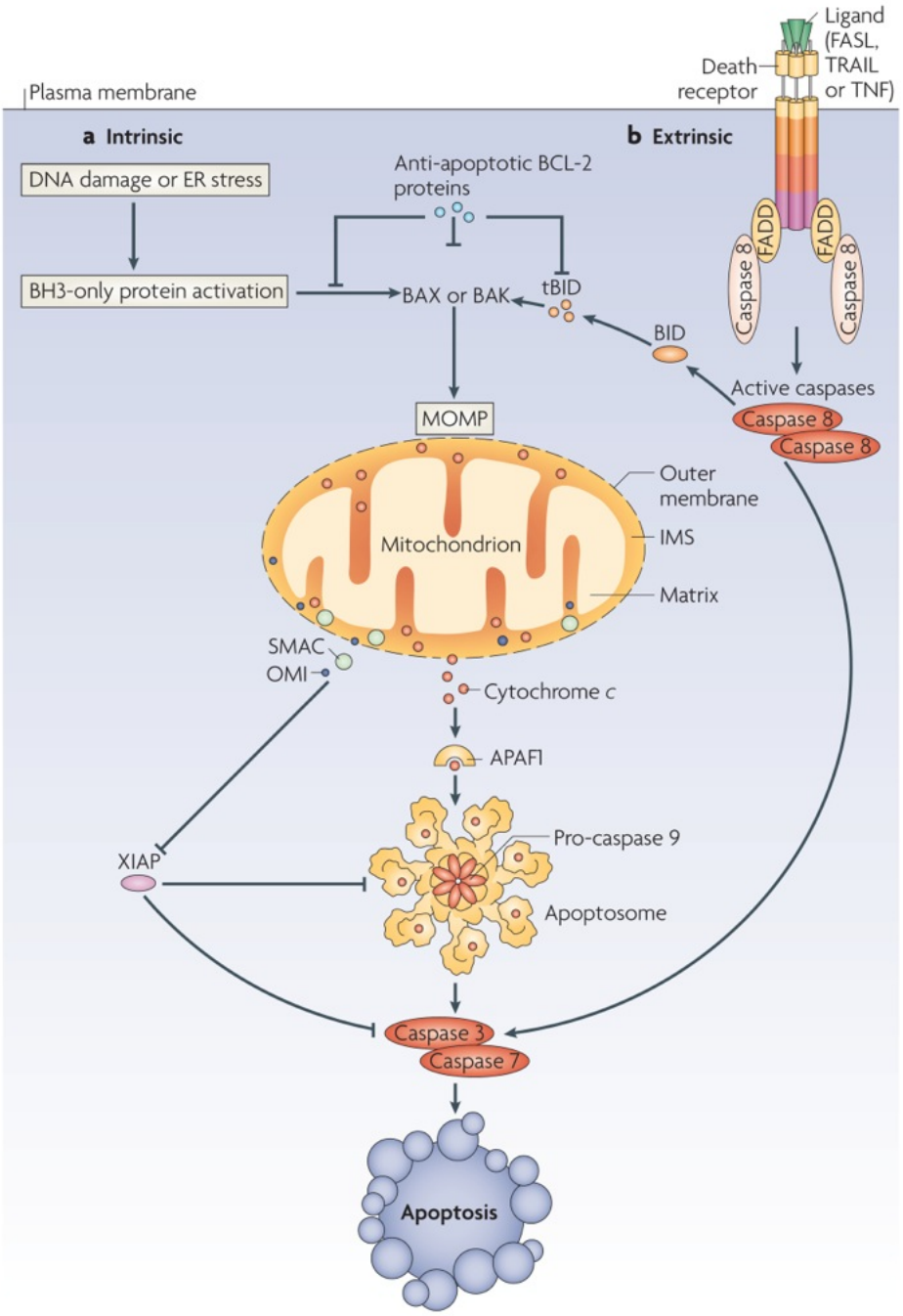

Figure 1.3: A schematic overview of the intrinsic and extrinsic apoptosis pathway - The intrinsic apoptosis pathway is initiated upon cellular stress leading to activation of BH3-only proteins which in turn activate Bax and Bak. Once activated, Bax and Bak lead to MOMP. Following MOMP, cytochrome c, Smac and Omi are released from the mitochondrial intermembrane space (IMS). Cytochrome c, Apaf1 and pro-caspase-9 form the apoptosome in which caspase-9 is activated. Caspase-9 in turn activates effector caspases, finally leading to apoptosis. Smac and Omi promote apoptosis by neutralizing XIAP. The extrinsic apoptosis pathway is initiated by binding of death ligands to their receptors. Subsequently, adaptor proteins (i.e. FADD) and pro-caspase-8, are recruited to the receptor leading to activation of caspase-8. Active caspase-8 promotes apoptosis directly by activation of executioner caspases or through cleavage and activation of Bid, leading to mitochondrial mediated apoptosis (Tait & Green, 2010).

The intrinsic apoptosis pathway is initiated by cellular stress such as DNA damage or endoplasmic reticulum (ER) stress leading to activation of pro-apoptotic members of the Bcl-2 family (Bcl-2: B cell lymphoma 2) as described in detail in the following chapter. The signaling cascade includes various Bcl-2 family members and finally results in permeabilization of the outer mitochondrial membrane (MOMP). Following MOMP, various pro-apoptotic factors are released from the mitochondrial intermembrane space into the cytosol (i.e. cytochrome c, Smac and Omi) (Saelens *et al.*, 2004). Cytosolic cytochrome c associates, in the presence of dATP, with Apaf1 and procaspase-9 molecules. This leads to the formation of a complex called the ”apoptosome”, in which procaspase-9 molecules are activated and in turn activate effector caspases eventually leading to cell death (Li *et al.*, 1997; Yuan *et al.*, 2010). Besides cytochrome c, the second mitochondria-derived activator of caspase (Smac) and Omi are released from mitochondria. They promote apoptosis by neutralizing X-linked inhibitor of apoptosis protein (XIAP), a caspase-9 and executioner caspase inhibitor (Eckelman *et al.*, 2006). Moreover, the two proteins, apoptosis-inducing factor (AIF) and endonuclease G, which are also released following MOMP, are suggested to kill cells in a caspase-independent manner by causing DNA-fragmentation (Li *et al.*, 2001; Susin *et al.*, 1999).

1.3.2 Bcl-2 family

The human B cell lymphoma 2 (Bcl-2) gene was originally discovered at the t(14;18) chromosome translocation breakpoint resulting in its overexpression in follicular B-cell lymphoma (Tsujimoto *et al.*, 1985). Subsequently, overexpression of Bcl-2 was shown to promote carcinogenesis by inhibiting cell death (Dohlman *et al.*, 1988). To date, many different Bcl-2 homologues have been described, together forming the large ”Bcl-2 family”.

All Bcl-2 family members contain one or more Bcl-2 homology domains (BH1, BH2, BH3, BH4), which enable interaction between Bcl-2 proteins (Youle & Strasser, 2008). Based on their structure (number and kind of BH-domains) and their biochemical function they are divided into three groups as shown in Figure 1.4. The anti-apoptotic Bcl-2 family group includes Bcl-2 itself, as well as Bcl-x_L, Bcl-w, A1 and Mcl-1. All anti-apoptotic family members are structurally closely related to Bcl-2. The second Bcl-2 family group, the pro-apoptotic Bcl-2 proteins, are subdivided into the BH123-proteins Bax, Bak and Bok and the BH3-only proteins (Bid, Bim, Bad, Bmf, Noxa, Hrk, Puma and Bik). In healthy cells, Bax and Bak are held in an inactive state by anti-apopotitic Bcl-2 proteins. If the cell is stressed, Bax and Bak are activated and form large protein complexes leading to pore formation and MOMP.

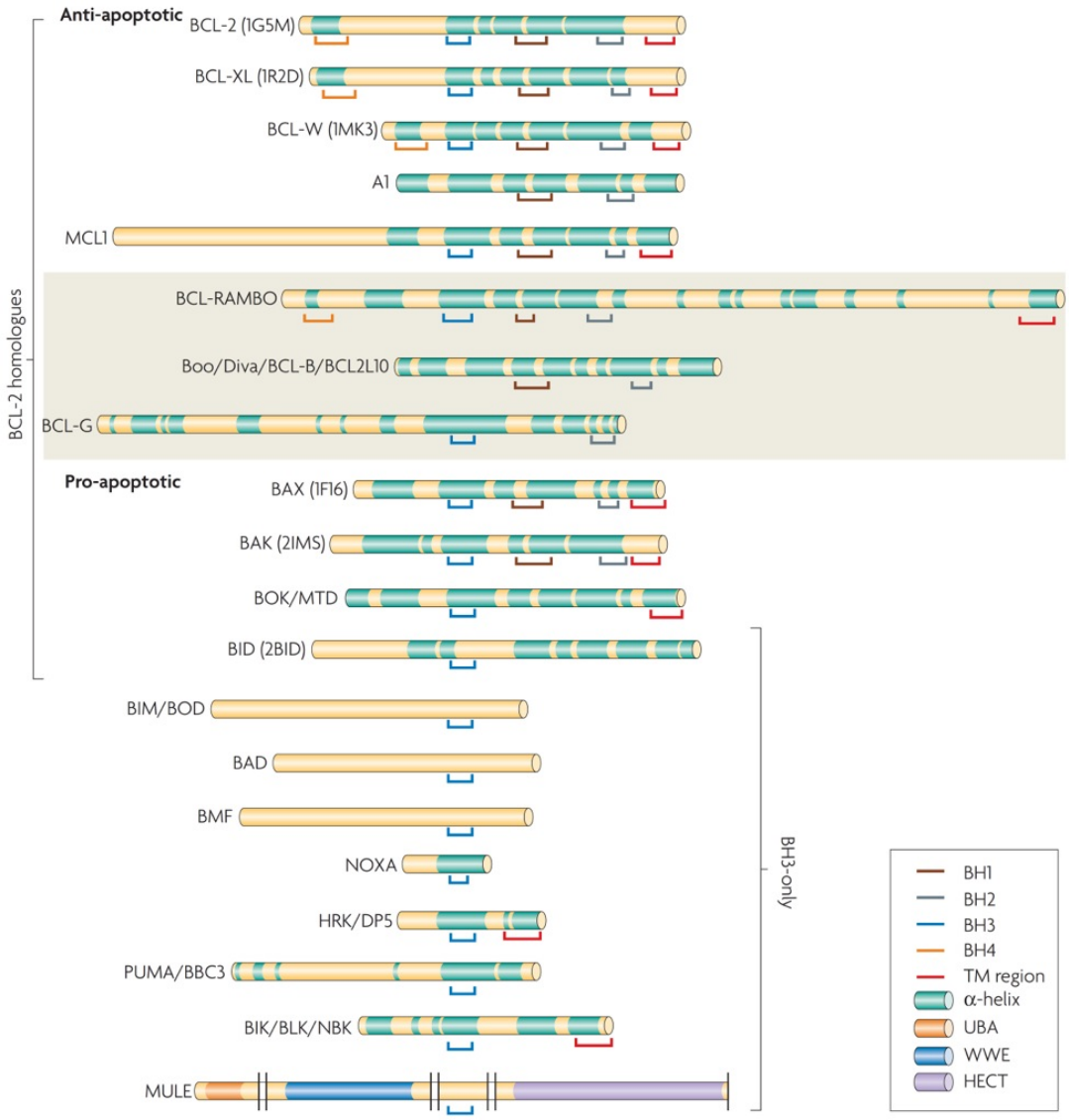

Figure 1.4: Bcl-2 family members - The Bcl-2 family members can be divided into three groups based on various structural and functional features: (1) anti-apoptotic members Bcl-2, Bcl-x_L, Bcl-w, A1 and Mcl-1, (2) pro-apoptotic BH123-proteins Bax, Bak and Bok and (3) pro-apoptotic BH3-only members Bid, Bim, Bad, Bmf, Noxa, Hrk, Puma, Bik. The Mcl-1 specific E3 ubiquitin-ligase MULE also contains a BH3 domain. The Bcl-2 homology domains (BH1-4) are essential for protein-protein interaction. The BH1, BH2 and BH3 domains form a hydrophobic groove, which is able to bind BH3-only peptides. The BH3 domain, especially the one of BH3-only proteins, is essential for interaction with core Bcl-2 family proteins. The grey box depicts proteins less well studied so far. transmembrane (TM); ubiquitin-associated domain (UBA); Trp-Trp-Glu interaction module (WWE); HECT ubiquitin ligase domain; (Youle & Strasser, 2008).

Bax and Bak activation is initiated by the action of BH3-only proteins which express only the short BH3 motif, an amphipathic α-helix with around 26 residues. This domain allows high affinity binding to the hydrophobic groove of anti-apoptotic Bcl-2 family proteins (Sattler *et al.*, 1997) formed by BH1, BH2 and BH3. Thereby, anti-apoptotic Bcl-2 proteins are inactivated, and Bax and Bak are activated. Thus, the balance between pro- and anti-apoptotic Bcl-2 family proteins determines whether a cell survives or dies ("Bcl-2 rheostat"). Besides the BH-domains, many Bcl-2 family members contain a hydrophobic transmembrane domain (TM), which enables constitutive or apoptotic signal-mediated translocation and anchoring into membranes such as the mitochondrial outer membrane and the ER (Strasser *et al.*, 2011). Different localization has been shown to be associated with different function, for example ER-Bcl-2 is involved in calcium flux (Rong & Distelhorst, 2008). It is still unclear how the three Bcl-2 family subgroups interact with each other. To date, two distinct models have been proposed, the indirect and direct activation model as depicted in Figure 1.5 (Happo *et al.*, 2012; Kuwana *et al.*, 2005).

The direct activation model (Chipuk *et al.*, 2010; Letai *et al.*, 2002) suggests that BH3-only proteins can be divided into activators (e.g. Bim, tBid and maybe Puma (Cartron *et al.*, 2004)) and sensitizers (e.g. Noxa, Bmf and Bad). Whereas both subgroups can bind to and inhibit anti-apoptotic Bcl-2 proteins, only the former can bind transiently to and activate Bax and Bak. In this model, apoptosis is promoted upon displacement of activators bound to anti-apoptotic Bcl-2 proteins by sensitizer BH3-only proteins. Thus, activator BH3-only proteins are freed and bind and activate Bax and Bak. In contrast, the indirect activation model (Uren *et al.*, 2007; Willis *et al.*, 2007) proposes that free Bax and Bak molecules are spontaneously activated. This model thus doesn't require activator BH3-only proteins. Apoptosis is initiated upon neutralization of the anti-apoptotic Bcl-2 proteins by BH3-only proteins and the release of Bax or Bak. Most probably, features of both models seem to be required for apoptosis initiation *in vivo* (Mérino *et al.*, 2009).

Independently of these two models it has been shown that only Bim, tBid and Puma are able to bind to all anti-apoptotic Bcl-2 proteins with high affinity. In contrast, Bad and Bmf bind selectively to Bcl-2, Bcl-x_L and Bcl-w, and Noxa only binds to Mcl-1 and A1 (Chen *et al.*, 2005; Kuwana *et al.*, 2005). Further downstream, Bax is proposed to be bound by all anti-apoptotic Bcl-2 proteins (Strasser *et al.*, 2011; Willis *et al.*, 2007), whereas Bak seems to be bound with high affinity only by Bcl-x_L, Mcl-1 (Willis *et al.*, 2005) and A1 (Strasser *et al.*, 2011).

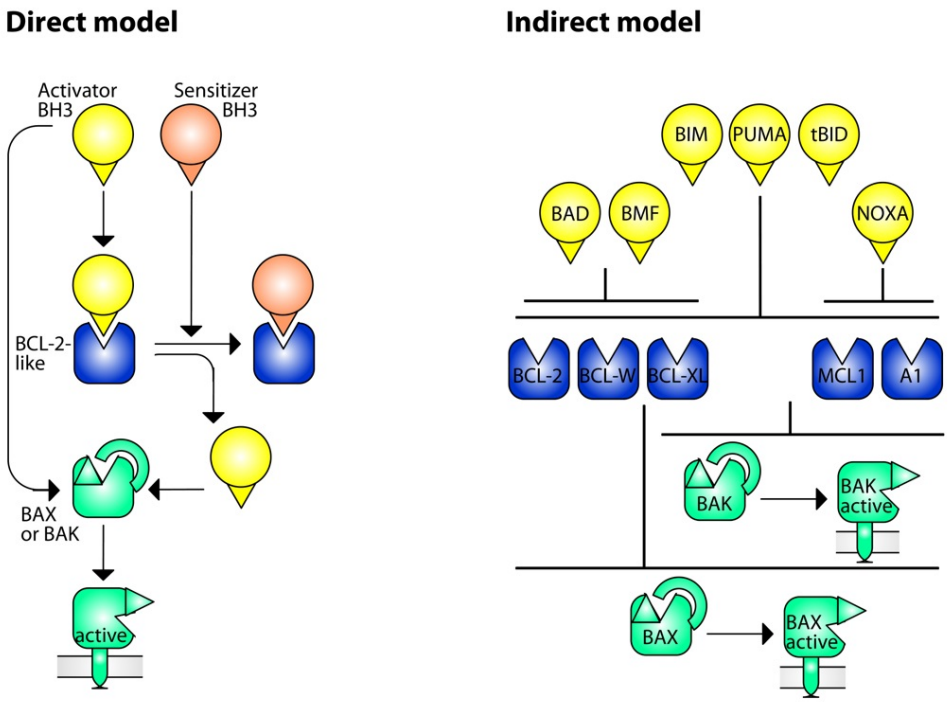

Figure 1.5: Model for the interplay between Bcl-2 family members - The direct activation model (left panel) suggests that an apoptotic signal induces sensitizer BH3-only proteins (e.g. Noxa, Bmf and Bad) to release activator BH3-only proteins (Bim, tBid and probably Puma), which are bound to anti-apoptotic Bcl-2 proteins. Subsequently, freed activator BH3-only proteins activate Bax and Bak. In the indirect model activated BH3-only proteins release Bax or Bak from anti-apoptotic Bcl-2 family proteins which are spontaneously activated (modified from (Happo *et al.*, 2012; Strasser *et al.*, 2011)).

Another open question is, how active Bax and Bak oligomerize and induce MOMP. One model suggests that an apoptotic signal gets Bak to expose its BH3 domain and thereby enables binding to another active Bak molecule via the surface groove (Dewson *et al.*, 2008). These symmetric dimers oligomerize via interaction of their α6 helix (Dewson *et al.*, 2009). Bax is proposed to oligomerise in a similar way (Westphal *et al.*, 2011). Another model proposes that upon apoptotic signaling, activated Bax molecules interact via a a rear site groove leading to the formation of a face-to-back dimers which recruits further active Bax molecules to form an oligomer (Shamas-Din *et al.*, 2011). These higher-order oligomers may promote MOMP through proteinaceous channels or lipidic pore formation (Tait & Green, 2010). Newmeyer and colleagues suggest a new model for apoptotic pore formation in the outer mitochondrial membrane. This model proposes that BH3-only proteins together with unknown membrane-remodeling factors (MRF) promote the Bax-mediated lipidic pore formation (Basañez *et al.*, 2012; Kushnareva *et al.*, 2012). This latter model strongly supports the above described direct activation model. Very recently the active conformation of Bax has been structurally resolved and shown to involve the direct binding of a BH3-domain (Czabotar *et al.*, 2013).

1.3.3 BH3-only proteins act as stress sensors

BH3-only proteins are activated selectively in a cell type-dependent and cell stress-dependent manner (Happo *et al.*, 2012). Accordingly, single BH3-only proteins have distinct physiological functions, as demonstrated using gene-targeted mice (Bouillet *et al.*, 1999; Coultas *et al.*, 2005, 2007; Erlacher *et al.*, 2005; Imaizumi *et al.*, 2004; Jeffers *et al.*, 2003; Kaufmann *et al.*, 2007; Labi *et al.*, 2008; Ranger *et al.*, 2003; Villunger *et al.*, 2003b; Yin *et al.*, 1999). Importantly, different BH3-only proteins can cooperate in apoptosis induction in response to some apoptotic stimuli (Erlacher *et al.*, 2006; Labi *et al.*, 2006; Michalak *et al.*, 2008; Strasser *et al.*, 2011). The activity of BH3-only proteins is regulated on the transcriptional as well as on post-translational level as shown for Bim, Puma, Noxa and Bmf in Figure 1.6 (Puthalakath *et al.*, 2002).

For example, the three major isoforms of Bim (BimEL, BimL and BimS) are generated by alternative splicing, with BimS beeing the most potent killer (O'Connor *et al.*, 1998). In healthy cells, the apoptotic activity of BimEL and BimL is repressed due to their association with the dynein light chain 1 (DLC1) of the dynein motor complex (Puthalakath *et al.*, 1999). Release from this complex can be triggered by phosphorylation of Bim through Jun N-terminal kinase (JNK) in response to environmental stress (Putcha *et al.*, 2003). Furthermore, Bim is regulated as depicted in Figure 1.6. BimEL and BimL are expressed in lymphocytes, myeloid cells, neurons and many other cell types, whereas BimS was not detected in any of these cell types (OReilly *et al.*, 2000). Gene targeting in mice indicates that Bim might be a critical physiological regulator of leukocyte homeostasis, since *bim*$^{-/-}$ mice show highly elevated levels of B cells, mature T cells, granulocytes and monocytes (Bouillet *et al.*, 1999). Indeed, Bim has been reported to be essential during lymphocyte development for negative selection of autoreactive thymocytes and B cells and for the shutdown of acute and chronic immune responses (Bouillet *et al.*, 2002; Enders *et al.*, 2003; Hughes *et al.*, 2008; Pellegrini *et al.*, 2003). Moreover, *in vitro* experiments demonstrate that Bim mediates apoptosis upon growth factor deprivation in lymphocytes (Bouillet *et al.*, 1999) and a variety of other cell types such as osteoclasts and neurons (Youle & Strasser, 2008). Besides cytokine deprivation, Bim is required for lymphocyte apoptosis induced by highly elevated calcium ion flux and microtubule perturbation but seems to be less important for γ-irradiation or glucocorticoid induced apoptosis (Bouillet *et al.*, 1999; Erlacher *et al.*, 2005). Interestingly, the combined loss of Bim and Puma renders lymphocytes more resistant to apoptosis induced by γ-irradiation, glucocorticoid and ER stressor compared to loss of either Bim or Puma (Erlacher *et al.*, 2006).

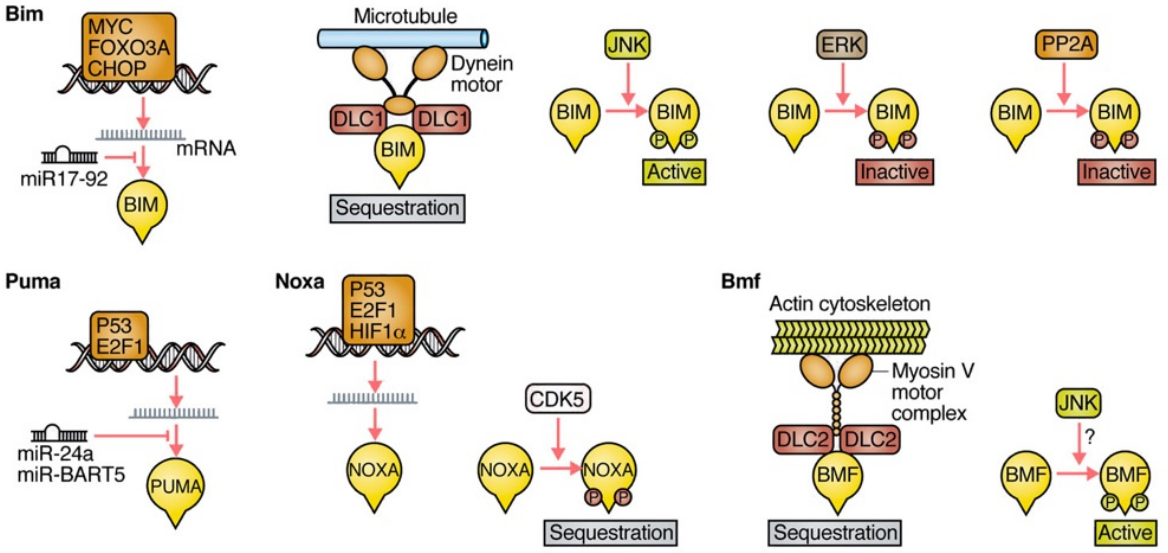

Figure 1.6: Regulation of BH3-only proteins - BH3-only proteins are regulated in response to various cell stress signals. These stress signals can induce expression of BH3-only proteins through different transcription factors. Cytokine deprivation induces expression of Bim via the forkhead transcription factor FOXO3A (Coffer *et al.*, 2000), while ER stress leads to Bim induction via CHOP-C/EBPα (Puthalakath *et al.*, 2007). Bim can also be induced by Myc (Egle *et al.*, 2004). In contrast, the miR-17-92 microRNA cluster represses Bim expression (Ventura *et al.*, 2008). DNA damage induces transcription of Noxa (Oda *et al.*, 2000) and Puma (Nakano *et al.*, 2001; Yu *et al.*, 2001) via the tumor suppressor p53. E2F1 also induces transcription of Noxa and Puma (Hershko & Ginsberg, 2004), and hypoxia-inducible factor HIF1α leads to Noxa induction (Kim *et al.*, 2004). Puma expression is inhibited by miR-BART5 (Choy *et al.*, 2008). BH3-only proteins are also regulated post-translationally by sequestration to intracellular cytoskeletal structures. While, interaction with the LC8 cytoplasmic DLC1 sequesters BimEL and BimL to the microtubular dynein motor complex (Puthalakath *et al.*, 1999), interaction with DLC2 leads to sequestration of Bmf to the myosin V actin motor complex (Puthalakath *et al.*, 2001) in healthy cells. Moreover, BH3-only proteins are regulated on a post-translational level by site-specific phosphorylation. Apoptotic function of Bim (Putcha *et al.*, 2003) and Bmf might be increased upon release from the dynein or myosin V motor complexes due to phosphorylation through JNK (Lei & Davis, 2003). The activity of Bim is also increased by protein phosphatase 2A (PP2A)-mediated dephosphorylation in response to ER-stress (Puthalakath *et al.*, 2007). In contrast, extracellular signal-regulated kinase (ERK) mediated phosphorylation leads to dissociation of BimEL from Mcl-1 and Bcl-x_L (Ewings *et al.*, 2007), as well as ubiquitylation and proteasomal degradation of BimEL (Ley *et al.*, 2003). Apoptotic function of Noxa is inhibited upon phosphorylation through cyclin-dependent kinase 5 (CDK5) in the presence of Glucose leading to cytosolic sequestration of Noxa (Lowman *et al.*, 2010). Modified from (Happo *et al.*, 2012).

The two major isoforms of Bmf (BmfCUG and BmfS) have been described to bind anti-apoptotic Bcl-2 proteins with comparable affinity (Grespi *et al.*, 2010). The pro-apoptotic function of Bmf is inhibited in healthy cells through association of Bmf to the myosin V motor complex via the DLC2. Bmf is freed from the motor complex upon loss of cell attachment in certain cell lines (Puthalakath *et al.*, 2001). However, Bmf seems to be dispensable for cell detachment induced apoptosis (anoikis) in endothalial cells and fibroblasts, indicating that other BH3-only proteins such as Bim (Mailleux *et al.*, 2007) might contribute to anoikis (Labi *et al.*, 2008). Moreover, Bmf might be relevant for growth factor withdrawal induced apoptosis, since Bmf was found to be accumulated in cytokine-deprived granulocytes (Villunger *et al.*, 2003a). Mice lacking Bmf show defects in B cell homeostasis, thus Bmf might cooperate with Bim in regulating lymphocyte apoptosis (Labi *et al.*, 2008).

Puma (p53-upregulated modulator of apoptosis) is a direct transcriptional target of the tumor suppressor p53 (Nakano *et al.*, 2001). Loss of Puma renders lymphocytes highly resistant to γ-irradiation and DNA damage-inducing chemotherapeutics (Erlacher *et al.*, 2005; Jeffers *et al.*, 2003; Villunger *et al.*, 2003b). Moreover, Puma can mediate apoptosis in response to p53-independent stress situations, such as growth factor deprivation or glucocorticoid treatment (Han *et al.*, 2001; Villunger *et al.*, 2003b; You *et al.*, 2006). In comparison to Puma, Noxa, another direct transcriptional target of p53 (Oda *et al.*, 2000) seems to be less important for γ-irradiation or etoposide-induced apoptosis of lymphocytes and fibroblasts (Shibue *et al.*, 2003; Villunger *et al.*, 2003b). However, ultraviolet (UV)-radiation induced apoptosis in fibroblasts and skin keratinocytes is mainly mediated by Noxa (Naik *et al.*, 2007). Combined loss of Noxa and Puma has been reported to protect thymocytes from γ-irradiation induced apoptosis as efficient as loss of p53, indicating that Noxa and Puma can cooperate in mediating DNA-damage induced apoptosis in some cell types (Michalak *et al.*, 2008).

1.4 Apoptosis signaling in HSPCs

1.4.1 Role of the intrinsic apoptosis pathway in HSPCs

Intrinsic apoptosis signaling is critically involved in the regulation of HSPC homeostasis as demonstrated in mice deficient or transgenic for anti-apoptotic Bcl-2 proteins. Bcl-x_L deficiency causes early embryonic death of mice and extensive apoptosis of immature haematopoietic stem cells in the fetal liver (Motoyama *et al.*, 1995). Mcl-1 has also been reported to be important for HSPC survival, since conditional depletion of Mcl-1 in mice leads to loss of HSPCs in the bone marrow (Opferman *et al.*, 2005). In contrast, Vav-gene promoter mediated overexpression of Mcl-1 causes malignant transformation of HSPCs in mice (Campbell *et al.*, 2010b). Moreover Mcl-1 has been described to be essential for self-renewal of human HSCs, demonstrated by knocking down of Mcl-1 in human CB cells followed by serial-transplantation of cells into immunodeficient mice (Campbell *et al.*, 2010a). Haematopoiesis in Bcl-2 deficient mice has been reported to be normal, whereas mature lymphoid cells rapidly die in the absence of Bcl-2. Accordingly, transplantation of Bcl-2 deficient LSK cells leads to an impaired lymphoid development, while long-term reconstitution of nonlymphoid cells is unaffected (Matsuzaki *et al.*, 1997; Veis *et al.*, 1993). On the other hand, transgenic overexpression of Bcl-2 in the haematopoietic compartment was shown to increase HSPC numbers in fetal haematopoietic organs (Ly-6E/A promoter) or adult BM (H2K and Vav promoter) (Domen *et al.*, 2000; Ogilvy *et al.*, 1999; Orelio *et al.*, 2004). Furthermore, transgenic overexpression of Bcl-2 in combination with Kitl/c-Kit signaling was reported to prevent apoptosis in HSPCs upon *in vitro* cultivation (Domen & Weissman, 2000). Additionally, Bcl-2 transgenic HSPCs are relatively resistant to chemotherapeutic agents and lethal irradiation *in vivo* (Domen & Weissman, 2003; Domen *et al.*, 1998), and show an enhanced repopulation potential *in vivo* as well as an increased clonogenic potential *in vitro* (Domen *et al.*, 2000; Ogilvy *et al.*, 1999).

Since Bcl-2 proteins play an important role in the regulation of HSPC survival, one might assume that their counterparts, the pro-apoptotic BH3-only proteins, are equally important for the maintenance of HSPC homeostasis. Indeed, initial competitive reconstitution experiments performed by our group in collaboration with Verena Labi and Andreas Villunger (Innsbruck Medical University) demonstrated a dramatically increased long-term haematopoietic reconstitution potential of Bim-deficient LSK cells compared to wt LSK cells (Figure 1.7). 16 weeks after transplantation of a 1:1 mixture of Ly5.1$^+$ wt and Ly5.2$^+$ *bim*$^{-/-}$ LSK cells in lethally irradiated Ly5.1 recipient mice almost all mature lymphocytes were derived from the Bim-deficient donor.

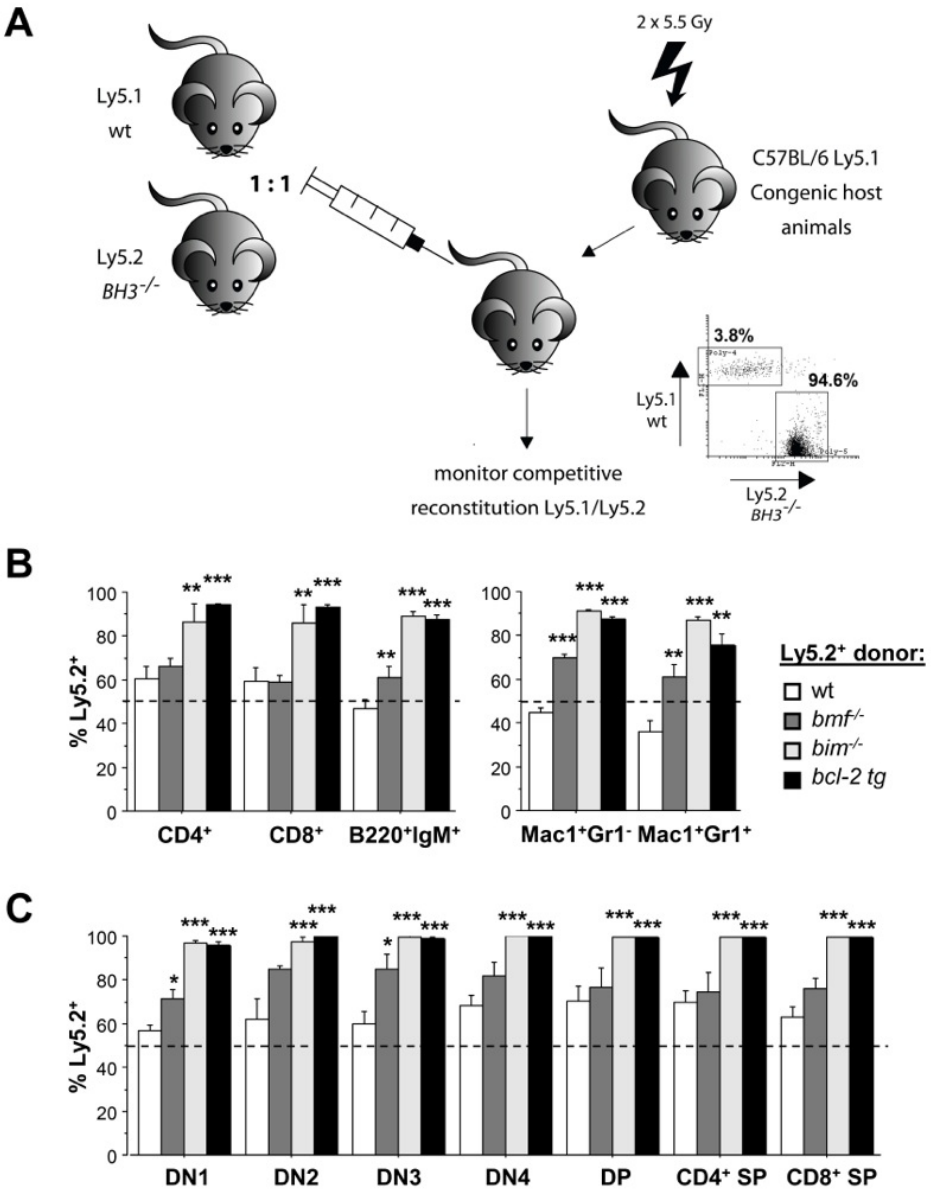

Figure 1.7: Displacement of wt haematopoiesis in wt:*bim*$^{-/-}$ and wt:*bcl-2 tg* BM chimeras - (A) Lethally irradiated Ly5.1^{+} recipient mice were transplanted with 15,000 LSK cells derived from a Ly5.1^{+} wt donor together with 15,000 LSK cells derived from a Ly5.2^{+} wt, *bim*$^{-/-}$, *bmf*$^{-/-}$ or *bcl-2 tg* donor. 16 weeks after competitive transplantation recipient mice were sacrificed and the percentage of Ly5.1^{+} and Ly5.2^{+} cells was determined in different cell subsets via cell surface marker staining and flow cytometry analysis. (B) The spleen was analyzed for T cells (CD4^{+}, CD8^{+}), B cells (B220^{+}IgM^{+}) and myeloid cells (Monocytes: Mac1^{+}Gr1^{-}; Granulocytes: Mac1^{+}Gr1^{+}). (C) The thymus was analyzed for immature thymocyte subsets (DN: CD4^{-}8^{-}; DN1: CD44^{+}25^{-}; DN2: CD44^{+}25^{+}; DN3: CD44^{-}25^{+}; DN4: CD44^{-}25^{-}; DP: CD4^{+}8^{+}) and mature T cells (CD4^{+} SP, CD8^{+} SP). (modified Figure 2 from (Labi *et al.*, 2012)).

The same results were observed upon transgenic Bcl-2 overexpression in LSK cells. Competitive reconstitution experiments with Bmf knockout LSK cells showed similar effects but they were weaker and cell type dependent. Interestingly, Bim also plays an important role in lymphocyte development (reviewed by (Strasser, 2005)) and therefore displacement of mature wt lymphocytes by *bim*$^{-/-}$ LSK cells might be due to accumulation of apoptosis-resistant lymphocytes over time. The fact that also the short-lived granulocytes (Pillay *et al.*, 2010) were mainly derived from the Bim-deficient donor might indicate that wt HSPCs were also displaced by *bim*$^{-/-}$ HSPCs. However, a closer look at the haematopoietic stem cell compartment is needed to confirm this observation (see first part of the result section).

1.4.2 Role of the extrinsic apoptosis pathway in HSPCs

While intrinsic apoptosis is critically involved in HSPC survival, extrinsic apoptosis signaling does not seem to be important for the maintenance of HSPC homeostasis. Murine HSPCs did not express the Fas receptor (Aguila & Weissman, 1996) and Fas-deficient mice showed normal numbers of colony-forming cells within the BM (Schneider *et al.*, 1999). Moreover, the resistance of CD34^{+} cells to death receptor induced apoptosis was suggested to rely on the exclusive expression of caspase-8L, a caspase-8 splice variant with anti-apoptotic function (Mohr *et al.*, 2005). Besides, human CD34^{+} HSPCs isolated from human UCB or adult mobilized peripheral blood were resistant to Fas-mediated apoptosis likely due to a high expression of FLIP (Kim *et al.*, 2002). However, Fas expression was reported to be induced in CD34^{+} HSPCs upon *in vitro* expansion with haematopoietic growth factors (Takenaka *et al.*, 1996) and stimulation with interferon-γ and TNFα (Maciejewski *et al.*, 1995). Induced Fas expression in LSK cells upon TNF-α exposure was associated with a reduced haematopoietic repopulation potential (Bryder *et al.*, 2001). Importantly, a recent study reported that although donor cells homed to the BM after transplantation displayed acute Fas expression, these cells remained highly resistant to Fas-mediated apoptosis (Pearl-Yafe *et al.*, 2007). Furthermore it was reported that TRAIL, a DR4 and DR5 ligand, did not induce apoptosis in haematopoietic stem cells (Gazitt *et al.*, 1999).

1.4.3 Role of other apoptotic and non-apoptotic cell death pathways in HSPCs

Although apoptosis signaling is mostly mediated through the mitochondrial (intrinsic) or the death-receptor (extrinsic) pathway, caspase activation can also be achieved by other mechanisms. One such apoptosis mechanism has been shown to occur in SLAM-HSCs (LSK CD150^{+}CD48^{-}) upon deletion of both c-myc and N-myc (Laurenti *et al.*, 2008). Myc proteins are potent oncogenes involved in a variety of cellular processes such as proliferation, differentation

and apoptosis (Murphy *et al.*, 2005). Laurenti and colleagues discovered, that depletion of c-myc and N-myc in SLAM-HSCs resulted in highly elevated levels of intracellular catalytically active Granzyme B. The highly toxic molecule Granzyme B was located throughout the cytoplasm and caused excessive apoptotic cell death in SLAM-HSCs. These data suggest that stem cell survival strongly depends on Myc activity, which is required to repress Granzyme B (Laurenti *et al.*, 2008). Furthermore, HSPCs have been shown to respond heterogeneously to TNF-α/Fas induced death signaling (Xiao *et al.*, 2011). While TNF-α/Fas induced necroptosis through RIP-1 in one part of HSPCs, unknown factors stimulate caspase-8-dependent type I or II apoptosis in the remaining part. However, TGF-β-activated kinase-1 (Tak1) is able to inhibit both death signals (Xiao *et al.*, 2011).

1.5 Engineering of HSPCs

Manipulation of autologous HSPCs by *ex vivo* gene transfer is an emerging and rapidly growing therapeutic option for various haematological and immunological monogenic diseases. For instance, several cellular dysfunctions associated with the Wiskott-Aldrich syndrom (WAS) have recently been restored by *ex vivo* transduction of $CD34^+$ HSPCs with WAS protein-expressing retroviral vectors and their subsequent transplantation (Boztug *et al.*, 2010). Despite promising results of early clinical trials, an intolerable high risk of leukemogenesis has emerged during the last years which can be explained by random integration of retroviral vectors into the host genome. These serious adverse effects of retroviral therapies call for the need of safer and more efficient technologies for the genetic modification of HSPCs (Naldini, 2011).

First generation retroviral vectors used for genetic HSPC modification contain two functional long terminal repeats (LTRs). However, strong enhancer and promoter elements within the LTRs can induce leukemia by activation of nearby proto-oncogenes (Kohn, 2010). Thus, retroviral self-inactivating (SIN) vectors lacking transcriptional control elements within the 3'LTR have been designed (Yu *et al.*, 1986). Deletions in the 3'LTR are transferred to the 5'LTR upon retroviral replication in the infected cells, leading to transcriptional inactivation of the provirus (Yee *et al.*, 1987; Yu *et al.*, 1986). Additional inclusion of the post-transcriptional regulatory element (PRE) of the woodchuck hepatitis virus enabled production of highly concentrated virus suitable for clinical application (Kraunus *et al.*, 2004). Moreover, weaker specific cellular promoters for transgene expression reduced the risk for activation of neighboring proto-oncogenes (Zychlinski *et al.*, 2008).

The use of lentiviruses, a subclass of retroviruses may be advantageous for gene delivery. Lentiviruses have been shown to be more efficient in transferring genes into human HSPCs thus requiring shorter *ex vivo* culture time for transduction resulting in an increased engraftment (Mazurier *et al.*, 2004). Furthermore, the lentiviral vector simian immunodeficiency virus (SIV) was discovered to integrate predominantly along transcription units, whereas the murine leukemia virus (MLV)-derived retroviral vector preferred promoter regions for integration, suggesting a safety advantage of lentiviral vectors (Hematti *et al.*, 2004). Plus in contrast to retroviruses, lentiviral expression of a candidate gene does not require nuclear envelop breakdown (cell proliferation), thus genes can be expressed in quiescent cells (Lewis & Emerman, 1994).

Direct gene correction using homologous recombination (HR) might further reduce genotoxicity. Targeted transgen addition in human naïve haematopoietic stem cells was achieved by integrase-defective lentiviral vector-mediated delivery of zinc-finger nucleases (ZFNs) together with homologous template DNA for gene correction (Lombardo *et al.*, 2007). ZFNs stimulate endogenous homologous recombination by introducing DNA-double strand brakes in target genes (Porteus & Carroll, 2005). Furthermore, nucleofection of HSPCs with engineered ZFNs was reported to mediate gene disruption while maintaining their repopulation ability (Holt *et al.*, 2010). Although the use of ZFNs seems to be very promising for targeted gene delivery, expression of ZFNs can lead to cell death caused by extensive DNA damage signaling or off-target cleavage (Porteus & Carroll, 2005).

Besides the described permanent modification of HSPCs commonly used for gene therapy, transient expression of molecules is required for some therapeutic issues. For transient gene expression, adenoviral vectors can be used. In contrast to lentiviral mediated gene transfer, adenoviral vectors do not integrate into the genome of the host. During proliferation adenoviral vectors are split amongst the daughter cells and finally are lost, thereby enabling temporarily expression of the exogenous gene (Järås *et al.*, 2007). However, conventional Adenovirus seroptype 5 (Ad5)-based vectors bind to coxsackie and adenovirus receptors (CAR), which are not sufficiently expressed on $CD34^+$ cells (Bergelson *et al.*, 1997; Rebel *et al.*, 2000). To circumvent CAR paucity, fiber-modified adenoviral vectors such as Ad5/F35 chimeric vectors, utilizing the ubiquitously expressed CD46 as a cellular receptor, have been developed (Gaggar *et al.*, 2003; Nilsson *et al.*, 2004a). Ad5/F35 vectors mediate efficient transient gene transfer into dividing and nondividing $CD34^+$ cells (Nilsson *et al.*, 2004a).

1.6 Aim of this study

Recently, our group in collaboration with Verena Labi and Andreas Villunger (Innsbruck Medical University) found that loss of Bim or Bmf in murine HSPCs dramatically increases long-term haematopoietic reconstitution (Figure 1.7). However, it was unclear whether this effect is caused by an increased survival of HSPCs during transplantation or whether it is due to an accumulation of apoptosis-deficient mature lymphatic and myeloid cells over time.

Therefore, the aim of the first part of this study was to better characterize the role of Bim and Bmf during different stages of haematopoietic reconstitution with special focus on the survival of HSPCs during early engraftment. We hypothesized that Bim and Bmf might be responsible for apoptotic cell death of HSPCs triggered in the absence of supportive survival signals (i.e. cytokines), which are normally provided by the stem cell niche.

The second aim was to analyze whether our findings could be used therapeutically for the improvement of HSCT. Increasing the resistance of donor HSPCs against transplantation-associated cell stress might be a new therapeutic approach to enhance HSCT efficiency and accelerate haematopoietic regeneration. One of the main clinical challenges in the context of haematopoietic stem cell transplantation is the risk of delayed engraftment, which is often associated with infection-related mortality. Delayed engraftment is suggested to correlate directly with the number of transplanted HSPCs (Demirer *et al.*, 2009). Thus, in the second part of this study we investigated whether lentiviral mediated downregulation of BIM or BMF renders human HSPCs more potent during their engraftment into a xenograft transplantation model.

Finally, in order to circumvent the possible risk of tumor formation upon transplantation of apoptosis resistant HSPCs, transient apoptosis inhibition in human HSPCs was of interest for this study.

2

Materials & Methods

2.1 Material

2.1.1 Cells, animals, cell culture reagents and material

Primary cells and cell lines	
LSK cells	lineage$^-$sca1$^+$c-kit$^+$ cells, isolated from BM of C57BL/6 mice
CD34$^+$ cells	provided by Department of Obstetrics and Gynecology, University Hospital Freiburg - informed consent given by parents - ethical approval by ethic committee
BL40 cells	P. Daniel, Max-Delbrck-Center, Berlin
LCL5 cells	P. Daniel, Max-Delbrck-Center, Berlin
HEK 293A cells	S. Geley, Biocenter, Innsbruck
HEK 293T cells	H. Pahl, Center for Clinical Research, Freiburg
HeLa cells	C. Flotho, Pediatrics and Adolescent Medicine, Freiburg
Mice	
C57BL/6 mice	Animal Facility ZKF, Freiburg
bad$^{-/-}$ mice	A. Villunger, Biocenter, Innsbruck
bim$^{-/-}$ mice	A. Villunger, Biocenter, Innsbruck
noxa$^{-/-}$ mice	A. Villunger, Biocenter, Innsbruck
puma$^{-/-}$ mice	A. Villunger, Biocenter, Innsbruck
bmf$^{-/-}$ mice	A. Villunger, Biocenter, Innsbruck
vav-bcl-2 tg mice	A. Villunger, Biocenter, Innsbruck
rag2$^{-/-}\gamma c^{-/-}$ mice	H. Eibel, CCI, Freiburg
Cytokines	All recombinant human and murine Cytokines were purchased from Immunotools or R&D systems
Cell culture reagents	
StemPro®-34 serum-free medium (SFM)	Invitrogen
StemPro®-Nutrient Supplement (40X)	Invitrogen

Fetal bovine serum (FBS) E.S. Cell Qualified US origin	Invitrogen
Penicillin/Streptomycin (P/S)	Invitrogen
L-Glutamine	Invitrogen
Bovine serum albumin(BSA)	Sigma-Aldrich
EDTA-Solution	Sigma-Aldrich
MethoCult SF H4436	Stemcell Technologies
RPMI 1640 medium	Invitrogen
DMEM	Invitrogen
IMDM	Invitrogen
DPBS	Invitrogen
Fetal calf serum (FCS)	Biochrom AG
0,25% Trypsin	Invitrogen
0,05% Trypsin-EDTA	Invitrogen
Trypan blue	Invitrogen
DMSO	Sigma-Aldrich
Aqua sterile	B.Braun
ProFection Mammalian Transfection Kit	Promega
BoosterExpress^{TM} Reagent Kit	Genlantis
Biocoll Separating Solution	Biochrome

2.1.2 Oligonucleotides

Oligonucleotides were purchased from Eurofins.

qRT-PCR

Actin (m)	forward	5'-ACTGGGACGACATGGAGAAG-3'
	reverse	5'-GGGGTGTTGAAGGTCTCAAA-3'
Bad (m)	forward	5'-GGACTTATCAGCCGAAGCAG-3'
	reverse	5'-GCTCAAACTCTGGGATCTGG-3'
Bcl-2 (m)	forward	5'-CTGGCATCTTCTCCTTCCAG-3'
	reverse	5'-GACGGTAGCGACGAGAGAAG-3'
Bcl-x_L (m)	forward	5'-TTCGGGATGGAGTAAACTGG-3'
	reverse	5'-TGGATCCAAGGCTCTAGGTG-3'
Bim (m)	forward	5'-GAGATACGGATTGCACAGGA-3'
	reverse	5'-TCAGCCTCGCGGTAATCATT-3'
Bmf (m)	forward	5'-CCCATAAGCCAGGAAGACAA-3'
	reverse	5'-AGGGAGAGGAAGCCTGTAGC-3'
Mcl-1 (m)	forward	5'-TAACAAACTGGGGCAGGATT-3'
	reverse	5'-GTCCCGTTTCGTCCTTACAA-3'
Noxa (m)	forward	5'-CCCACTCCTGGGAAAGTACA-3'
	reverse	5'-AATCCCTTCAGCCCTTGATT-3'
Puma (m)	forward	5'-CAAGAAGAGCAGCATCGACA-3'
	reverse	5'-TAGTTGGGCTCCATTTCTGG-3'
18S (h)	forward	5'-TCAAGAACGAAAGTCGGAGG-3'
	reverse	5'-GGACATCTAAGGGCATCACA-3'
BimEL (h)	forward	5'-TGACACAGACAGGAGCCCAGC-3'
	reverse	5'-CGCCGCAACTCTTGGGCGAT-3'
BMF (h)	forward	5'-GTGCTCGTCACGCTGGACCC-3'

	reverse	5'-GGTCACCGGCTCCCCATCCT-3'
PCR		
BCL-2 (h)	forward (*EcoR*I)	5'-CCGGAATTCACCATGGCGCACGCTGGGAGAACA-3'
	reverse (*Not*I)	5'-ATTTGCGGCCGCTTTATCACTTGTGGCCCAGATAGGCA-3'
BCL-XL (h)	forward (*EcoR*I)	5'-CCGGAATTCACCATGTCTCAGAGCAACCGGGAG-3'
	reverse (*Not*I)	5'-ATTTGCGGCCGCTTTATCATTTCCGACTGAAGAGTGAG-3'
RNAi		
(pLeGO-hU6)		
BIM shRNA (h)	top	5'-AACCCCTGATGTAAGTTCTGAGTGTGTTCAAGAGA CACACTCAGAACTTACATCATTTTTTC-3'
	bottom	5'-TCGAGAAAAAATGATGTAAGTTCTGAGTGTG TCTCTTGAACACACTCAGAACTTACATCAGGGGTT-3'
BMF shRNA (h)	top	5'-AACCCCTCAGCCGACTTCAGCTCTTTTCAAGAGA AAGAGCTGAAGTCGGCTGATTTTTTC-3'
	bottom	5'-TCGAGAAAAAATCAGCCGACTTCAGCTCTT TCTCTTGAAAAGAGCTGAAGTCGGCTGAGGGGTT-3'
Luci shRNA	top	5'-AACCCCCGCTGAGTACTTCGAAATGTCTTCAAGAGA GACATTTCGAAGTACTCAGCGTTTTTTC-3'
	bottom	5'-TCGAGAAAAAACGCTGAGTACTTCGAAATGTC TCTCTTGAAGACATTTCGAAGTACTCAGCGGGGGTT-3'
(pENTR-THT)		
BIM shRNA (h)	top	5'-GATCCCCTGATGTAAGTTCTGAGTGTGTTCAAGAGA CACACTCAGAACTTACATCATTTTTGGAAA-3'
	bottom	5'-AGCTTTTCCAAAAATGATGTAAGTTCTGAGTGTG TCTCTTGAACACACTCAGAACTTACATCAGGG-3'
BMF shRNA (h)	top	5'-GATCCCCTCAGCCGACTTCAGCTCTTTTCAAGAGA AAGAGCTGAAGTCGGCTGATTTTTGGAAA-3'
	bottom	5'-AGCTTTTCCAAAAATCAGCCGACTTCAGCTCTT TCTCTTGAAAAGAGCTGAAGTCGGCTGAGGG-3'
Sequencing		
pLeGO-hU6	forward	5'-ATATATCTTGTGGAAAGGACG-3'
	reverse	5'-TGGCCCAACGTTAGCTATTTTCAT-3'
pLeGO-iG	forward	5'-CCCTGCGCCTTATTTGAATTAACC-3'
	reverse	5'-GCTTCGGCCAGTAACGTTAGG-3'
pENTR-THT	forward	5'-CTGCAGGAATTCGAACGCTGACG-3'
	reverse	5'-GGGATATCAGCTGGATGGC-3'

2.1.3 DNA cloning

Plasmids	
pLeGO-hU6 (pGhU6)	H. Pahl, Center for Clinical Research, Freiburg
pLeGO-iG (piG)	H. Pahl, Center for Clinical Research, Freiburg
vsv.g-envelope plasmid	H. Pahl, Center for Clinical Research, Freiburg
gag/pol plasmid	H. Pahl, Center for Clinical Research,
Freiburg pENTR-THT III	S. Geley, Biocenter, Innsbruck
pAdTrack-DEST	S. Geley, Biocenter, Innsbruck
pAdEasy-1-F35	X. Fan, Lund University, Sweden
pAdEasy-1-F35 CMV-BCL-XL	S. Geley, Biocenter, Innsbruck
Bacteria	
E.coli DH5α	H. Pahl, Center for Clinical Research,
Freiburg *E.coli* Mach1	S. Geley, Biocenter, Innsbruck
E.coli BJ5183	S. Geley, Biocenter, Innsbruck
Enzymes and reagents	
Agarose	Serva
1 kb DNA ladder	Invitrogen
6X Loading Dye	Thermo Scientific (Fermentas)
QIAquick® Gel Extraction Kit	Qiagen
Alkaline phosphatase (calf intestinal phosphatase)	Roche Biochemicals
T4 Polynucleotide kinase	Promega
T4 DNA Ligase	Promega
Rapid DNA ligation kit	Roche Biochemicals
Gateway LR Clonase II Enzyme Mix	Invitrogen
GoTaq® Flexi DNA Polymerase	Promega
Pfu DNA Polymerase	Thermo Scientific
ATP	Invitrogen
LB-Medium	Roth
LB-Agar	Roth
Ampicillin	Sigma-Aldrich
Kanamycin	Sigma-Aldrich
Gentamicin	Sigma-Aldrich
SOC Medium	Invitrogen
FastPlasmid Mini Kit	5Prime
Plasmid Mini Kit	Qiagen
Plasmid Maxi Kit	Qiagen

All other enzymes were purchased from Thermo Scientific (Fermentas) or New England Biolabs.

2.1.4 RNA analysis

Quick RNA Micro Prep	Zymo Research

qRT-PCR

QuantiTect Reverse Transcription Kit	Qiagen
Absolute Q-PCR SYBR Green Mix	Thermo Scientific
96 well Reaction Plate (Standard)	Peqlab
Absolute Q-PCR Seal	Thermo Scientific

RT-MLPA

M-MLV Reverse Transcriptase	Promega
SALSA RT-MLPA Kit Apoptosis mRNA	MRC-Holland MLPA
DEPC	Sigma-Aldrich
HiDi Formamide	Applied Biosystem
Gene Scan 500 Rox Size Standard	Applied Biosystem

2.1.5 Antibodies

Antibodies for Western blot analysis		
Monoclonal rat anti-Bim S/EL/L antibody (3C5)	1:200	Enzo Life Sciences
Polyclonal rabbit anti-Puma antibody	1:1000	ProSci Incorporated
Monoclonal rat anti-Bmf antibody (9G10)	1:1000	Enzo Life Sciences
Monoclonal mouse anti-Bcl-2 antibody (Bcl-2/100)	1:1000	Ancell
Monoclonal mouse anti- Bcl-x_L antibody (44/Bcl-x)	1:500	BD Biosciences
Monoclonal mouse anti-β-Actin antibody (AC-15)	1:10000	Sigma-Aldrich
goat anti-mouse IgG-HRP	1:5000	Santa Cruz Biotechnology
goat anti-rabbit IgG-HRP	1:5000	Santa Cruz Biotechnology
goat anti-rat IgG-HRP	1:5000	Santa Cruz Biotechnology

Antibodies for cell surface staining conjugated to FITC, PE, Biotin or APC used for flow cytometry or MACS and FACS-based cell sorting	
Lineage Cell Depletion Kit	Miltenyi Biotec
anti-mouse CD45 antibody (30-F11)	BD Biosciences
anti-mouse CD45.1 (Ly5.1) antibody (A20)	Biolegend
anti-mouse CD45.2 (Ly5.2) antibody (104)	Biolegend
anti-mouse c-kit antibody (2B8)	eBioscience
anti-mouse Sca-1 antibody (D7)	Biolegend
anti-mouse CD150 antibody (TC15-12F12.2)	
CD34 Microbead Kit, human	Miltenyi Biotec
anti-human CD45 antibody (HI30)	BD Biosciences
anti-human CD33 antibody (WM53)	BD Biosciences
anti-human CD19 antibody (HIB19)	BD Biosciences

anti-human CD3 antibody (SK7)	BD Biosciences
anti-human CD34 antibody (AC136)	Miltenyi Biotec
anti-human CD38 antibody (IB6)	Miltenyi Biotec

2.1.6 Protein analysis

Cell lysis buffer (10x)	Cell signaling technology
phenylmethylsulfonyl fluoride (PMSF)	Sigma-Aldrich
ammonium persulfate (APS)	Sigma-Aldrich
Polyacrylamid Rotiphoese 30	Roth
N,N,N',N'-tetramethylethane-1,2-diamine (TEMED)	Merk
sodium dodecyl sulfate (SDS)	Serva
1,4-Dithiothreitol (DTT)	Roth
Bromophenolblue	Sigma-Aldrich
Trizma base	Sigma-Aldrich
Tween 20	Sigma-Aldrich
Glycine	AppliChem
Spectra Multicolor Broad Range Protein	Fermentas
Nonfat dried milk powder	AppliChem
DC™ protein assay kit	Bio-Rad
Pure Nitrocellulose Membrane (0,2 μm)	Bio-Rad
ECL Plus Western Blotting Detection System	Amersham
ECL Advance Western Blotting Detection kit	Amersham
High performance chemiluminescencefilm	Amersham

2.1.7 Flow cytometry analysis

Streptavidin-Phycoerythrin/Cyanine dye 7 (PE/Cy7)	Biolegend
7-Amino-Actinomycin D (7-AAD)	Sigma-Aldrich
Alexa Fluor® 647-conjugated Annexin V	Biolegend
FITC-conjugated Annexin V	BD Bioscience
APC-conjugated anti Ki-67 antibody (B56)	BD Bioscience
4',6-diamidino-2-phenylindole (DAPI)	Sigma-Aldrich
BD™ Phosflow Fix Buffer I	BD Bioscience
BD™ Phosflow Perm/Wash Buffer I	BD Bioscience

2.1.8 Further chemicals and reagents

Etoposide	Pediatrics and Adolescent Medicine hospital pharmacy, Freiburg
Treosulfan	Pediatrics and Adolescent Medicine hospital pharmacy, Freiburg
Tunicamycin	Sigma-Aldrich

Taxol	Pediatrics and Adolescent Medicine hospital pharmacy, Freiburg
Vivapure Adenopack 20	Sartorius Stedim Biotec
DNase I	Roche Applied Science
Collagenase D from Clostridium histolyticum	Roche Applied Science
Ethanol	Merck
Methanol	Sigma-Aldrich
Glacial Acetic Acid	Merck
Glycerol	Roth
HEPES	Sigma-Aldrich
NaCl	VWR
KCl	Roth
$MgSO_4$	Roth
$MgCl_2$	Roth
tryptone	Sigma-Aldrich
yeast extract	Sigma-Aldrich
$MnCl_2$	Sigma-Aldrich
PIPES	Roth
NaN_3	Sigma-Aldrich
Phenol/Chloroform/Isoamylalcohol	Sigma-Aldrich
HCl	Roth
NaOH	Merck
$CaCl_2$	Sigma-Aldrich
$NaHCO_3$	Merck
NH_4Cl	Roth

2.1.9 Equipment and plastic ware

All plastic ware was purchased from BD Falcon, except listed below.

Cord blood collection set	MacoPharma
MS-Columns	Miltenyi Biotec
LS-Columns	Miltenyi Biotec
Rotilabo-Syringefilter, PVDF, sterile (0,22 μm)	Roche Applied Science
Vacuum Filtration System (0,2 μm)	VWR
145x20mm Cellstar® cell culture dish	Greiner

2.1.10 Hardware and Software

Hardware

Milli-Q®	Merck
Axiovert 40C microscope	Zeiss
Fluorescence microscope	Zeiss
Flow (Hera Safe)	Heraeus Instruments
Incubator Hera cell 240	Heraeus Instruments
FACSCalibur	BD Biosciences
BD LSRFortessa™ cell analyzer	BD Bioscience
MoFlo® Astrios™ cell sorter	Beckman Coulter
Agilent Bioanalyzer 2100	Agilent Technologies
ABI-3100 16 capillary sequencer	Applied Biosystems
MACS Multi Stand	Miltenyi Biotec
MiniMACS™ Separator	Miltenyi Biotec
MidiMACS™ Separator	Miltenyi Biotech
Pipettes	Eppendorf
Hamilton syringe 710 lT 100 µl	Chromatographie Service
Hamilton KF-needles (Ga30/40mm/pst.4)	Chromatographie Service

Software

StatView 5.0.1	SAS Institute Inc.
Cyflogic 1.2.1	CyFlo Ltd.
GeneMapper® 4.1	Applied Biosystems
Plasm 2.1.5.30	biofreesoftware
Project ROME 0.9.0	Adobe
GraphPad PRISM® 5.0	GraphPad Software, Inc.

2.2 Methods

2.2.1 Methods in cell biology

2.2.1.1 Cryopreservation and thawing of cells

For long term preservation cells were collected, resuspended in FCS or ES-FBS ($CD34^+$ cells) supplemented with 10% DMSO and slowly frozen to -80°C in an isopropyl alcohol containing freezing container. After three days cells were transferred to liquid nitrogen at -196°C.
When required, cells were quickly thawed at 37°C and washed once in appropriate medium. Cryopreserved cord blood (CB) $CD34^+$ cells were thawed and washed twice in complete stem cell medium (StemPro®-34 serum-free medium (SFM), 1XStemPro®-Nutrient Supplement, 1% L-Glutamine, 1% P/S) supplemented with 20% ES-FBS for the first washing step and with 10% ES-FBS for the second time.

2.2.1.2 Mycoplasma test

Cell lines were tested for *Mycoplasma* contamination using the Venor®*GeM* Advance kit based on specific PCR-amplification of the highly conserved 16S rRNA region within the mycoplasma genome. *Mycoplasma* detection was performed according to the manufacturer's instructions. In brief, 100 µl cell culture supernatant was heat-inactivated, cleared from cellular debris by centrifugation and subsequently used for PCR. Contamination of cell lines with *Mycoplasma* is indicated by a 270 bp band in agarose gel electrophoresis.

2.2.1.3 Cultivation of cell lines

All cells were cultured at 37°C and 5% CO_2 . Human cervical cancer HeLa and human embryonic kidney 293T (HEK 293T) cells were cultured in DMEM high glucose with sodium pyruvate supplemented with 10% FCS, 1% penicillin/streptomycin (P/S) and 1 mM L-Glutamine. HEK 293A cells were maintained in IMDM supplemented with 10% FCS and 1% P/S. The Burkitt lymphoma cell lines BL40 and LCL5 were cultured in RPMI medium contianing 10% FCS and 1% P/S.

2.2.2 Methods in stem cell biology

2.2.2.1 Isolation and cultivation of murine HSPCs: LSK cells

Bone marrow (BM) of 2 femurs and 2 tibiae was isolated by flushing bones twice with PBS. To remove erythrocytes, cells were incubated for 10 min with red cell lysis buffer containing 0.15 M NH_4Cl , 0.01 M $NaHCO_3$ and 0.001 M EDTA and washed once with PBS. For magnetic

cell seperation cells were incubated for 10 min with a Biotin-labeled lineage-marker specific antibody cocktail followed by an incubation for 15 min with anti-Biotin-MicroBeads. Cells were washed, resuspended and put on a MACS column placed in a MACS magnet. Unlabeled cells (lineage$^-$ cells) which were not retained in the column, were collected and stained with antibodies for Sca-1 and c-Kit (1:50 dilution). After washing, cells were sorted for sca-1$^+$ and c-kit$^+$ cells with an MoFlo® Astrios™ cell sorter. All steps were performed at 4°C in MACS buffer (PBS, 0.5% BSA, 2 mM EDTA, 1% P/S) or in PBS/10% FCS (before and after sorting, respectively). Lineage$^-$sca1$^+$c-kit$^+$ (LSK) cells were cultured in IMDM supplemented with 10% FCS, 1% P/S and recombinant murine (rm) TPO, SCF and Flt3L (100 ng/ml each) in 96-well flat bottom cell culture plates.

2.2.2.2 Isolation and cultivation of human HSPCs: CD34$^+$ cells

Human umbilical cord blood (CB) was collected with a sterile collection set immediately after caesarean section. Using density gradient centrifugation (Ficoll) mononuclear cells were separated from erythrocytes, granulocytes and dead cells. In brief, cord blood was mixed with an equal amount of PBS/2 mM EDTA and layered carefully above Ficoll reagent. After centrifugation a cloudy mono-nuclear cell-containing interphase became visible between plasma and Ficoll reagent. Interphase was collected and washed with PBS/2 mM EDTA, and cells were resuspended in PBS/2 mM EDTA and centrifuged for 15 min at 200 g in order to deplete thrombocytes. Mononuclear cells were enriched for CD34$^+$ cells with MACS cell separation technology. To this end, cells were labeled with magnetically labeled anti-CD34-antibodies. A magnetic field built in magnetic columns placed into a MACS™ Separator separated labeled from unlabeled cells. CD34$^+$ cells were obtained after removing the magnetic column from the MACS™ Separator by flushing the column once with MACS buffer (PBS, 0.5% BSA, 2 mM EDTA, 1% P/S).

CD34$^+$ cells were cultured at a density of 500,000 cells/ml in a 96-well flat bottom cell culture plate in StemPro®-34 serum-free medium (SFM) supplemented with 1X StemPro®-Nutrient Supplement, 10% ES-FBS, 1% L-Glutamine, 1% P/S and recombinant human (rh) TPO (10 ng/ml), rh SCF, rh Flt3L and IL-6 (100 ng/ml each) unless otherwise indicated.

2.2.2.3 Colony forming unit (CFU) assay

250 GFP$^+$CD34$^+$ cells were plated on a semi-solid medium containing SCF, GM-CSF, G-CSF, IL3, IL5 and EPO (Methocult®) and cultured at 37°C for 11 days. Quantitative determination of different types of colonies, based on typical morphological features was performed by light microscopy. After 14 days of culture cells were washed and replated into secondary Methocult®

plates. Part of the cells was stained after 14 and 31 days with Annexin V and 7-AAD as described in 2.2.6.2 to determine the amount of apoptotic cells by flow cytometry. Cells were treated accordingly after 17 days of culture within the secondary plate.

2.2.2.4 Transplantation assays

For competitive reconstitution experiments, Ly5.1$^+$C57BL/6 recipient mice were lethally irradiated (9.5 Gy). 6-8 h later mice were transplanted with 15,000 Ly5.1$^+$ LSK cells and 15,000 Ly5.2$^+$ LSK cells derived from wt, *bim*$^{-/-}$, *bmf*$^{-/-}$ or *vav-bcl-2 tg* mice. LSK cells were transplanted intravenously (i.v.) in a final volume of 200 µl. After 10 days or 16 weeks, mice were sacrificed and BM was isolated by flushing femurs with 3 ml PBS/10% FCS. Well resuspended BM was analyzed for Ly5.2$^+$ LSK cells and LSK CD150$^+$ cells by flow cytometry as described in 2.2.6.1.

Limiting dilution assays were performed by using decreasing numbers of Ly5.2$^+$ total BM cells which were transplanted together with 200,000 Ly5.1$^+$ total BM cells. Thereby, 10,000 BM cells were shown to be limiting for successful reconstitution as defined by Akala et al ($>$1% Ly5.2$^+$ myeloid and $>$1% Ly5.2$^+$ lymphatic splenic cells indicated successful engraftment (Akala *et al.*, 2008)). Therefore, all further experiments were performed with 10,000 Ly5.2$^+$ donor cells. 14 weeks after transplantation mice were sacrificed, BM was isolated and the percentage of Ly5.2$^+$ cells was analyzed by flow cytometry.

2.2.2.5 Humanized xenograft mouse model

Xenograft experiments were performed according to the protocol published by Traggiai et al (Traggiai *et al.*, 2004). 1-4 day old *rag2*$^{-/-}\gamma c^{-/-}$ mice which lack B, T and functional NK cells due to double-deficiency for rag2 and the common y-chain, were irradiated with 2.5 Gy. After 6-8 h the progeny cells of 10^5 human CD34$^+$ or lentivirally transduced human CD34$^+$ cells were injected intrahepatically in a final volume of 25 µl. Animals were sacrificed 8 weeks after transplantation. Liver, spleen, BM and thymus were removed and processed on ice. Liver tissue was cut into small pieces and digested with collagenase (1 mg/ml) and DNase (50 µg/ml) for 30 min at 37°C. Afterwards cells were strained through a 70 µm mesh and washed once. Mononuclear cells were isolated by density gradient centrifugation (Ficoll). Femurs were flushed with 3 ml PBS/10% FCS and BM was resuspended well. Spleen and thymus were filtered through a 70 µm mesh and afterwards a 40µm mesh to get single cell suspensions. BM, spleen and thymus were incubated for 10 min at 37°C with red cell lysis buffer (0.15 M NH_4Cl , 0.01 M $NaHCO_3$ and 0.001 M EDTA) and washed once with PBS. Single cell suspensions were stained as described in 2.2.6.1.

2.2.2.6 Homing assay

Homing describes the crossing of haematopoietic stem cells from blood into BM through the endothelial barrier (Lapidot *et al.*, 2005). In BM, haematopoietic stem cells move to the endosteum where the bona fide stem cell niche is located. For homing analysis 30,000 freshly isolated Ly5.2$^+$ LSK cells (wt or *bim*$^{-/-}$) were injected into lethally irradiated Ly5.1$^+$ recipient mice. 15 h after transplantation, mice were sacrificed according to the protocol published by Williams and Nilsson (Williams *et al.*, 2009). 2 femurs, 2 tibiae and 2 iliac crests containing about 30% of the total BM were isolated. First, the central BM was obtained by flushing bones with PBS/10% FCS. For isolating endosteal cells the remaining empty bones were pestled, washed with PBS/10%FCS and digested in DMEM/10% FCS with 3 mg/ml collagenase for 40 min at 37°C under on and off vortexing. Cells were pooled in PBS and filtered to remove bone particles. Mononuclear cells were isolated by density gradient centrifugation (Ficoll). Finally, the percentage of viable (7-AAD negativ) Ly5.1$^+$ and Ly5.2$^+$ cells was analyzed in both fractions obtained (central BM and endosteal BM).

2.2.3 Methods in molecular biology

2.2.3.1 Polymerase chain reaction (PCR)

Polymerase chain reaction (PCR) is a method for exponential amplification of specific DNA sequences. A PCR reaction starts with DNA denaturation at 95°C to form DNA single strands. Next, short oligonucleotides (primers) with complementary sequences to the DNA sequence of interest hybridize to these single strands (annealing). Optimal annealing temperature which is dependent on the length and sequence of the primers is determined using gradient PCR. Finally, a thermostable DNA polymerase elongates annealed primers from the 3' end by adding new deoxinucleotides. Optimal temperatures for polymerase reaction range between 68 and 72°C. After several rounds of amplification PCR products are separated on an ethidium bromide containing agarose gel and made visible by exposure to ultraviolet light.

PCR was used for the amplification of BCL-2 and BCL-XL cDNAs using pcDNA3-hBCL-2 or pcDNA3-hBCL-XL (kindly provided C. Borner, Institute for Molecular Medicine and Cell Research Freiburg) as a template. PCR was performed using a proofreading *Pfu* polymerase with the PCR program shown below. Primers for BCL-XL amplification were annealed at 54°C and for BCL-2 amplification at 57°C.

program		cycles	temperature [°C]	Time
initial denaturation		1	94	3 min
amplification		35		
	denaturation		94	30 s
	annealing		54/57	30 s
	extension		72	1 min 20 s
final extension		1	72	3 min
cooling		4	forever	

Furthermore, individual cloning steps were controlled by using colony PCR. Single colonies resuspended in sterile water served as templates for PCR amplification. A plasmid without insert served as positive and sterile water as negative controls, respectively. PCR was performed according to the manufacturer's instruction (Promega Kit M8305) using a GoTaq® DNA polymerase. Primers used for amplification of the inserts cloned into pLeGO-hU6 or pLeGO-iG are listed in 2.1.2 and are the same as used for sequencing. pLeG0-hU6 primer were annealed at 60 °C for 50 s and pLeGO-iG primer at 51°C for 50 s with an subsequent extension at 72°C for 1 min or 1 min 30 s respectively.

2.2.3.2 Agarose gel electrophoresis

DNA fragments resulting from PCR or digestion with restriction enzymes were analyzed by agarose gel electrophoresis. Negatively charged DNA molecules move in an electrical field through the pores of the gel matrix towards the anode, and smaller fragments move faster than larger ones. By using the DNA intercalating fluorescent dye ethidium bromide separated DNA fragments can be visualized after exposure to ultraviolet light. Molecular weight size marker enable size determination of separated DNA fragments. For preparation of agarose gels Tris-Acetate (TAE) buffer (40 mM Tris Base, 1 mM EDTA, 20 mM Glacial Acetic Acid) was boiled with 1 to 2% agarose depending on the size of the DNA fragments, shortly before gelation ethidium bromide was added. Samples mixed with DNA loading dye were run together with an appropriate size standard on the gel at 90 V.

2.2.3.3 DNA purification and concentration determination

DNA fragments such as linearized vectors were extracted from the agarose gel using the QIAquick® Gel Extraction Kit according to the manufacturer's instructions. Briefly, the DNA fragment was cut out of the agarose gel, dissolved and purified based on adsorption of negatively charged DNA molecules to positively charged silica particle in high-salt buffer. DNA was eluted from silica particles containing columns using low-salt conditions. Purified linearized vectors were processed as described in the DNA cloning section.

Furthermore, phenol-based extraction and subsequent precipitation in ethanol was used to purify DNA prior to electroporation (described in 2.2.3.8). For that purpose dissolved DNA was vigorously mixed with an equal volume of phenol:chloroform:isoamylalcohol (25:24:1) followed by phase separation using centrifugation. The upper aqueous phase containing DNA was removed from the phenol phase containing proteins (lower polarity) and washed once with chloroform/isoamylalcohol in order to eliminate phenol. DNA was precipitated from the aqueous phase by adding 3 M NaOAc pH 5.2 and ethanol followed by vigorous vortexing and centrifugation for 20 min at 4°C. The DNA pellet was washed once with 70% ethanol, air-dried and finally resuspended in an appropriate buffer or in DEPC-water. DNA concentration and purity were determined with a NanoDrop Spectrometer.

2.2.3.4 DNA cloning

For gene knockdown (i.e. Luciferase, BIM or BMF), oligonucleotides containing a 19-21 bp shRNA, a nine-nucleotide loop (TTC AAG AGA), a polymerase III-termination sequence (5-6 thymidins) and vector compatible cohesive ends were designed. Complementary oligonucleotides were annealed and phosphorylated using T4 polynucleotidkinase. For gene overexpression, BCL-2 or BCL-XL cDNAs were PCR-amplified from pcDNA3-hBCL-XL or pcDNA3-hBCL-2 as described in 2.2.3.1. Primers designed for the amplification of BCL-2 or BCL-XL contained vector compatible restrictions sites, and a Kozak consensus sequence for efficient initiation of eukaryotic translation was added to the forward primer (Kozak *et al.*, 1987). Vectors were digested with specific restriction enzymes and dephosphorylated using Calf Intestinal Alkaline Phosphatase (CIP) to prevent vector religation. After agarose gel electrophoresis and extraction 2.2.3.3 vectors were ligated (T4 Ligase) with annealed oligonucleotides or digested cDNAs.

2.2.3.5 Lentiviral backbone plasmid cloning

For stable knockdown of BIM and BMF in human $CD34^+$ cells the lentiviral short hairpin expression vector pLeGOhU6-G (Figure 2.1) was used (Roelz *et al.*, 2010). This vector harbors a human U6 promotor for shRNA expression as well as a GFP marker under the control of a SFFV promoter. Annealed oligonucleotides were cloned into the *Hpa*I-*Xho*I site of pLeGO-hU6-G. pLeGO-hU6-G expressing shRNA sequence targeting Luciferase, which is absent in human cells, served as a negative control as well as the empty vector pLeGO-hU6-G. BCL-2 and BCL-XL were overexpressed in pLeGO-iG (Figure 2.1) vectors. PCR amplicons were cloned into the *EcoR*I-*Not*I site of the pLeGO-iG vector under control of the SFFV promotor. The marker gene GFP was expressed by an internal ribosome entry site (IRES). Lentivirus production was

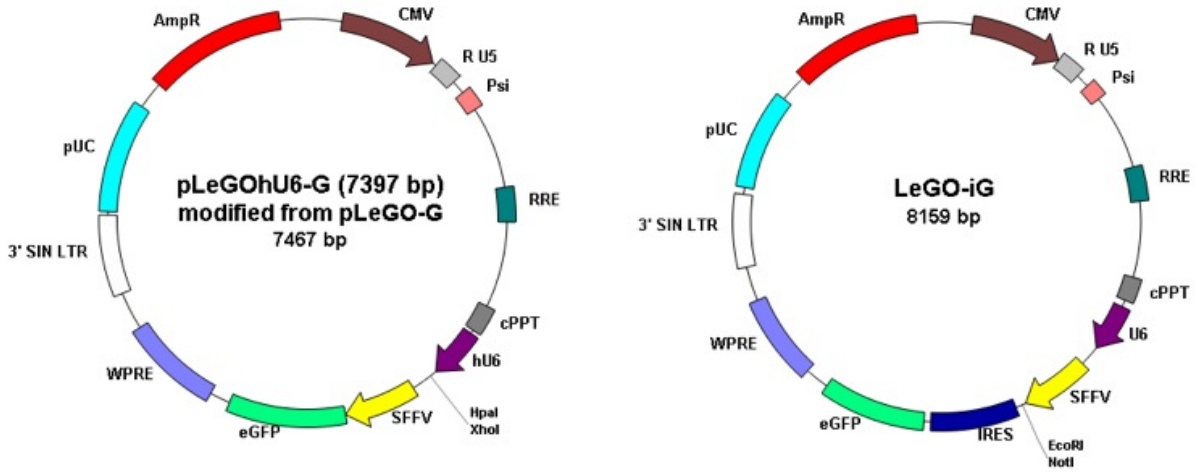

Figure 2.1: Lentiviral gene ontology (LeGO) vectors - Lentiviral vectors for short-hairpin RNA (shRNA) expression under the control of the human U6 (hU6) promoter (left panel) and for expression of a gene of interest via the spleen focus-forming virus (SFFV) promoter (right panel). eGFP = enhanced green fluorescent protein; CMV = cytomegalovirus promoter; SIN-LTR = self-inactivating-long-terminal repeat; WPRE = Woodchuck hepatitis virus post-trancriptional regulatory element; Psi = lentiviral packaging signal; RRE = rev responsive element; cPPT = central polypurine tract; AmpR = ampicillin resistance gene; pUC = bacterial origin of replication; modified from (Roelz *et al.*, 2010; Weber *et al.*, 2008).

performed as described in 2.2.4.1.

2.2.3.6 Adenoviral backbone plasmid cloning

For transient knockdown of BIM or BMF, recombinant Ad5/F35-adenoviruses were generated using restriction enzymes and ligases, Gateway® Cloning Technology (Invitrogen) and the AdEasy system as depicted in Figure 2.2 (Luo *et al.*, 2007). Processed oligonucleotides targeting BIM or BMF were cloned into the *Bgl*II-*Hind*III site of pENTR-THT (kindly provided by S. Geley). The pENTR vector contains the RNA polymerase III dependent tetracycline-sensitive RNAse P H1 (THT) promoter for shRNA expression and the DNA recombination sequences *att*L1 and *att*L2 for site-specific recombination. Sequence-verified clones were recombined (LR) with pAdTrack-Destination vectors harboring green fluorescent protein (GFP) marker under the control of a CMV promoter and two viral DNA recombination sequences (Ad5 left arm, Ad5 right arm). The LR reaction was mediated by λ recombination proteins (Gateway LR Clonase II Enzyme Mix) which cut within the *att*L recombination sites flanking the shRNA sequence in the pENTR-THT vector and ligate it to the corresponding *att*R recombination sites in the pAdTrack-Dest vector. Restriction enzyme digestion-verified pAdTrack-THT-shRNA plasmids were linearized with *Pme*I, purified by phenol/chloroform extraction and ethanol precipitation (see 2.2.3.3) and electroporated into *E.coli* BJ5183 cells containing the super-coiled

backbone vector pAdEasy-1-F35 (see 2.2.3.8). BJ5183 cells are *rec*A proficient and efficiently execute stable homologous recombination. Successful recombination was confirmed by restriction mapping. Verified plasmids were linearized with *Pac*I, thereby liberating both inverted terminal repeats (ITRs) to efficiently initiate viral DNA replication. The pAdEasy-1-F35-CMV-GFP/CMV-BCL-XL plasmid was kindly provided by Stephan Geley (Biocenter, Innsbruck). Finally, adenoviruses were produced as described in 2.2.4.3.

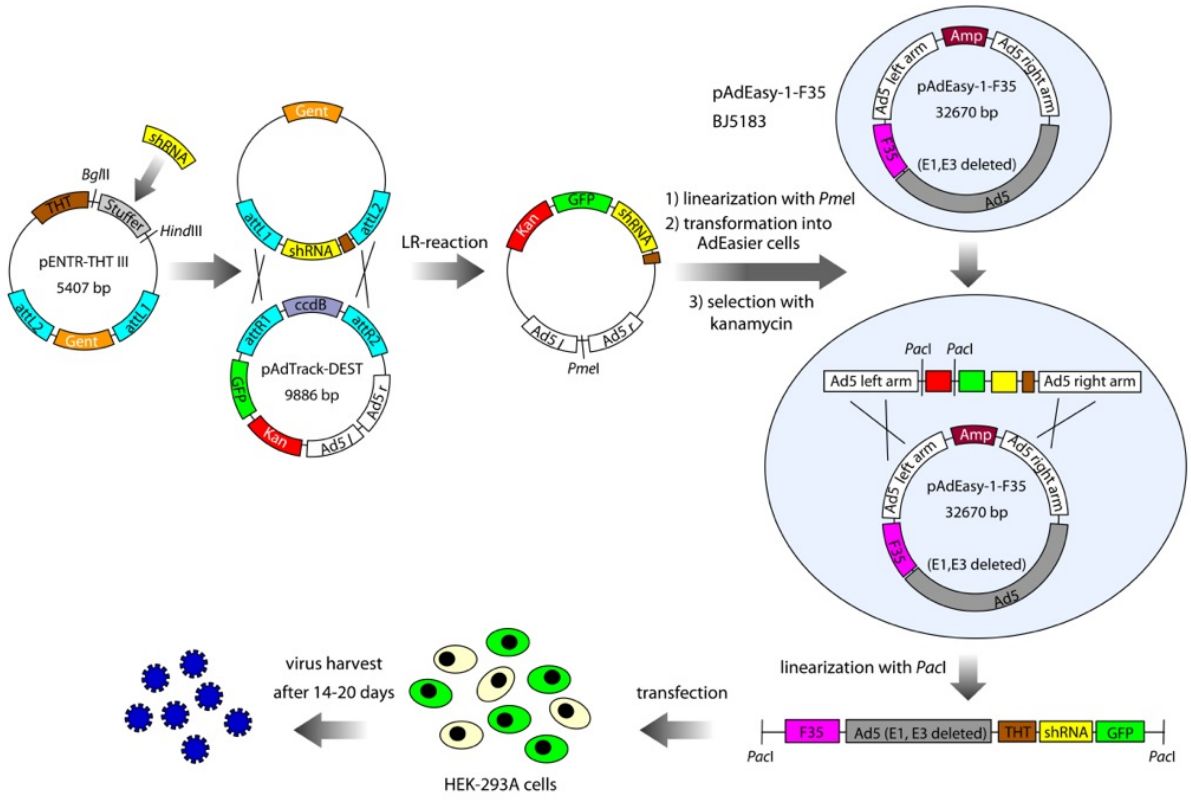

Figure 2.2: Adenoviral backbone cloning - shRNA was cloned into pENTR-THT-III and recombined with pAdTRACK. Resulting recombinant vectors were linearized and transformed into BJ5183 cells, where the viral sequences (Ad5 left arm, Ad5 right arm) recombined with the pAdEasy-1-F35 adenoviral backbone plasmid. Finally, recombinant adenoviral DNA was linearized with *Pac*I and transfected into HEK 293A cells for virus production. CcdB = a protein that poisons *E.coli* gyrase (Loris *et al.*, 1999); Gent = gentamicin resistance gene; Kan = kanamycin resistance gene; Amp = Ampicillin resistance gene. Modified from (Luo *et al.*, 2007)

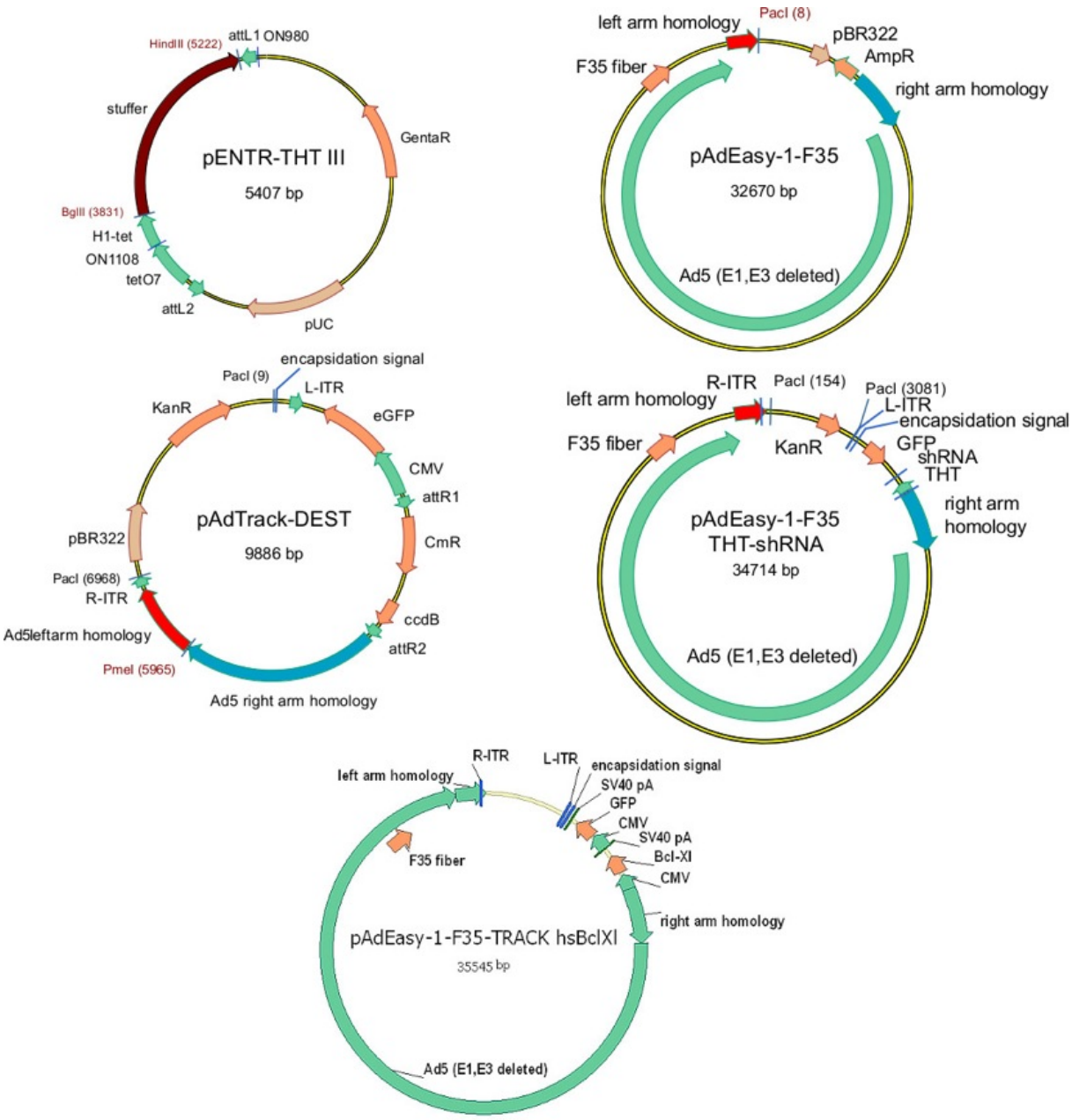

Figure 2.3: Adenoviral vectors and plasmids used for construction - For shRNA expression: pENTR-THTIII, pAdTrack-DEST, pADEasy-1-F35, pAdEasy-1-F35-THT-shRNA; For BCL-XL over-expression: pAdEasy-1-F35-TRACK hsBCL-XL; THT = tetracyclin-sensitive RNAse P H1 promoter; L-ITR = left-hand ITR and packaging signal; R-ITR = right-hand ITR .

2.2.3.7 Preparation of competent bacteria

To enable uptake of hydrophilic DNA molecules, bacteria were rendered ”competent”. Chemo-competent *E.coli* cells were generated by resuspending bacterial cell pellets in a solution with high calcium concentration leading to pore formation and thereby enabling DNA uptake upon heat shock. Briefly, a single colony was inoculated in 250 ml SOB medium (20 g tryptone, 5 g yeast extract, 0.6 g NaCl, 0.2 g KCl, 2 g $MgCl_2$, 2.5 g $MgSO_4$ in 1 l sterile water) and incubated at 19°C and 200 rpm until OD_{600}=0.55-0.65 (log phase growth) was reached. Culture was chilled on ice and split into 8 pre-cooled Falcon tubes. Bacterial cells were pelleted, gently resuspended in TB buffer (10 mM PIPES, 15 mM $CaCl_2$, 250 mM KCl, 55 mM $MnCl_2$, pH=6.7) and pooled down to 2 Falcon tubes. This step was repeated and 7% DMSO was finally added to the total pellet resuspended in 20 ml TB. Chemo-competent bacteria were aliquoted on ice, frozen down in liquid nitrogen and stored at -80°C. For the preparation of electro-competent *E.coli* cells, bacterial pellets were washed several times with 10% glycerol to reduce conductivity. Briefly, an overnight culture was diluted 1/200 in LB-Medium and incubated at 37°C and 200 rpm until OD_{600}=0.7 was reached. Afterwards culture was chilled on ice, split into 8 pre-cooled Falcons followed by centrifugation (3000 rpm, 4°C, 10 min). Bacterial cell pellets were gently resuspended in 10% glycerol and pelleted. The washing step with glycerol was repeated for three more times with each time pooling two cell pellets. Finally, the total pellet was diluted in 10% glycerol to get a OD_{600}=0.2 of a 400-fold dilution. Electro-competent bacteria were aliquoted on ice, frozen down in liquid nitrogen and stored at -80°C. The transformation efficiency of the competent bacterial cells was calculated by counting bacterial colonies on selection plates using defined amounts of input plasmid DNA (efficiency = colonies/μg plasmid DNA).

2.2.3.8 Plasmid amplification and isolation

Plasmid DNA was transformed into chemically competent *E.coli* DH5α (lentiviral vectors), *E.coli* Mach1 (adenoviral vectors) bacteria or for *in vivo* homologous recombination in electrocompetent *E.coli* BJ5183 cells containing the pAdEasy-1-F35 viral backbone.

For heat shock transformation chemically competent bacteria were thawed on ice, gently mixed with ligation or LR-reaction mix and incubated for 30 min on ice. Followed by a heat shock for 45 s at 42°C for vector uptake, the mixture was replaced on ice for 2 min. Transformed bacteria were incubated with prewarmed SOC medium for 60 min at 37°C at 250 rpm. Finally, bacteria were plated on LB-agar-plates containing the corresponding antibiotic (i.e. gentamicin, kanamycin or ampicillin).

For *in vivo* recombination electrocompetent pAdEasy-1-F35 BJ5183 were thawed on ice and gently mixed with the linearized and purified pAdTrack-THT-shRNA vector. Bacteria were electroporated for vector uptake within a cuvette inserted into an electroporator at 2.5 kV, 25 μFd and 200 Ω. Immediately after electroporation prewarmed SOC medium was added and the mixture was incubated for 1 h at 37°C and 200 rpm. Bacteria were plated on LB-agar-plates containing kanamycin and incubated overnight at 37°C. Small colonies indicate successful *in vivo* recombination, since recombinants of pAdEasy-1-F35 and pAdTrack grow slowly due to larger size of pAdEasy-1-F35 compared to religated pAdTrack-THT-shRNA plasmids.

After an overnight incubation of transformed bacteria at 37°C single colonies were picked and transferred to LB-medium containing the appropriate antibiotic. Following overnight replication, plasmid DNA was extracted from bacteria using Mini- or Maxi-kit according to the manufacturer's instructions.

2.2.3.9 Plasmid verification

Plasmid DNA was verified using colony PCR, restriction mapping or by sequencing. Colony PCR was performed as described in 2.2.3.1. To verify the correct orientation of the cloned insert, plasmid DNA was digested with various restriction enzymes, cutting within the insert and the vector leading to different sized DNA fragments, which were subsequently analyzed by agarose gel electrophoresis. Detailed validation of generated vectors was performed by DNA sequencing done by GATC-Biotech. To this end, 30-50 ng/μl purified DNA was send together with 10 pmol/μl primers summarized in material section. Sequences were aligned with the software CodonCode Aligner.

2.2.3.10 RNA isolation

To avoid degradation, RNA was always handled using DNAse, RNAse and pyrogen-free tips and reaction tubes as well as DEPC-water. RNA was isolated from 100,000-200,000 human $CD34^+$ or murine LSK cells using Spin-columns (ZymoResearch) containing positively charged silica particles with high affinity to negatively charged RNA under high salt conditions. Low ionic strength allows elution of RNA molecules from silica columns. According to the manufacturer's instructions cells were lysed in RNA Extraction Buffer, incubated on ice for 20 min and vortexed every 10 min. After addition of 99% ethanol, cells were vortexed briefly and incubated on ice for 10 min. Mixture was transferred to a spin column centrifuged at 10,000 rpm for 1 min, washed once with RNA Wash Buffer and centrifuged again to dry the column. Elution was finally achieved by RNAse-free water.

2.2.3.11 RNA concentration and quality control

RNA concentration and purity were determined with a NanoDrop Spectrometer (absorption maximum of nucleic acids at OD 260 nm). Purity of the isolated RNA was determined by measuring the ratio of absorbance at 260 nm (nucleic acids) and 280 nm (proteins) and should lay between 1.8-2.0.

To verify RNA integrity the Agilent® 2100 Bioanalyzer was used. This technique is based on gel electrophoresis in chip format to analyze size and quantity of RNA. The method was performed according to the manufacturer's instructions. Briefly, a chip containing sample wells, gel wells and a well for an RNA size standard (ladder), all interconnected with micro-channels was filled with a sieving polymer and fluorescence dye (intercalating into RNA strands). RNAs were fractionated based on their molecular size and detected by a laser. Intact total RNA is indicated by a 1:2 ratio of the 18S and 28S rRNA peak ares (Figure 2.4).

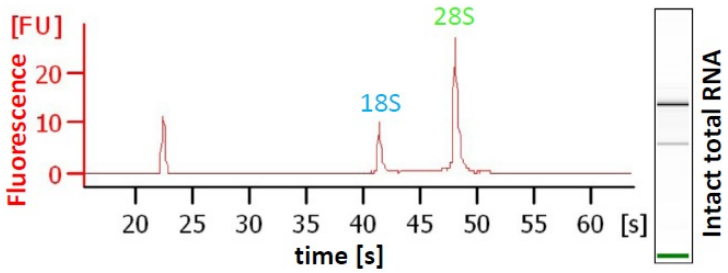

Figure 2.4: RNA quality control using Agilent® technology - A 1:2 ratio of the 18S and 28S rRNA in the electropherogram and the gel-like image indicates intact total RNA.

2.2.3.12 Reverse transcription from RNA into cDNA

Reverse transcription was performed using QuantiTect® Reverse Transcription Kit from Qiagen. To eliminate genomic DNA, 50 or 100 ng of RNA were incubated with 2 µl gDNA Wipeout Buffer at 42°C for 2 min. Afterwards, samples were immediately put on ice and ice-cold reverse transcription mastermix was added. The latter consists of Quantiscript Reverse Transcriptase, Reverse Transcriptase Buffer and Reverse Transcriptase Primer mix. For cDNA synthesis samples were incubated for 15 min at 42°C and afterwards for 3 min at 95°C to inactivate reverse transcriptase. cDNA was either stored on ice to proceed with qRT-PCR or at -20°C.

2.2.3.13 Quantitative reverse transcription PCR (qRT-PCR)

Quantitative reverse transcription PCR was performed using the Mastercycler® ep realplex from Eppendorf, where DNA is quantified by the intercalating dye SYBR green, which fluoresces when bound to double-stranded DNA. Therefore, the increase of fluorescence is proportional

to the increase of synthesized double stranded DNA. To ensure that only a specific product is detected, qRT-PCR is followed by a melting point determination. Since the melting point depends on length, GC content and complementarity of two DNA strands the desired amplicon can easily be distinguished from primer dimers, misannealed primers and contaminating DNA.

For amplification the cDNA template was pipetted into a 96 Low Profile Reaction Plate (PEQLAB) and water, forward and reverse primer and SYBR® green (Thermo scientific) were added. Directly after sealing the plate with an optically clear Q-PCR seal (Thermo scientific) and removing air bubbles, samples were measured at the Mastercycler® ep realplex from Eppendorf according to the program shown below.

Primers used for qRT-PCR are listed in the material section. The optimal annealing temperature of primers was determined initially. All primers for murine targets were annealed at 60°C, and qRT-PCR was run for 40 cycles. For human targets primers were annealed at 61°C (BIM, BMF) or 62°C (PUMA) and PCR was run for 40 cycles or 50 cycles for PUMA.

program		**cycles**	**temperature [°C]**	**Time**
initial denaturation		1	95	15 min
amplification		40		
	denaturation		95	15 s
	annealing		59-62	30 s
	extension		72	30 s
melting Curve		1	95	30 s
			60	30 s
			gradient 0,4	
			95	15 s
cooling		1		

All samples were measured in triplicates. Results were normalized to the expression level of the housekeeping gene 18S rRNA (human samples) or to β-actin (mouse samples). Relative quantification was calculated with the -$\Delta\Delta$CT method.

2.2.3.14 Reverse transcriptase multiplex ligation-dependent probe amplification (RT-MLPA®)

The multiplex reverse transcriptase PCR method RT-MLPA® (MRC-Holland) enables simultaneous profiling of 42 mRNAs involved in apoptosis regulation. Specific mRNA was reversely transcribed into cDNA (M-MLV reverse transcriptase) and hybridized to MLPA probes (two separated oligonucleotides for each target sequence as shown in Figure 2.5). In addition to homologous region both oligonucleotides contain a PCR primer sequence (either ”X” or ”Y”) and one contains a stuffer sequence of individual length. Only two MLPA probes that were bound

to directly adjacent target sequences were subsequently ligated by a thermostable ligase thus resulting in probes of a defined length. Next, ligated probes were amplified in a PCR reaction performed with a 6-carboxyfluorescein-(FAM) labeled forward primer (X) and an unlabeled reverse primer (Y).

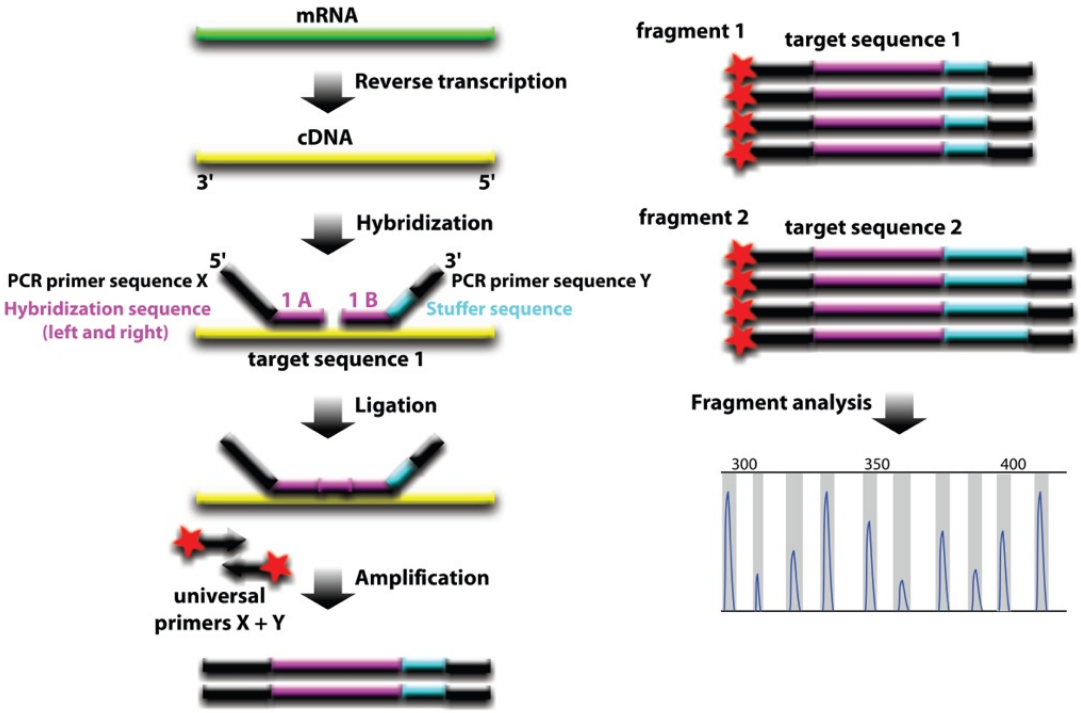

Figure 2.5: Reverse transcriptase multiplex ligation-dependent probe amplification (RT-MLPA®) - After reverse transcription of specific mRNAs into cDNAs, two separated oligonucleotides (MLPA probes) were hybridized directly adjacent to their target sequence and subsequently ligated. Ligated probes were amplified by PCR, separated by capillary electrophoresis according to the size of their stuffer sequence and quantified using GeneMapper® Software (MRC-Holland mRNA MLPA®, modified).

Amplification products were mixed with HiDi formamide and size standards (Rox 500) and separated by capillary electrophoresis (ABI-3100 16 capillary sequencer) followed by quantification with the software GeneMapper® from Applied Biosystems (Eldering *et al.*, 2003). To normalize for variations between different samples single peaks were calculated relative to the sum of all peak areas, which was set to 100% (Kater *et al.*, 2004). Calculation was performed with StatView.

2.2.4 Methods in virology

2.2.4.1 Lentivirus production

For lentivirus production the generated lentiviral backbone plasmids were transfected into HEK 293T cells by using the $CaPO_4$ method. vsv.g-envelope plasmid and a gag/pol plasmid were cotransfected. To obtain 90% confluency upon transfection, 14x10^6 HEK 293T cells were cultured in a 15 cm^2 tissue culture plate for 4-6 h. Transfection medium was replaced by fresh medium 16 h after transfection. Within the following 48 h, supernatant containing viral particles was harvested twice. After removal of cell debris by sterile filtration, supernatant was pooled and ultracentrifuged at 4°C with 19,500 rpm for 2.5 h to concentrate the lentiviral particles. Lentiviruses were resuspended in 100-200 µl IMDM supplemented with 1% BSA and centrifuged at 13,000 rpm for 1 min to remove residual cell debris. Small aliquots of lentiviruses were stored at -80°C. Viral concentration was determined by infecting HeLa cells with different amounts of 10-fold diluted viral suspension for 24 h. Afterwards, medium was replaced by fresh medium. The percentage of cells expressing GFP was analyzed by flow cytometry 48 h later. Virus concentration (IU/ml) was determined using a well with 10-20% GFP^+ cells (linear correlation): (%GFP^+ cells/100) x (1000 µl/V) x dilution factor x cell number plated.

2.2.4.2 Lentiviral transduction of $CD34^+$ cells

For lentiviral transduction cryopreserved or fresh $CD34^+$ cells were thawed and seeded at 1x10^5 cells/well in a 96 well flat bottom tissue culture plate and prestimulated for 20-24 h with complete stem cell medium containing 10% ES-FBS and the following cytokines: 50 ng/ml TPO, 100 ng/ml SCF, 100 ng/ml Flt3L and 20 ng/ml IL3. After prestimulation medium was replaced by serum-free complete stem cell medium supplemented with cytokines, and lentivirus was added at a multiplicity of infection (MOI) of 10. Since MOI stands for the number of viral particles added per cell, MOI=10 means that 10-fold more viral particles were added than cells were plated. On the following day the transduction was repeated. 24 h after second infection the medium was changed to fresh complete stem cell medium supplemented with 10% ES-FBS and cytokines. Cells were cultured for an additional day and then sorted for GFP expression. For *in vivo* experiments the progeny of 10^5 $CD34^+$ cells was directly harvested 24 h after second virus exposure, washed twice with PBS and resuspended in 25 µl 0.9% NaCl solution. GFP expression was determined by FACSCalibur.

2.2.4.3 Adenovirus production

Adenovirus amplification was adapted from the protocol for AdEasy system-based generation of recombinant adenoviruses (Luo *et al.*, 2007). Briefly, 2x10^6 HEK 293A cells were seeded in a 25 cm^2 tissue culture flask and cultured for 4-6 h at 37°C and 5% CO_2 to obtain a cell density of 50-70%. Following medium exchange cells were transfected with the linearized adenoviral plasmid using a $CaPO_4$ kit according to the manufacturer's instructions.

The virus was harvested 2-3 weeks later, when a high GFP expression was monitored under the fluorescence microscope and 30-50% of the cells were detached. To this end, cells were scraped off the tissue culture flask, centrifuged and vortexed in 2 ml of supernatant. Afterwards, four cycles of freezing in liquid nitrogen, thawing in a 37°C water bath and vigorously vortexing were performed to release viruses from cells. Following centrifugation to remove cell debris half of the lysate was added to 80-90% confluent HEK 293A cells grown in a 25 cm^2 for 4-6 h. 3-5 d after infection, as soon as 30-50% of the infected cells were detached, cells were harvested, centrifuged and resuspended in 5 ml of supernatant by vortexing. Virus lysate was obtained after four freeze-thaw-vortex cycles and centrifugation for cell debris removal. In order to get a high-titer adenovirus four additional amplification steps were performed in 75 cm^2 flasks with increasing cell numbers. Finally, adenoviruses were purified with the Vivapure Adenopack 20 columns. Purification with Maxi spin columns is based on binding of adenoviral particles to an ion exchange membrane adsorber. Small aliqouts of adenoviruses were stored in buffer containing 50 mM HEPES (pH 7.4), 150 mM NaCl, 0.1% BSA and 2.5% glycerol at -80°C.

2.2.4.4 Adenoviral transduction of CD34$^+$ cells

For the establishment and optimization of adenoviral transduction, cryopreserved CD34$^+$ cells were thawed and seeded at 1x10^5 cells/well in a 96 well flat bottom tissue culture plate and prestimulated for 1, 4 or 20 h with complete stem cell medium containing 10% ES-FBS and the following cytokines: 50 ng/ml TPO, 100 ng/ml SCF, 100 ng/ml Flt3L with or without 20 ng/ml IL3. After prestimulation the medium was replaced by serum-free complete stem cell medium supplemented with the above mentioned cytokines, and adenovirus was added at a multiplicity of infection of 1-60. 3, 16 or 24 h after infection in the presence or absence of BoosterExpress^{TM} reagent for 4, 20 or 24 h, the medium was changed to fresh complete stem cell medium supplemented with 10% ES-FBS and cytokines. Afterwards cells were cultured for 24 h or 48 h or up to 15 days. Transduction efficiency, indicated by the percentage of GFP$^+$ cells was determined by flow cytometry. For *in vivo* experiments cells were prestimulated for 1 h with TPO (50 ng/ml), SCF, Flt3L (100 ng/ml each) and IL3 (20 ng/ml) and incubated with Ad5/F35-PGK-GFP or Ad5/F35-CMV-GFP/CMV-BCL-XL (10-20 MOI) for 24 h in the presence of BoosterExpress^{TM}

reagent for the last 4 h. 24 h later cells were sorted for GFP expression and cultured for 24 h. The progeny of 10^5 GFP^+ cells was washed twice with PBS and resuspended in 25 µl 0.9% NaCl solution. In a second approach 10^5 $CD34^+$ cells were transduced with adenoviruses in the absence of BoosterExpress™ reagent, cultured for an additional day and resuspended in 25 µl 0.9% NaCl solution after washing with PBS.

2.2.5 Methods in protein chemistry

2.2.5.1 Protein extraction

Proteins were extracted from whole cell lysates. To this end, collected cells were washed once with ice-cold PBS and lysed in cell lysis buffer (Cell signaling technology) supplemented with 1 mM PMSF for 20 min on ice with brief vortexing every 10 min. PMSF inhibits serine proteases like trypsin, chymotrypsin and thrombin and the cysteine protease papain. After removal of cell debris and insoluble membrane proteins by centrifugation at 14,000 rpm for 20 min the protein content of the supernatant was determined using DC™ protein assay kit based on the Lowry assay. Briefly, copper is reduced by proteins under alkaline conditions and the radical groups of tyrosine, tryptophan and cysteine reduce Folin reagent leading to a blue color with an absorbance maximum at 750 nm. Protein concentration was determined relative to a BSA standard using an ELISA-reader.

2.2.5.2 Western blot analysis

Proteins were size-fractioned under reducing conditions using sodium dodecyl sulfate polyacrylamide gel electrophoresis (SDS-PAGE). For this purpose equal amounts of protein were mixed with 5X sample buffer (0.5 M Tris/HCl pH 6.5, 10% SDS, 20% glyerol, 0.02% bromophenol) freshly supplemented with 50 mM DTT denatured at 96°C for 5 min and loaded on a 12% SDS-polyacrylamid gel together with a protein size marker for each gel. After separation at 120 V proteins were transferred on to a nitrocellulose membrane using a semidry blotting system. Transfer was performed with a blotting buffer containing 48 mM Tris, 39 mM glycine, 20% methanol and 0.04%SDS, at 1 mA/cm^2 for 90 min. To reduce unspecific protein binding membranes were blocked directly after blotting in PBS supplemented with 5% milk powder and 0.1% Tween 20 for 1 h at RT. Next, membranes were incubated overnight at 4°C with primary antibodies directed against specific proteins as indicated in the material section. Following incubation with the corresponding horseradish peroxidase-conjugated secondary antibody for 1 h at RT signals were detected by enhanced chemiluminescence. β-Actin was used as a loading control.

2.2.6 Flow cytometry analysis

2.2.6.1 Cell surface staining

For cell surface staining FITC, PE, APC or Biotin conjugated monoclonal antibodies were diluted 1:100 in 50 µl PBS/10% FCS. Antibodies used are listed in 2.1.5 Cells were stained for 30 min at 4°C in the dark, washed and either analyzed directly or stained with Streptavidin-PE-Cy7 diluted 1:100 in 50 µl PBS/10% FCS to detect biotinylated antibodies.

2.2.6.2 Apoptosis analysis

Apoptosis was determined by a combined 7-AAD and Annexin V staining (Figure 2.6). Annexin V binds Ca^{2+}-dependent to phosphatidylserine (PS) which is translocated from the inner to the outer leaflet of the lipid bilayer (surface membrane) during early phases of apoptosis. Late apoptotic and necrotic cells loose cell and nuclear membrane integrity enabling 7-AAD to intercalate into the DNA.

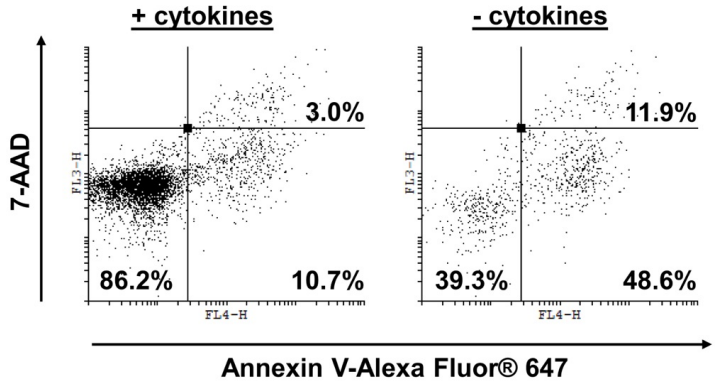

Figure 2.6: Apoptosis analysis by flow cytometry - Mouse LSK cells were cultured for 48 h with (left panel) or without cytokines (right panel) and stained subsequently with Annexin V-Alexa Fluor® 647 and 7-AAD. Viable cells are negativ for 7-AAD and Annexin V, whereas early apoptotic cells are Annexin V positive. Annexin V/7-AAD double-positive cells are either late apoptotic or necrotic cells.

At indicated time points cells were harvested and washed once with ice-cold PBS. Cells were resuspended in 100 µl binding buffer (10 mM HEPES pH 7.4, 140 mM NaCl and 2.5 mM $CaCl_2$ in Millipore purified water) supplemented with 2.5 µg/ml 7-AAD and 2.5 µg/ml Annexin V coupled with either FITC or Alexa Fluor® 647. After incubation for 5-10 min at 4°C in the dark the percentage of early apoptotic cells (7-AAD negative, Annexin V positive) and viable cells (7-AAD and Annexin V negative) was analyzed via FACS. Specific apoptosis was calculated as follows: (induced apoptosis - spontaneous apoptosis)/(100 - spontaneous apoptosis).

2.2.6.3 Proliferation assay

The proliferation status of murine and human haematopietic stem and progenitor cells was analyzed combining the DNA binding dye DAPI with an anti-Ki-67 antibody. Since the Ki-67 antigen is only expressed in cycling cells, its expression can be used to discriminate between cells in G_0 or G_1 phase. The DNA amount of cells determined by DAPI intensity furthermore identifies cells in S or G_2/M phase.

Proliferation was measured prior to and 4 or 8 weeks after transplantation as well as after *in vitro* stimulation with cytokines. Cells were washed once with ice-cold PBS and subsequently fixed and permeabilized with 75% ethanol for at least 2 h at -20°C. Subsequently, cells were washed twice with PBS wash buffer (PBS, 1% FCS, 0.09% NaN_3) and incubated with 50 µl PBS wash buffer supplemented with 10 µl anti-Ki-67 antibody for 30 min at room temperature (RT) in the dark. Cells were washed twice with PBS wash buffer, resuspended in PBS with 1.25 µg/ml DAPI and analyzed by flow cytometry (BD LSRFortessa™ cell analyzer). Since GFP is lost upon ethanol treatment lentivirally transduced $CD34^+$ cells were sorted for GFP expression prior to ethanol fixation. For analysis of HSPCs 4 weeks after transplantation cells were fixed using BD™ Phosflow protocols instead of using ethanol. To this end, cells were fixed with pre-warmed BD™ Phosflow Fix Buffer I at 37°C for 10 min and frozen at -80°C for later usage or centrifuged directly and washed twice with BD™ Phosflow Perm/Wash Buffer I. Finally $2x10^6$ cells were resuspended in 100 µl BD™ Phosflow Perm/Wash Buffer I together with 20 µl anti-Ki-67 antibody and incubated for 30 min at RT in the dark. Cells were washed once with BD™ Phosflow Perm/Wash Buffer I, resuspended in PBS with 1.25 µg/ml DAPI and analyzed by flow cytometry (BD LSRFortessa™ cell analyzer).

2.2.7 Statistical analysis

For statistical analysis the Mann-Whitney-test, the Student's t-test (unpaired) with Welch's correction or the Fisher exact test were performed as indicated, considering p-values$<$0.05 as statistically significant (StatView 4.1 software program).

3

Results

3.1 Importance of BH3-only proteins in murine HSPCs

3.1.1 Various BH3-only proteins are induced in murine HSPCs subjected to cytokine deprivation

Although transplantation of haematopoietic stem and progenitor cells (HSPCs) is often used to cure haematological and immunological diseases, the efficacy of this treatment is still limited by the risk of graft failure or delayed engraftment. Clinical experience has shown that these risks can be reduced by using higher numbers of transplanted stem cells (Demirer *et al.*, 2009; Mavroudis *et al.*, 1996). In search for novel strategies to increase donor cell numbers, we focused on cell death signaling in HSPCs in general and on the role of the pro-apoptotic BH3-only proteins in particular.

In order to mimic cell stress and cell death induction of HSPCs during stem cell transplantations *in vitro*, we first subjected isolated HSPCs to cytokine withdrawal. It is known, that upon cytokine deprivation the intrinsic apoptosis pathway is triggered by BH3-only proteins (Coffer *et al.*, 2000). The first question arising was, which BH3-only protein(s) is/are important for HSPCs in the absence of cytokine mediated survival signals. To address this question, LSK cells (lineage$^-$sca1$^+$c-kit$^+$) were isolated from the bone marrow (BM) of wild type (wt) mice and cultured for 48 h in the presence and absence of cytokines. As expected, cytokine deprivation led to rapid apoptosis induction (21.3 +/- 6.3% viable cells), whereas the addition of the cytokines TPO, SCF and Flt3L (100 ng/ml each) led to an almost complete protection of the cells (78.3 +/- 4.5% viable cells).

To analyze which BH3-only proteins were induced prior to cell death induction we isolated mRNA after 14 h of culture (+/- cytokines), and determined relative changes in their mRNA expression by the RT-MLPA® technique as explained in the method section (Eldering *et al.*, 2003). As shown in Figure 3.1 cytokine deprivation led to an increased mRNA expression of Bim (2.0-fold), Bmf (3.3-fold), Puma (2.3-fold) and Noxa (1.9-fold), whereas Bad and Bid were not upregulated. The BH3-only proteins Bik and Hrk were not expressed in HSPCs. Next to the regulation of BH3-only proteins we also analyzed changes in mRNA levels of the two downstream pro-apoptotic Bcl-2 proteins, Bax and Bak, and the anti-apoptotic Bcl-2 family members. Neither Bax nor Bak were upregulated on the mRNA level (Figure 3.1). However, simultaneously to the upregulation of BH3-only proteins, the mRNAs of the anti-apoptotic antagonists Bcl-2 and Bcl-x_L were downregulated (0.5-fold each). Almost no changes were observed in the mRNA levels of Mcl-1 and A1 (Figure 3.1).

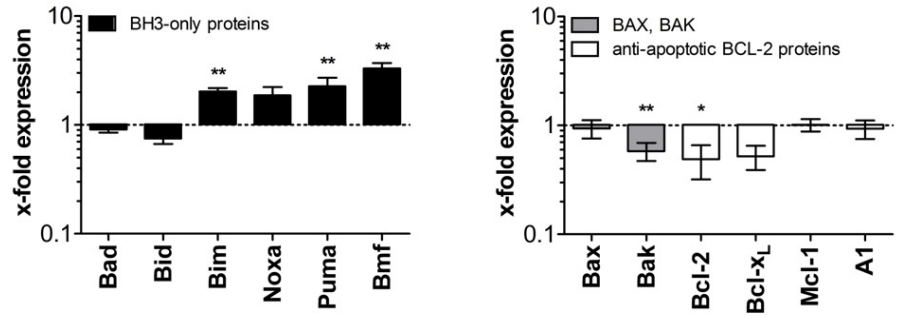

Figure 3.1: Expression of Bcl-2 family members in cytokine-deprived murine LSK cells - LSK cells were isolated from BM of wt mice and cultured for 14 h with or without TPO, SCF and Flt3L (100 ng/ml each). mRNA levels of BH3-only proteins (left panel), Bax, Bak and anti-apoptotic Bcl-2 proteins (right panel) were analyzed by RT-MLPA. X-fold expression of mRNA levels in the absence of cytokines compared to mRNA levels in the presence of cytokines (=1) is shown. Data represent mean values +/-SEM of n=5-6 from four independent experiments. Significant p-values (Mann-Whitney-test): Bim p=0.01; Puma p=0.01; Bmf p=0.01; Bak p=0.01; Bcl-2 p=0.04.

Table 3.1 shows all other genes tested with RT-MLPA®. No relevant mRNA changes were found. The results obtained by RT-MLPA® were independently confirmed by qRT-PCR (Figure 3.2).

Table 3.1: Expression of apoptosis-related genes in cytokine-deprived murine LSK cells

- cytokines/ + cytokines	Mean ±SEM	p-value	- cytokines/ + cytokines	Mean ±SEM	p-value
Bcl-G	0.30 ±0.30	0.36	Naip1	2.01 ±0.36	0.10
Bcl-rambo	0.95 ±0.04	0.20	cIAP1	2.35 ±0.68	0.07
Bcl-w	0.76 ±0.32	0.72	cIAP2	1.28 ±0.06	0.07
Moap1	0.53 ±0.15	0.06	XIAP	1.81 ±0.26	0.07
AIF	0.62 ±0.09	0.20	Survivin	0.65 ±0.07	0.27
Apaf1	1.22 ±0.23	0.36	Apollon	1.25 ±0.21	0.72
Smac/Diablo	0.43 ±0.43	0.47	FLIP	0.89 ±0.24	0.86
Omi	0.70 ±0.24	0.14	p21	0.90 ±0.31	0.86
Pak2	0.38 ±0.24	0.41	B2m	1.42 ±0.34	0.27

LSK cells were isolated from BM of wt mice and cultured for 14 h with or without TPO, SCF and Flt3L (100 ng/ml each). mRNA levels of the indicated genes were analyzed by RT-MLPA®. X-fold expression of mRNA levels in the absence of cytokines compared to mRNA levels in the presence of cytokines is shown. Data represent mean values +/-SEM of n=5-6 from four independent experiments. P-values were calculated with Mann-Whitney-test.

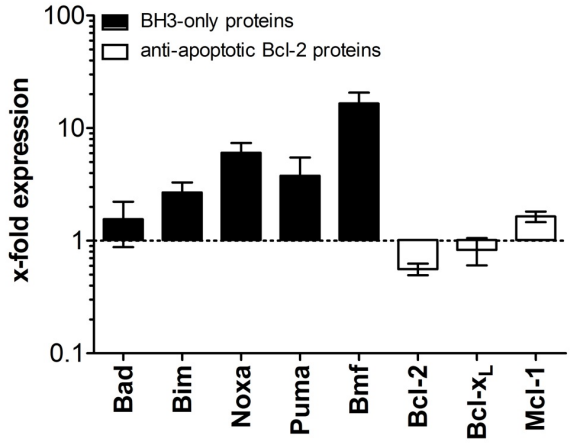

Figure 3.2: Validation of RT-MLPA® data by qRT-PCR - Wt LSK cells were isolated and cultured for 14 h with or without cytokines. mRNA levels of the indicated Bcl-2 family members were assessed by qRT-PCR. Relative expression of mRNA levels in the absence of cytokines compared to mRNA levels in the presence of cytokines (=1) is shown. Data were normalized to β-actin and calculated using the -ΔΔCT relative quantification method. Data represent mean values +/-SD of two independent experiments with n=2, no statistical analysis was performed.

3.1.2 Cytokine deprivation-induced cell death in murine HSPCs depends mainly on Bim

As shown in 3.1.1 the balance between pro- and anti-apoptotic Bcl-2 family members is shifted towards a pro-apoptotic state. To analyze whether upregulation of Bim, Bmf, Noxa and Puma indeed mediates apoptosis induction we isolated murine LSK cells from mice deficient for various BH3-only proteins and exposed them to cytokine deprivation for 48 h (Figure 3.3). Surprisingly, only loss of Bim and to a minor extent loss of Puma prevented cytokine deprivation-induced apoptosis, whereas loss of Bad, Noxa, or Bmf did not protect LSK cells. Overexpression of Bcl-2 under control of the *Vav*-gene promoter almost completely prevented cytokine deprivation-induced apoptosis in LSK cells, which is in line with previously published data (Domen & Weissman, 2000; Ogilvy *et al.*, 1999).

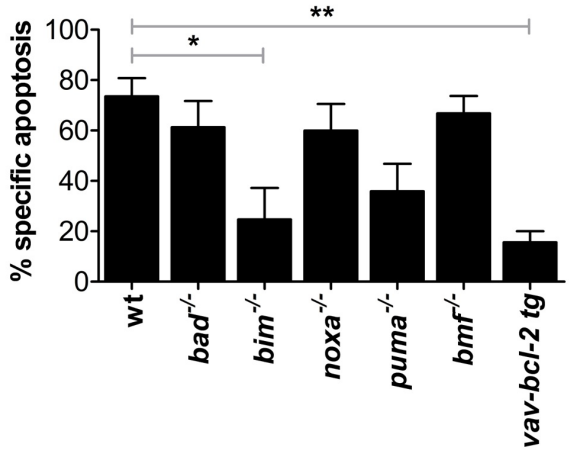

Figure 3.3: Bim or Puma deficiency protects LSK cells from cytokine deprivation-induced apoptosis *in vitro* - LSK cells were isolated from BM of mice lacking the indicated BH3-only proteins or from mice overexpressing Bcl-2. After 48 h of culture in the presence or absence of cytokines, cells were stained with Annexin V-FITC and 7-AAD, and cell death was determined by flow cytometry. Specific apoptosis was calculated as indicated in the method section. Data represent mean values +/-SEM from n=3-4/genotype of two independent experiments. Significant differences (Student's t-test with Welch's correction) compared to wt LSK cells were observed in *bim*$^{-/-}$ (p=0.04) and *bcl-2 tg* (p=0.003) LSK cells.

3.1.3 Bim- and Bmf-dependent apoptosis limits both early engraftment and long-term haematopoiesis

The finding that loss of Bim prolonged the survival of LSK cells upon cytokine deprivation *in vitro* urged us to investigate whether *bim*$^{-/-}$ LSK cells would also perform better *in vivo* during the reconstitution of lethally irradiated mice. Although *bmf*$^{-/-}$ LSK cells were not protected from apoptosis *in vitro*, mRNA levels of Bmf were highly increased upon cytokine deprivation in wt LSK cells (Figure 3.1). Thus we wondered whether Bmf might also play a role *in vivo* and we therefore included *bmf*$^{-/-}$ LSK cells in our analysis.

In order to compare the reconstitution ability of *bim*$^{-/-}$ or *bmf*$^{-/-}$ LSK cells directly to that of wt LSK cells, we performed competitive reconstitution experiments. Therefore, Ly5.1^{+} recipient mice were lethally irradiated (9.5 Gy) and reconstituted with LSK cells derived from a Ly5.1^{+} wt mouse (50%) and from a Ly5.2^{+} mouse of the indicated genotype (50% wt, *bim*$^{-/-}$, *bmf*$^{-/-}$ or *vav-bcl-2 tg*). 10 days or 16 weeks after transplantation mice were sacrificed and the percentage of Ly5.2^{+} cells in the HSPC compartment within the BM was analyzed by flow cytometry. As shown in Figure 3.4 mice transplanted with the same amount of Ly5.1^{+} and Ly5.2^{+} wt LSK cells displayed, as expected, almost the same amount of Ly5.1^{+} and Ly5.2^{+} donor HSPC cells 10 days (43% Ly5.2^{+} LSK cells + 57% Ly5.1^{+} LSK cells) as well as 16 weeks (53% Ly5.2^{+} LSK cells + 47% Ly5.1^{+} LSK cells; 51% Ly5.2^{+} LSK CD150^{+}cells + 49% Ly5.1^{+} LSK CD150^{+}cells) after transplantation. Surprisingly, already 10 days after transplantation, Bim (64% Ly5.2^{+}) and Bmf (66% Ly5.2^{+}) deficient LSK cells showed a clear engraftment advantage compared to wt LSK cells. This effect was strongly increased in wt:*bim*$^{-/-}$ BM chimeras (90% *bim*$^{-/-}$ LSK; 86% *bim*$^{-/-}$ LSK CD150^{+}) after 16 weeks. At this time point nearly all the LSK and LSK CD150^{+} cells were derived from the Bim-deficient donor indicating a complete displacement of wt HSPCs.

Given the fact, that the engraftment advantage of *vav-bcl-2 tg* or *bim*$^{-/-}$ LSK cells was always comparable, these results indicate that Bim accounts for all Bcl-2 inhibited apoptotic cell death during reconstitution. Similar to Bim-deficiency, Bmf-deficiency displaced wt HSPCs within 16 weeks after transplantation, although to a less extent. These data explain why wt myelopoiesis and lymphopoiesis are displaced in wt:*bim*$^{-/-}$ and wt:*bmf*$^{-/-}$ chimeras, as it has been previously shown (Figure 1.7B/C).

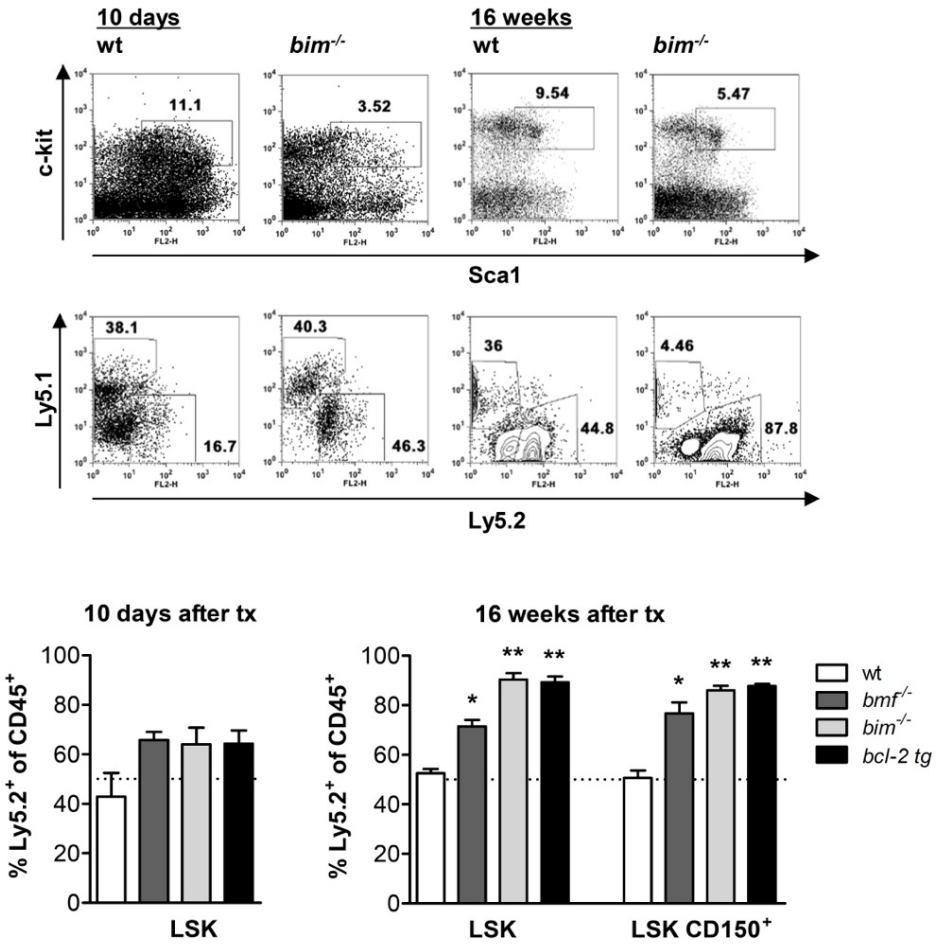

Figure 3.4: Displacement of wt HSPCs in wt:*bmf*$^{-/-}$, wt:*bim*$^{-/-}$ and wt:*bcl-2 tg* BM chimeras - Lethally irradiated Ly5.1^{+} recipient mice were transplanted with 50% Ly5.1^{+} wt LSK cells and 50% LSK cells from wt, *bmf*$^{-/-}$, *bim*$^{-/-}$ or *bcl-2 tg* Ly5.2^{+} mice. 10 days and 16 weeks after competitive reconstitution, recipient mice were sacrificed and percentages of Ly5.2 LSK and more immature LSK CD150^{+} cells were determined by flow cytometry. Dot blots of representative experiments are shown (upper panel). Data represent mean values of three independent experiments +/-SEM with n=3-6 animals/genotype. Significant differences (Mann-Whitney-test) compared to wt LSK and wt LSK CD150^{+} were observed 16 weeks after transplantation in *bmf*$^{-/-}$ (p=0.03) *bim*$^{-/-}$ (p=0.01) and *bcl-2 tg* (p=0.01) LSK and LSK CD150^{+} cells. tx: transplantation.

Since both early engraftment and long-term haematopoiesis of LSK cells seem to be limited by Bim-dependent apoptosis, we next transplanted a limited amount of total BM cells (10,000) derived from Ly5.2$^+$ wt or *bim*$^{-/-}$ mice together with 200,000 Ly5.1$^+$ wt BM competitor cells into lethally irradiated Ly5.1$^+$ recipient mice. One would expect that less *bim*$^{-/-}$ BM cells are required for successful reconstitution. Indeed, successful reconstitution defined by $>$1% Ly5.2$^+$ myeloid and lymphoid splenic cells, was achieved in 4 out of 5 mice transplanted with 10,000 *bim*$^{-/-}$ BM cells, whereas 0 out of 6 mice transplanted with 10,000 wt BM cells succeeded in engrafting recipient mice efficiently.

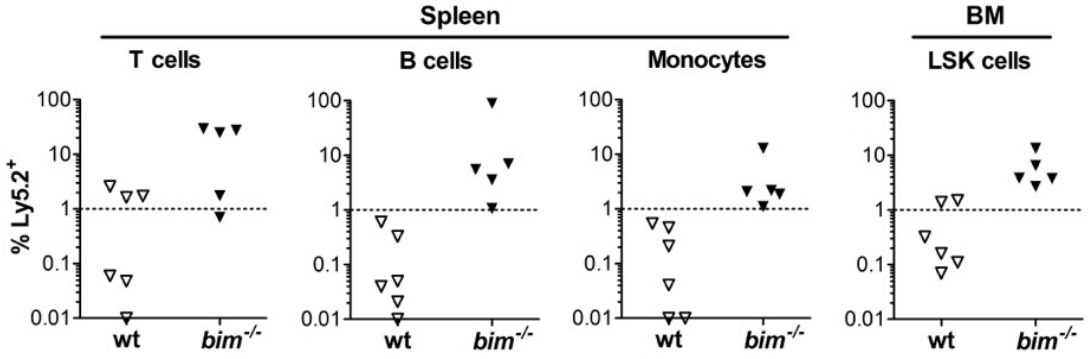

Figure 3.5: Superior reconstitution potential of *bim*$^{-/-}$ BM - A mixture of 10,000 BM cells derived from Ly5.2$^+$ wt or *bim*$^{-/-}$ mice and 200,000 Ly5.1$^+$ wt BM competitor cells was transplanted into lethally irradiated Ly5.1$^+$ recipient mice. 14 weeks later, the percentage of Ly5.2$^+$ cells was analyzed within different splenic cell populations and BM derived LSK cells. $>$ 1% Ly5.2$^+$ myeloid and $>$1% Ly5.2$^+$ lymphatic splenic cells indicated successful engraftment. Engraftment was significantly different between wt and *bim*$^{-/-}$ cells (Fisher exact test; p=0.015).

3.1.4 Apoptosis resistance, but not advantages during homing or proliferation account for the superior performance of *bim*$^{-/-}$ HSPCs

So far these results demonstrate that loss of Bim highly increases the transplantation efficacy of HSPCs due to inhibition of apoptosis. To exclude that mechanisms other than apoptosis contribute to this superior performance of *bim*$^{-/-}$ HSPCs, we analyzed their homing capacity and proliferation in detail (Figure 3.6).

For homing analysis, we transplanted Ly5.2^{+} wt or *bim*$^{-/-}$ LSK cells into lethally irradiated Ly5.1 recipient mice. 15 h later, when many of the Ly5.1^{+} donor cells have reached the recipient's BM but apoptosis is not yet limiting, mice were sacrificed. The percentage of viable Ly5.2^{+} cells in the central BM was determined by flow cytometry. Additionally, we analyzed Ly5.2^{+} cells residing in the endosteal niche of the BM, where LT-HSC are predominantly located. As shown in Figure 3.6A there were no detectable differences in homing ability between wt and *bim*$^{-/-}$ LSK cells, neither in the central BM nor in the endosteal niche.

Secondly, proliferation capacity of wt and *bim*$^{-/-}$ LSK cells was analyzed using a combined Ki-67 and DAPI staining (Figure 3.6B/C). There were no significant differences in the cell cycle state between *bim*$^{-/-}$ and wt LSK cells directly before transplantation. 4 weeks after transplantation more LSK cells were in the S-G_2-M phases indicating that stress haematopoiesis aiming to refill both the HSPC pool and the periphery was still ongoing. However, there was no difference between wt an *bim*$^{-/-}$ cells. Furthermore, entry into and progression through the cell cycle was tested by *in vitro* stimulating LSK cells for 72 h in the presence of the cytokines TPO, SCF and Flt3L (100ng/ml each). Again, there was no difference between *bim*$^{-/-}$ and wt LSK cells (Figure 3.6C). Taken together these results strongly confirm that apoptosis triggered by Bim limits the reconstitution potential of HSPCs *in vivo*, whereas Bim plays no role for HSPC homing and proliferation.

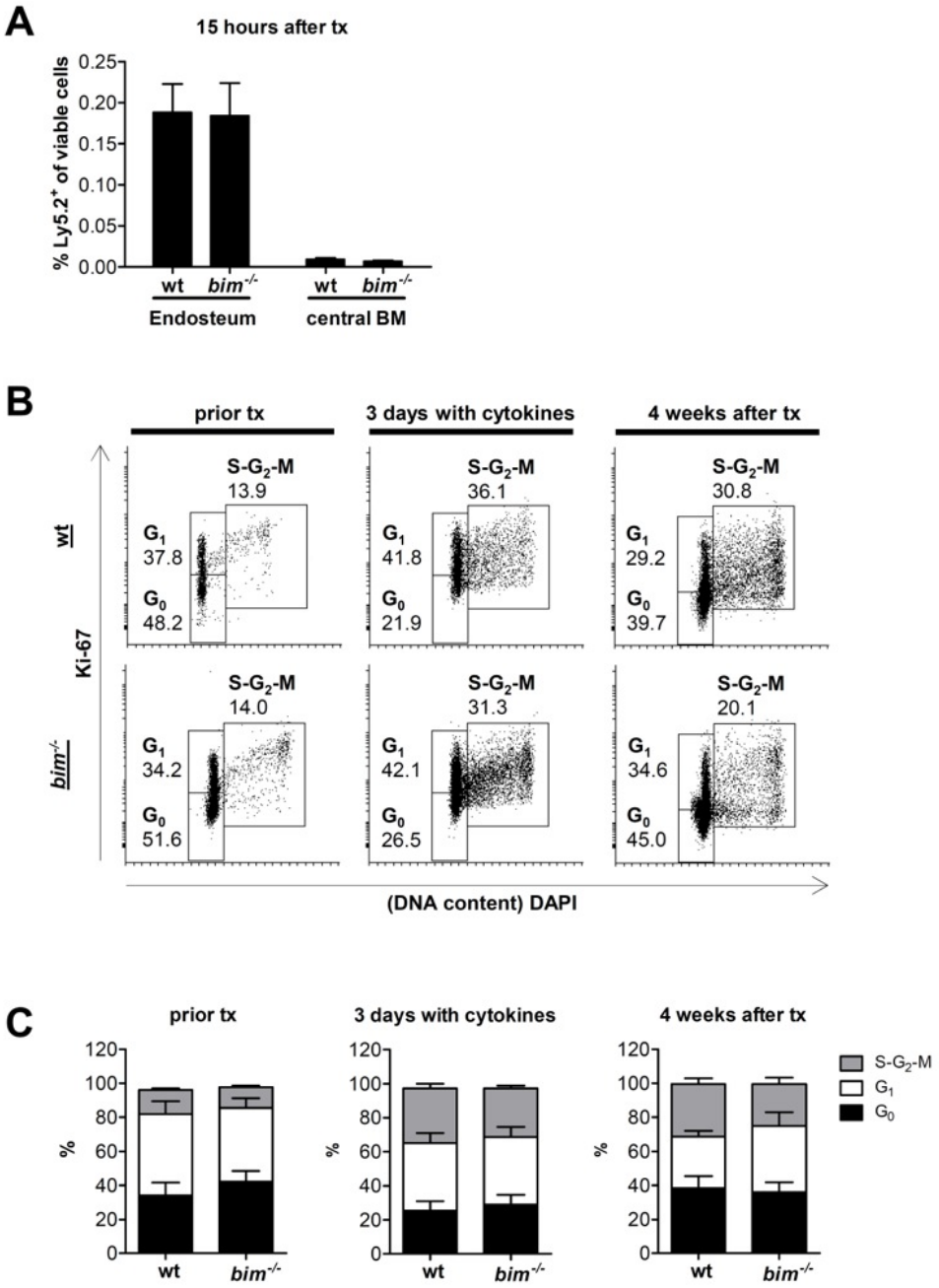

Figure 3.6: Knockout of Bim does not influence homing or proliferation potential of LSK cells - (A) Homing ability was analyzed 15 h after transplantation of lethally irradiated Ly5.1$^+$ recipient mice reconstituted with wt or *bim*$^{-/-}$ LSK cells. Mice were sacrificed and the endosteum as well as central BM were stained with antibodies against Ly5.1 and Ly5.2 and analyzed by flow cytometry (n=6-8). (B-C) Proliferation potential of wt and *bim*$^{-/-}$ LSK cells was tested directly after isolation from donor mice (prior tx; n=3), 4 weeks after tx (n=3-4) and 3 days after *in vitro* cultivation with TPO, SCF and Flt3L (n=4). LSK cells were stained with an anti-Ki-67 antibody and DAPI and analyzed by flow cytometry. Bars represent means +/-SEM of two (A) and three (C) independent experiments. No significant differences were observed (Mann-Whitney-test). tx: transplantation.

3.2 Bim and Bmf have conserved functions between murine and human HSPCs

Next we asked whether BIM and BMF are also important in the regulation of cytokine deprivation-induced apoptosis in human HSPCs. Human studies were performed with cord blood (CB) derived $CD34^+$ cells. This cell population is enriched for HSPCs and used for haploidentical transplantations in the clinic. In contrast to LSK cells, human $CD34^+$ cells were less sensitive to cytokine deprivation-induced apoptosis (compare Figure 3.3 and Figure 3.7).

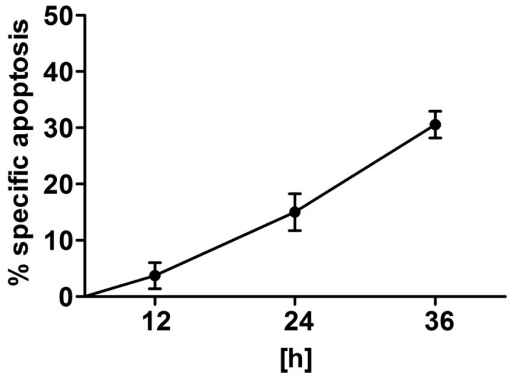

Figure 3.7: Cytokine withdrawal induces apoptosis in human $CD34^+$ cells - Human $CD34^+$ cells were freshly isolated from CB and cultured in the presence and absence of cytokines. Apoptosis was determined at the indicated time points by FACS analysis of Annexin V and 7-AAD stained cells. Specific apoptosis was calculated as indicated in the method section. Data represent mean values +/-SEM of three independent experiments with n=3-4.

To test the relevance of BH3-only proteins in human HSPCs for cytokine withdrawal mediated cell death, freshly isolated $CD34^+$ cells were cultured for 14 h with or without the cytokines TPO (10 ng/ml), SCF, Flt3L and IL6 (100 ng/ml each). RT-MLPA® was used to detect mRNA expression changes of BCL-2 family members (Figure 3.8) as well as various apoptosis-related genes (Table 3.2) in the absence or presence of cytokines. In comparison to LSK cells (Figure 3.1), upregulation of BH3-only proteins upon cytokine deprivation was more restricted in $CD34^+$ cells. Only BIM (2.1-fold), BMF (9.5 fold) and to a minor extend PUMA (1.6-fold) were upregulated (Figure 3.8 left panel). Simultaneously their anti-apoptotic antagonists BCL-XL and A1 were significantly downregulated (0.4-fold and 0.6-fold, respectively). These data were independently confirmed by qRT-PCR (Figure 3.9). Significant upregulation of mRNA expression was only observed for BIM and BMF.

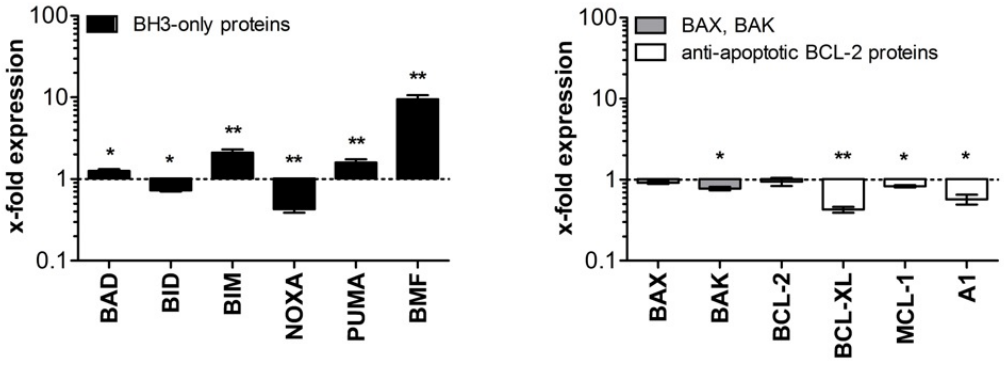

Figure 3.8: Expression of BCL-2 family members in cytokine deprived human CD34⁺ cells - Human CD34⁺ cells were freshly isolated from CB and cultured for 14 h with or without TPO (10 ng/ml), SCF, Flt3L and IL6 (100 ng/ml each). mRNA levels of BH3-only proteins (left panel), BAX, BAK and antiapoptotic BCL-2 proteins (right panel) were analyzed by RT-MLPA®. x-fold expression of mRNA levels in the absence of cytokines compared to mRNA levels in the presence of cytokines (=1) is shown. Data represent mean values +/-SEM of n=7 from five independent experiments. Significant p-values (Mann-Whitney-test): BAD p=0.05; BID p=0.02; BIM p=0.009; NOXA p=0.002; PUMA p=0.009; BMF p=0.002; BAK p=0.05; BCL-XL p=0.002; MCL-1 p=0.05; A1 p=0.03.

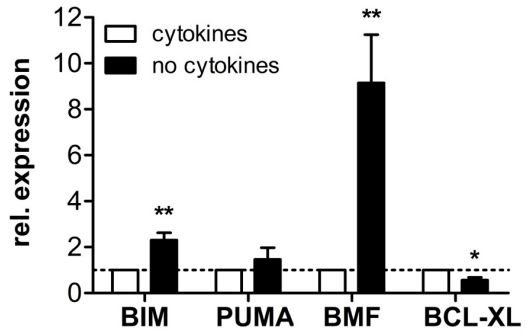

Figure 3.9: Validation of RT-MLPA® data by qRT-PCR - Human CD34⁺ cells were freshly isolated from CB and cultured for 14 h with or without TPO (10 ng/ml), SCF, Flt3L and IL6 (100 ng/ml each). mRNA levels of BIM, BMF and BCL-XL were analyzed by qRT-PCR. Relative expression of mRNA levels in the absence of cytokines compared to mRNA levels in the presence of cytokines is shown. Data represent mean values +/-SEM with n=3-5 of three independent experiments. Significant differences (Mann-Whitney-test) compared to cytokine treated cells: BIM p=0.01; BMF p=0.01; BCL-XL p=0.02.

The mRNA levels of BAX and BAK (Figure 3.8 right panel) as well as other genes analyzed (Table 3.2) remained largely unchanged with the notable exception of those of NAIP and BNIP-3L which were upregulated 4 fold and Survivin which was downregulated 3 fold.

Table 3.2: Expression of apoptosis-related genes in cytokine-deprived human CD34⁺ cells

- cytokines/ + cytokines	Mean ±SEM	p-value	- cytokines/ + cytokines	Mean ±SEM	p-value
BNIP-3L	4.13 ±0.35	0.002	NAIP	3.94 ±0.80	0.002
BNIP-3	1.29 ±0.14	0.11	cIAP1	1.66 ±0.08	0.03
BCL-RAMBO	1.11 ±0.06	0.18	cIAP2	1.29 ±0.12	0.22
BCL-W	1.12 ±0.19	0.85	XIAP	1.20 ±0.08	0.08
DR-6	1.04 ±0.09	0.57	Survivin	0.27 ±0.02	0.002
FAS	1.64 ±0.32	0.14	Apollon	0.93 ±0.06	0.22
AIF	0.80 ±0.07	0.14	FLIP	2.18 ±0.19	0.002
APAF1	1.49 ±0.15	0.02	SERPIN-B	0.95 ±0.04	0.95
SMAC/DIABLO	0.84 ±0.06	0.18	p21	0.54 ±0.10	0.02
OMI	1.26 ±0.06	0.11	GUSB	1.16 ±0.04	0.06
PERFORIN	0.86 ±0.58	0.75	PARN	0.71 ±0.05	0.18

Human CD34⁺ cells were freshly isolated from CB and cultured for 14 h with or without TPO (10 ng/ml), SCF, Flt3L and IL6 (100 ng/ml each). mRNA levels of the indicated genes were analyzed by RT-MLPA®. x-fold expression of mRNA levels in the absence of cytokines compared to mRNA levels in the presence of cytokines is shown. Data represent mean values +/-SEM of n=7 from five independent experiments. P-values were calculated with Mann-Whitney-test.

In addition, CD34⁺ cells were cultured with single cytokines for 4 days. As shown in Figure 3.10 SCF or Flt3L alone were sufficient to protect CD34⁺ cells from apoptosis. A closer look at the mRNA levels of BIM and BMF after exposure to single cytokines revealed that BIM induction was almost completely repressed by SCF, whereas BMF induction was diminished by either SCF or Flt3L (Figure 3.11). TPO had no effect on the expression of BIM or BMF. Accordingly, TPO had no protective effects on the *in vitro* survival of CD34⁺ cells (Figure 3.10).

Together, these findings indicate that BIM and BMF trigger apoptosis upon cyotkine deprivation in human CD34⁺ cells. This is in line with the data obtained in murine LSK cells and suggests a conserved function of BIM and BMF between murine and human HSPCs.

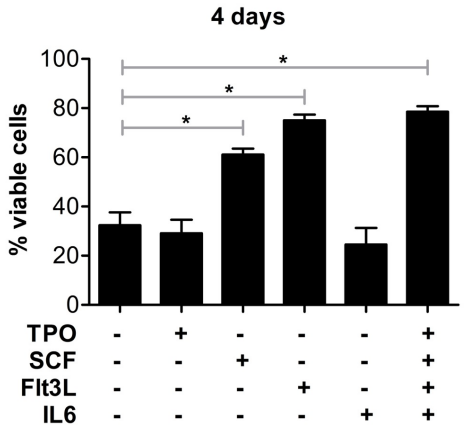

Figure 3.10: SCF or Flt3L alone protect human CD34⁺ cells from cytokine deprivation-induced apoptosis - CB derived CD34⁺ cells were cultured for 4 days with the indicated cytokines. Apoptosis was determined by FACS analysis of Annexin V and 7-AAD stained cells. Percentages of viable cells are shown (Annexin V- and 7-AAD-). Data represent mean values +/-SEM of three independent experiments with n=3-5. Significant p-values (Mann-Whitney-test): no cytokines versus SCF, p=0.03; no cytokines versus Flt3L, p=0.05; no cytokines versus all cytokines, p=0.03.

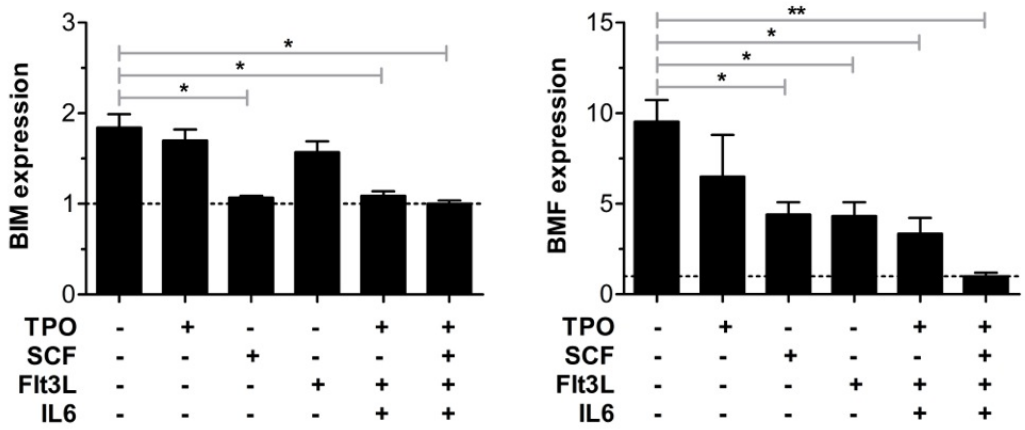

Figure 3.11: Expression of BIM and BMF in human CD34⁺ cells cultured under various conditions - CD34⁺ cells were freshly isolated from CB and cultured for 14 h with serum and 10 ng/ml TPO, 100 ng/ml SCF, Flt3L or IL6 alone or combinations thereof (as indicated). BIM and BMF expression were analyzed by RT-MLPA®. Data represent mean values +/-SD with n=3-7 of three independent experiments. Significant differences (Mann-Whitney-test) compared to complete cytokine deprivation: BIM expression: +SCF p=0.03, +TPO/Flt3L/IL6 p=0.05, all cytokines p=0.03; BMF expression: +SCF p=0.03, +Flt3L p=0.01, +TPO/Flt3L/IL6 p=0.03, all cytokines p=0.002.

3.3 BH3-only protein mRNA induced in human HSPCs is cell stress dependent

To gain further insight into the regulation of BH3-only proteins in human HSPCs, other typical stimuli that are known to trigger the intrinsic apoptosis pathway were applied to CD34$^+$ cells. As shown in Figure 3.12 human HSPCs were highly sensitive to DNA damage-induced apoptosis triggered by γ-irradiation, the topoisomerase II inhibitor etoposide or the DNA alkylating agent treosulfan (Hande *et al.*, 1998; Lanvers-Kaminsky *et al.*, 2006). Furthermore, CD34$^+$ cells underwent apoptosis upon exposure to taxol, which stabilizes microtubules and thereby inhibits mitosis (Xiao *et al.*, 2006). Apoptosis was also induced in CD34$^+$ cells upon tunicamycin treatment, an agent inducing ER-stress by inhibiting N-linked glycosylation of lumenal ER proteins (Zou *et al.*, 2009).

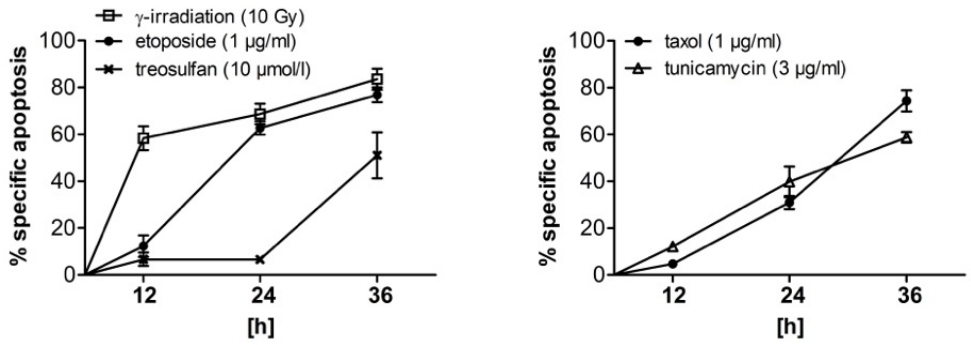

Figure 3.12: CD34$^+$ cells undergo apoptosis in response to cytotoxic agents - Human CD34$^+$ cells were freshly isolated from CB and cultured for 24 h with cytokines (10 ng/ml TPO, 100 ng/ml SCF, Flt3L and IL6) followed by exposure to γ-irradiation, etoposide, treosulfan, taxol or tunicamycin. Apoptosis was determined by FACS analysis of Annexin V and 7-AAD stained cells at the indicated time points. Percentage of specific apoptosis was calculated as indicated in the method section. Data represent mean values +/-SEM of n=3-5 from at least three independent experiments

The relevance of BH3-only proteins in CD34$^+$ cells for DNA damage, ER-stress or microtubule stabilization mediated cell death was determined by mRNA expression analysis using RT-MLPA®. After cultivating freshly isolated CD34$^+$ cells for 24 h with cytokines (10 ng/ml TPO, 100 ng/ml SCF, Flt3L and IL6) and exposing them to the above mentioned cell death stimuli for 4 h (treosulfan for 14 h), RNA was isolated and mRNA levels of BCL-2 family members (Figure 3.13) and other apoptosis-related genes (Table 3.3) were determined. Expression analysis revealed that PUMA is highly induced upon DNA damage (etoposide: 14-fold; γ-irradiation: 20-fold; treosulfan: 8-fold), which is in line with previously published data (Erlacher *et al.*, 2005; Villunger *et al.*, 2003b) (Figure 3.13A). This PUMA induction was confirmed on the protein level

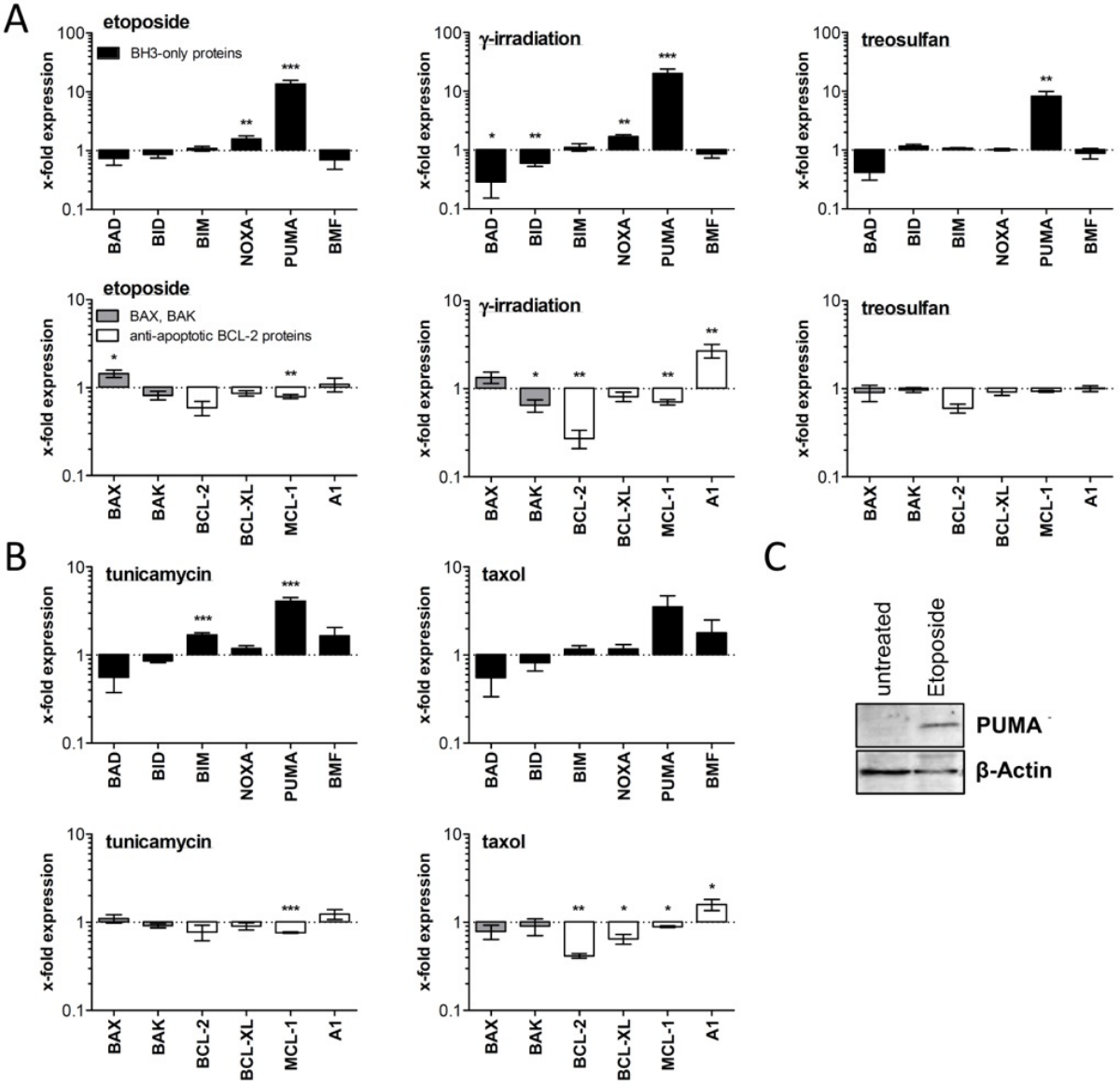

Figure 3.13: Expression of BCL-2 family members in CD34⁺ cells exposed to cytotoxic drugs - Freshly isolated CD34⁺ cells were cultured for 24 h with cytokines and exposed to (A) DNA damage inducing agents like etoposide (1 μg/ml) or γ-irradiation (10 Gy) for 4 h or to treosulfan (10 μmol/l) for 14 h and to the (B) ER-stress inducing agent tunicamycin (3 μg/ml) or the microtubuli stabilisator taxol (1 μg/ml) for 4 h. mRNA levels of the indicated BCL-2 family members were analyzed by RT-MLPA®. x-fold expression of mRNA levels in the presence of death stimuli compared to mRNA levels in the absence of death stimuli (=1) is shown. Data represent mean values +/-SEM with n=4-10 of four independent experiments. (C) Upregulation of PUMA on protein level. Significant p-values (Mann-Whitney-test) for etoposide: NOXA p=0.01; PUMA p=0.0002; BAX p=0.03; MCL-1 p=0.003; for γ-irradiation: BAD p=0.02; BID p=0.003; NOXA p=0.005; PUMA p=0.001; BAK p=0.02; BCL-2 p=0.002; MCL-1 p=0.002; A1 p=0.01; for treosulfan: PUMA p=0.003; for tunicamycin: BIM, PUMA, MCL-1 p=0.001; for taxol: BCL-2 p=0.01; BCL-XL p=0.02; MCL-1 p=0.02; A1 p=0.05.

Table 3.3: Expression of apoptosis-related genes in CD34⁺ cells exposed to stimuli inducing the intrinsic apoptosis pathway

	etoposide		γ-irradiation		treosulfan		taxol		tunicamycin	
- cytok./ + cytok.	Mean ± SEM	P	Mean ± SEM	P	Mean ± SEM	P	Mean ± SEM	P	Mean ± SEM	p
BNIP-3L	0.56 ±0.06	0.03	0.43 ±0.06	0.01	0.70 ±0.10	0.39	1.07 ±0.43	0.89	0.85 ±0.07	0.56
BNIP-3	0.65 ±0.16	0.12	0.42 ±0.04	0.003	0.68 ±0.08	0.95	0.56 ±0.04	0.09	0.62 ±0.12	0.10
BCL-RA.	1.00 ±0.08	0.87	1.08 ±0.10	>0.99	0.99 ±0.02	0.74	1.08 ±0.09	0.67	1.61 ±0.08	0.002
BCL-W	1.35 ±0.28	0.33	1.37 ±0.16	0.23	0.94 ±0.11	0.32	2.01 ±0.68	0.16	2.26 ±0.42	0.03
DR-6	0.56 ±0.62	0.01	0.23 ±0.03	0.001	0.77 ±0.08	0.05	1.74 ±0.61	0.23	0.52 ±0.03	0.001
MOAP1	0.70 ±0.08	0.02	0.60 ±0.04	0.01	0.90 ±0.10	0.40	0.83 ±0.05	0.32	0.73 ±0.03	0.05
B2M	0.66 ±0.08	0.05	0.37 ±0.01	0.001	0.94 ±0.05	0.64	0.80 ±0.24	0.26	0.61 ±0.02	0.10
AIF	0.76 ±0.07	0.03	0.55 ±0.03	0.002	0.89 ±0.10	0.39	0.74 ±0.08	0.07	1.10 ±0.07	0.49
APAF1	0.76 ±0.06	0.02	0.89 ±0.09	0.39	0.81 ±0.02	0.13	1.13 ±0.17	0.89	0.95 ±0.04	0.92
SMAC	0.81 ±0.08	0.07	0.95 ±0.08	0.75	1.11 ±0.02	0.84	0.98 ±0.23	0.89	1.09 ±0.06	0.44
OMI	0.57 ±0.04	0.0003	0.41 ±0.04	0.001	0.79 ±0.03	0.10	0.84 ±0.04	0.16	0.78 ±0.04	0.01
CTLA1	0.58 ±0.10	0.10	1.40 ±0.37	0.45	0.54 ±0.13	0.32	0.56 ±0.36	0.12	0.60 ±0.08	0.05
NAIP	0.74 ±0.10	0.10	1.74 ±0.41	0.13	1.38 ±0.07	0.01	0.84 ±0.28	0.48	1.43 ±0.13	0.02
cIAP2	1.37 ±0.23	0.12	2.18 ±0.29	0.01	1.10 ±0.18	0.64	1.92 ±0.20	0.02	1.74 ±0.37	0.14
XIAP	0.88 ±0.07	0.22	0.91 ±0.13	0.28	1.00 ±0.02	0.95	1.14 ±0.20	0.16	1.46 ±0.05	0.001
Survivin	0.55 ±0.06	0.001	0.52 ±0.06	0.002	0.90 ±0.05	0.26	0.74 ±0.37	0.67	0.79 ±0.06	0.05
Apollon	0.74 ±0.06	0.02	0.61 ±0.09	0.01	1.10 ±0.05	0.55	0.95 ±0.08	0.78	0.80 ±0.03	0.04
FLIP	0.68 ±0.08	0.003	0.64 ±0.11	0.01	1.04 ±0.04	0.55	1.00 ±0.13	0.57	0.81 ±0.08	0.04
SERP.-B	0.91 ±0.09	0.68	1.03 ±0.15	0.83	1.19 ±0.04	0.26	1.13 ±0.22	0.89	1.13 ±0.08	0.56
p21	7.45 ±0.61	0.0002	6.20 ±0.75	0.001	3.40 ±0.77	0.003	2.63 ±0.61	0.02	0.62 ±0.04	0.10
GUSB	0.66 ±0.08	0.01	0.60 ±0.05	0.005	0.99 ±0.05	0.95	0.71 ±0.08	0.03	0.90 ±0.04	0.28
PARN	0.76 ±0.05	0.01	0.66 ±0.06	0.003	1.00 ±0.05	0.32	0.97 ±0.10	>0.99	1.20 ±0.02	0.01

Freshly isolated CD34⁺ cells were cultured for 24 h with cytokines and exposed to etoposide (1 μg/ml for 4 h), γ-irradiation (10 Gy for 4 h), treosulfan (10 μmol/l for 14 h), tunicamycin (3 μg/ml for 4 h) or taxol (1 μg/ml for 4 h). mRNA levels of the indicated genes were analyzed by RT-MLPA®. x-fold expression of mRNA levels in the presence of death stimuli compared to mRNA levels in the absence of death stimuli is shown. Data represent mean values +/-SEM with n=4-10 of four independent experiments. P-values were calculated using Mann-Whitney-test. BCL-RA.=BCL-RAMBO; SERP.-B=SERPIN-B

(Figure 3.13C). Etoposide and γ-irradiation led to a further upregulation of the second p53 target NOXA (etoposide: 1.6-fold; γ-irradiation: 1.7-fold) together with a simultaneous downregulation of their antagonists BCL-2 and to a minor extend MCL-1 (Figure 3.13A). In contrast, the ER stressor tunicamycin significantly increased the mRNA levels of PUMA (4.1-fold) and BIM (1.7-fold) (Figure 3.13B), which is consistent with recently published data, showing that Puma and Bim cooperate in tunicamycin-induced apoptosis (Erlacher *et al.*, 2006). MCL-1 was downregulated upon tunicamycin treatment. Exposure of $CD34^+$ cells to the mitotic inhibitor taxol induced upregulation of PUMA (3.5-fold) and simultaneous downregulation of BCL-2, BCL-XL and MCL-1 (Figure 3.13B). Interestingly, the pro-survival protein A1 (1.6-fold) was upregulated upon taxol treatment. Furthermore the mRNA level of DR-6 was significantly downregulated upon γ-irradiation, wherease the p53 target and cell cylce inhibitor p21 was highly upregulated in $CD34^+$ cells after exposure to etoposide, γ-irradiation, treosulfan as well as taxol (Table 3.3).

Thus, the results so far demonstrate that BH3-only proteins are important for regulation of apoptosis in human HSPCs, and that mRNA induction strongly depends on the cell death stimulus.

3.4 Stable modulation of the BCL-2 rheostat

3.4.1 Knockdown of BIM but not BMF partially inhibits cytokine deprivation-induced apoptosis in human HSPCs *in vitro*

In order to validate the relevance of BIM and BMF for cytokine deprivation-induced apoptosis in human HSPCs, we next examined whether downregualtion of BIM or BMF prolongs the survival of $CD34^+$ cells *in vitro*. Therefore, $CD34^+$ cells were transduced with lentiviruses expressing shRNA specific for BIM or BMF (Figure 3.14). Lentiviral expression of shRNA targeting Luciferase gene was used as a negative control. As a positive control the anti-apoptotic BCL-2-family members BCL-XL and BCL-2, which inhibit both BIM and BMF, were overexpressed

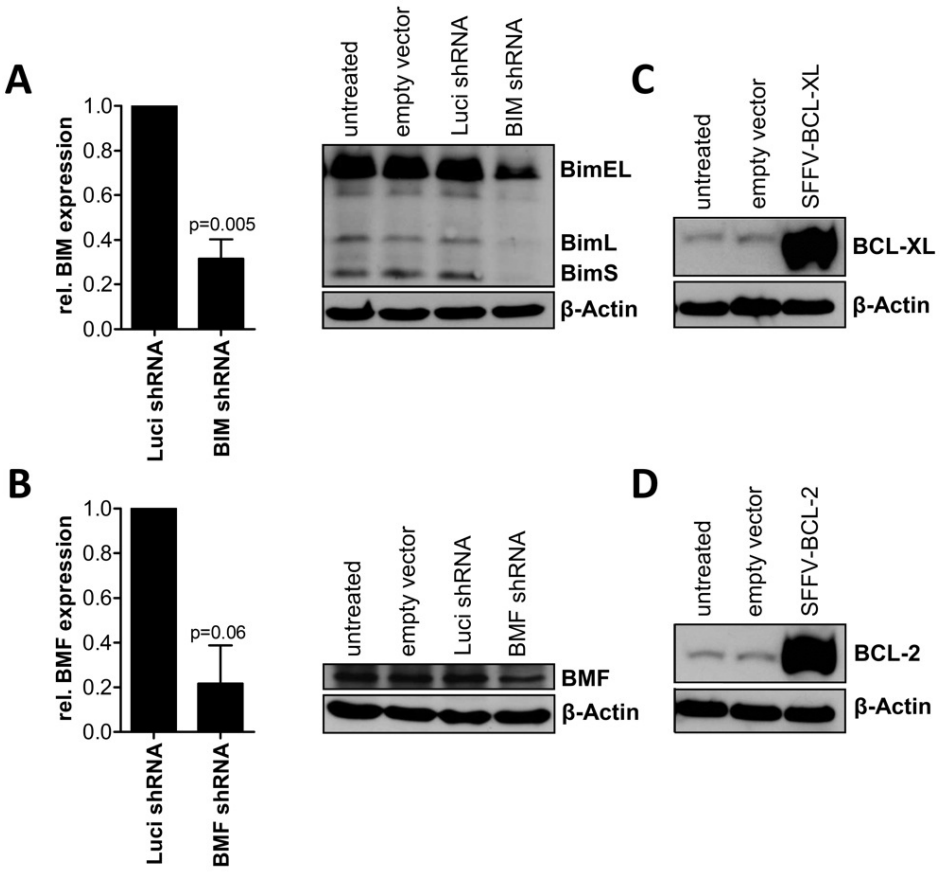

Figure 3.14: Efficient downregulation of BIM or BMF and overexpression of BCL-XL or BCL-2 in lentivirally transduced human $CD34^+$ cells - Cord blood derived human $CD34^+$ cells were transduced with lentiviruses expressing shRNA against BIM or BMF or overexpressing BCL-2 or BCL-XL. After sorting for GFP^+ cells, the RNAi efficacy was tested for both vectors on mRNA as well as on protein level using qRT-PCR and Western blot analysis (A/B). Upregulation of BCL-XL or BCL-2 in GFP^+CD34^+ cells is shown (C/D). β-Actin served as a loading control. Bars represent mean values +/-SD with n=3-5 of three independent experiments. BIM shRNA led to significant downregulation of BIM expression (Mann-Whitney-test).

under the control of the SFFV promotor using the pIG vector. The empty pIG vector served as a negative control for overexpression analysis. The RNAi efficacy was determined in sorted GFP$^+$CD34$^+$ cells by qRT-PCR and Western blot analysis. As shown in Figure 3.14A/B shRNA against BIM or BMF led to downregulation of BIM (69%) or BMF (78%) on mRNA level as well as on protein level. Furthermore, BCL-XL and BCL-2 were highly upregulated in GFP$^+$CD34$^+$ cells transduced with lentiviruses expressing the according genes under control of the SFFV promoter (Figure 3.14C/D).

Next, survival assays were performed with sorted GFP$^+$CD34$^+$ cells. In line with the findings in murine HSPCs, knockdown of BIM prolonged the survival of human HSPCs within the first 2 days of cytokine deprivation. However, the protection observed in CD34$^+$ cells was only weak and completely gone after 4 days of cytokine deprivation, whereas BCL-2 or BCL-XL overexpression efficiently increased survival after 2 or even 4 days of culture without cytokines (Figure 3.15).

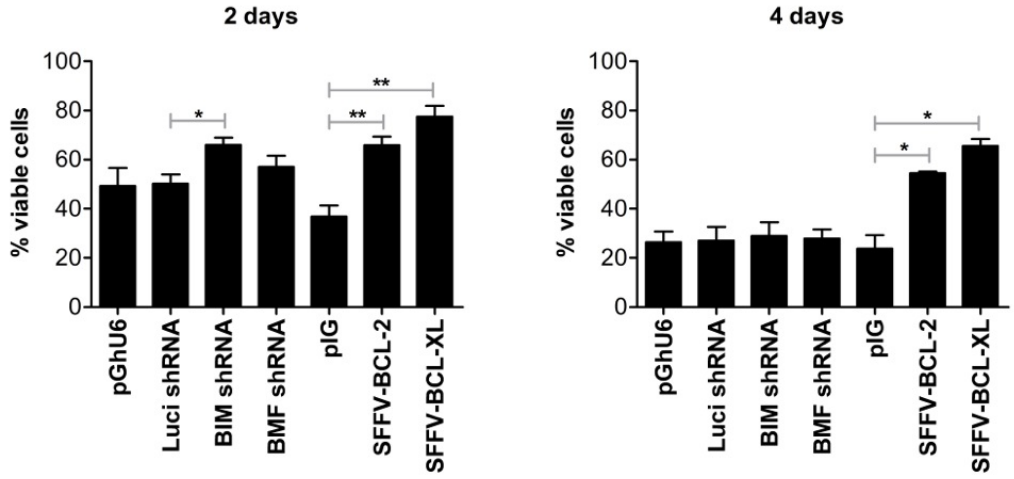

Figure 3.15: Downregulation of BIM but not BMF partially protects CD34$^+$ cells from cytokine deprivation-induced apoptosis *in vitro* - Lentivirally transduced CD34$^+$ cells were sorted for GFP expression and cultured for 2 or 4 days in the absence of cytokines. Apoptosis was determined by FACS analysis of Annexin V and 7-AAD stained cells. Percentage of viable cells is shown. Bars represent mean values +/-SEM with n=4-5 of three independent experiments. Significant p-values (Mann-Whitney-test): 2 days: Luci shRNA versus BIM shRNA p=0.03; pIG versus BCL2 and pIG versus BCL-XL p=0.01; 4 days: pIG versus BCL-2 and pIG versus BCL-XL p=0.05.

Similar to our mouse data, BMF downregulation did not play any role in cytokine deprivation-induced apoptosis in human HSPCs *in vitro*. Interestingly, a prolonged survival was observed when BIM expression was inhibited in CD34$^+$ cells cultured in the presence of SCF alone (4 days) as depicted in Figure 3.16. This effect was however not observed when BIM knockdown

CD34+ cells were cultured in TPO, Flt3L or IL6. Overexpression of BCL-XL increased the survival of CD34+ cells in the presence of either TPO, SCF, Flt3L or IL6 (data not shown).

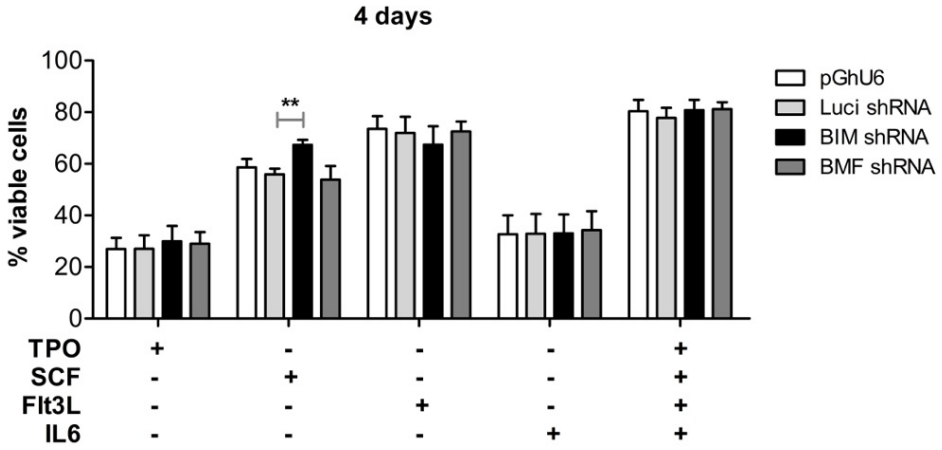

Figure 3.16: Downregulation of BIM in combination with SCF treatment increases survival of CD34+ cells - Lentivirally transduced CD34+ cells were sorted for GFP expression and cultured for 4 days in the presence of the indicated cytokines. Apoptosis was determined by FACS analysis of Annexin V and 7-AAD stained cells. Bars represent mean values +/-SEM of three independent experiments with n=3-5. Significant differences were observed between Luci shRNA versus BIM shRNA p=0.01 (Mann-Whitney-test).

In order to further analyze the protection conferred by BIM shRNA during longer periods of culture, we performed colony-forming unit (CFU) assays as described in the method section. Colony viability was determined after 14 days by FACS analysis of 7-AAD and Annexin V stained cells (Figure 3.17). Surprisingly, significantly more viable cells were found within colonies originated from CD34+ cells expressing shRNA specific for BIM or overexpressing BCL-2 or BCL-XL. This effect was still visible on day 31 after cells were replated.

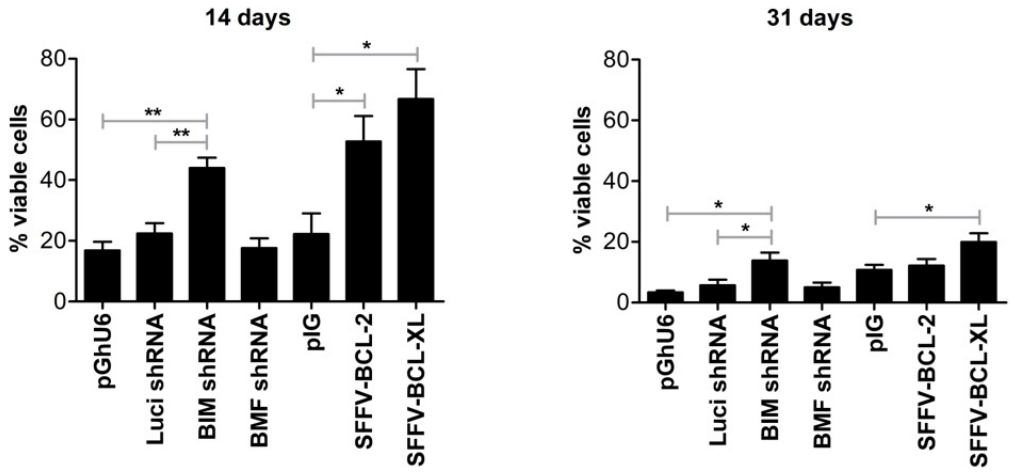

Figure 3.17: Downregulation of BIM but not BMF protects CD34⁺ cells from apoptosis induced during long term cultivation in Methocult® medium - Lentivirally transduced CD34⁺ cells were sorted for GFP expression and cultured in Methocult medium supplemented with cytokines. Following 14 days of culture cells were analyzed for apoptosis, while part of the cells were replated and cultured for another 17 days. Apoptosis was determined by FACS analysis of Annexin V and 7-AAD stained cells. Percentage of viable cells (Annexin V- and 7-AAD-) is shown. Bars represent mean values +/-SEM of n=4-8 from at least four independent experiments (14 days) and n=3-6 of three independent experiments (31 days). Significant p-values (Mann-Whitney-test): 14 days: pGhU6 versus BIM shRNA and Luci versus BIM shRNA p=0.003; pIG versus BCL-2 and pIG versus BCL-XL p=0.03; 31 days: pGhU6 versus BIM shRNA p=0.02; Luci shRNA versus BIM shRNA p=0.03; pIG versus BCL-XL p=0.05.

Taken together, these results demonstrate that reduced BIM levels partially protect CD34⁺ cells from apoptosis induced by complete cytokine deprivation or cytokine decline during long-term cultivation. Furthermore, survival assays suggest that the knockdown of BIM obtained by RNAi is synergised by SCF mediated inhibition of BIM induction (Figure 3.16 and Figure 3.11). In contrast, BMF knockdown does not protect human HSPCs subjected to cytokine withdrawal.

3.4.2 BIM or BMF downregulation does not influence HSPC differentiation

Next, we investigated whether downregulation of BIM or BMF affected human HSPC differentiation. We therefore performed CFU assays as described in the method section. In brief, GFP^+CD34^+ cells were cultured in Methocult® medium supplemented with cytokines for 11 days followed by quantification of mixed (GEMM), myeloid (GM, M, G) and erythroid (E) colonies by light microscopy. No significant differences were observed in the colony formation between all the groups analyzed (Figure 3.18). Thus, HSPC differentiation is neither affected by lentiviral transduction nor by the expression of BIM- or BMF-specific shRNA.

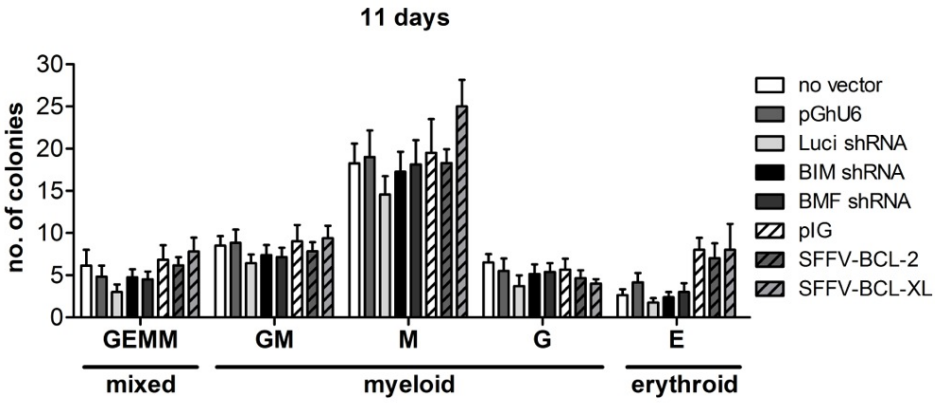

Figure 3.18: Downregulation of BIM or BMF does not influence $CD34^+$ cell differentiation - Lentivirally transduced $CD34^+$ cells were sorted for GFP expression and cultured for 11 days in Methocult® medium supplemented with G-CSF, GM-CSF, IL3, IL6 and EPO. Mixed, myeloid and erythroid colonies were quantified by light microscopy based on their morphology (Colony-forming units (CFU): GEMM=granulocyte, erythrocyte, macrophage, megakaryocyte; GM=granulocyte, macrophage; Colony/Burst-forming units: E=erythroid;). Bars represent mean values of n=6-8 of five independent experiments +/-SEM. No significant differences were observed (Mann-Whitney-test).

3.4.3 Analysis of human HSPCs in a humanized mouse model

In addition to the *in vitro* studies we performed *in vivo* assays to gain further insight into the role of BIM and BMF for apoptosis signaling in human HSPCs. Initially we established and optimized a transplantation protocol to get efficient human engraftment in xenograft recipient mice. We chose newborn *rag2*$^{-/-}\gamma c^{-/-}$ recipient mice according to the protocol published by Traggiai (Traggiai *et al.*, 2004). In brief, CD34$^+$ cells were injected into the liver of sublethally irradiated *rag2*$^{-/-}\gamma c^{-/-}$ mice within their first week of life. Before transplantation, CD34$^+$ cells were cultured in the presence of TPO (50 ng/ml), SCF and Flt3L (100 ng/ml each) with or without IL3 (20 ng/ml) according to a protocol of Choi (Choi *et al.*, 2008). 8 weeks after transplantation mice were sacrificed and the percentage of human CD45$^+$ cells was analyzed in the liver, BM, spleen and thymus by flow cytometry.

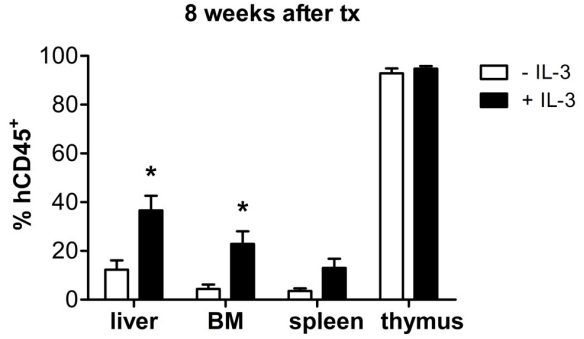

Figure 3.19: Enhanced human engraftment after *ex vivo* culture of CD34$^+$ cells in the presence of IL3 - Human CB derived CD34$^+$ cells were cultured for 3 days in the presence or absence of IL3 (20 ng/ml) combined with TPO (50 ng/ml), SCF and Flt3L (100 ng/ml each). The progeny of 10^5 cells was transplanted into the liver of 3 day old *rag2*$^{-/-}\gamma c^{-/-}$ mice. 8 weeks later animals were sacrificed and the percentage of human CD45$^+$ cells was determined in the indicated haematopoietic organs. n=5-6 mice from two independent experiments. Significant differences (Mann-Whitney-test) between the percentage of CD45$^+$ cells arising from CD34$^+$ cells cultured with or without IL3 prior to transplantation were obtained in the liver and BM (p=0.03) 8 weeks later.

In line with the data published by Choi et al. (Choi et al. 2008) human HSPC engraftment was highly increased when donor cells were cultured in the presence of IL3 before transplantation (Figure 3.19). Thus, for all further experiments, CD34$^+$ cells were cultured in the presence of TPO (50 ng/ml), SCF, Flt3L (100 ng/ml each) and IL3 (20 ng/ml). Pre-transplantation culture was required to allow lentiviral transduction of CD34$^+$ cells.

3.4.4 Increased reconstitution potential of human CD34+ cells with reduced levels of BIM or BMF

Next we asked whether the prolonged survival observed in human CD34+ cells expressing BIM shRNA *in vitro* may also be relevant *in vivo* and increase reconstitution efficiency. Because of the above described results observed in wt:*bmf*$^{-/-}$ chimeric mice and since BMF was highly upregulated (9.5-fold) upon cytokine deprivation in human cells as well (Figure 3.8), we also examined the role of BMF in human HSPCs *in vivo*.

Based on the humanized mouse model established before, the progeny of 10^5 lentivirally transduced CD34+ cells were transplanted into the liver of sublethally irradiated *rag2*$^{-/-}\gamma c^{-/-}$ mice within their first week of life. The transduction efficiency of donor cells, indicated by the percentage of GFP+ cells, was determined by flow cytometry directly prior to transplantation (Figure 3.20) and was comparable between CD34+ cells expressing shRNA specific for Luciferase (Luci), BIM or BMF or between pIG (empty vector) and BCl-2 overexpressing CD34+ cells.

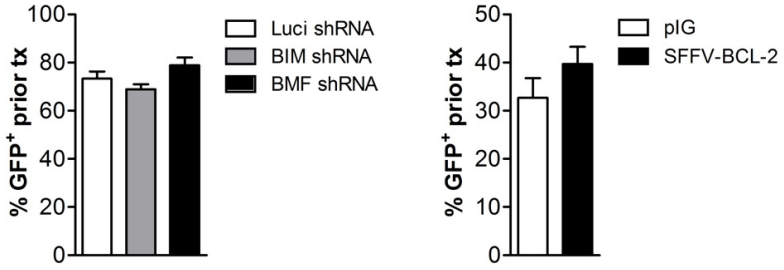

Figure 3.20: Comparable transduction efficiency before transplantation - After 1 day of culture CB derived human CD34+ cells were transduced twice (24 h and MOI=10 each) with the indicated lentiviruses. After 2nd infection the percentage of GFP+ cells was analyzed by flow cytometry. Bars represent mean values +/-SEM of n=7-14 mice from four to six independent experiments (left panel) and of n=4 mice from two independent experiments (right panel). No significant differences were observed (Mann-Whitney-test).

8 weeks after intrahepatic transplantation mice were sacrificed and the human engraftment, defined by the percentage of human CD45+ cells, was determined by flow cytometry in the liver and in the haematological organs BM, spleen and thymus. As shown in Figure 3.21B the proportion of human CD45+ cells was comparable in all recipient mice, independently of the lentiviruses used and organs analyzed. However, we observed a substantially increased number of GFP+ cells within the human CD45+ cell-populations, when cells expressed BIM or BMF shRNAs (Figure 3.21C left panel; BM: 29% Luci shRNA, 55% BIM shRNA, 63% BMF shRNA

expressing hCD45$^+$ cells). This effect was observed in all organs analyzed. Transplantation of BCL-2 overexpressing CD34$^+$ cells (Figure 3.21B/C right panel) provided similar results, being advantageous in reconstitution as compared to the control group.

Significant competitive advantages of CD34$^+$ donor cells expressing BIM or BMF shRNAs were also found in differentiated CD33$^+$ myeloid cells as well as in CD19$^+$ B-cells isolated from liver, BM and spleen (Figure 3.22). Interestingly, significantly increased percentages of GFP$^+$ cells expressing BIM or BMF shRNAs were already present in immature human CD34$^+$ cells. (Figure 3.23 left panel; liver: 35% Luci shRNA, 57% BIM shRNA, 58% BMF shRNA expressing hCD34$^+$ cells; BM: 22% Luci shRNA, 65% BIM shRNA, 67% BMF shRNA expressing hCD34$^+$ cells; spleen: 26% Luci shRNA, 55% BIM shRNA, 56% BMF shRNA expressing hCD34$^+$ cells). Again BCL-2 expressing cells behaved similarly to those expressing shRNAs against BIM or BMF (Figure 3.23 right panel). Unfortunately, very immature haematopoietic cells (CD34$^+$38$^-$ cells) could not be analyzed in detail due to very low cell numbers available.

Taken together, these findings lend strong support to the results obtained from murine transplantation experiment and indicate a conserved function of BIM and BMF in murine and human cells (compare Figure 3.4 with Figure 3.23). Since overexpression of their antagonist BCL-2 did not exceed the effects observed upon downregulation of either BH3-only protein, BIM and BMF seem to be the major BH3-only proteins involved in the reconstitution-associated cell death.

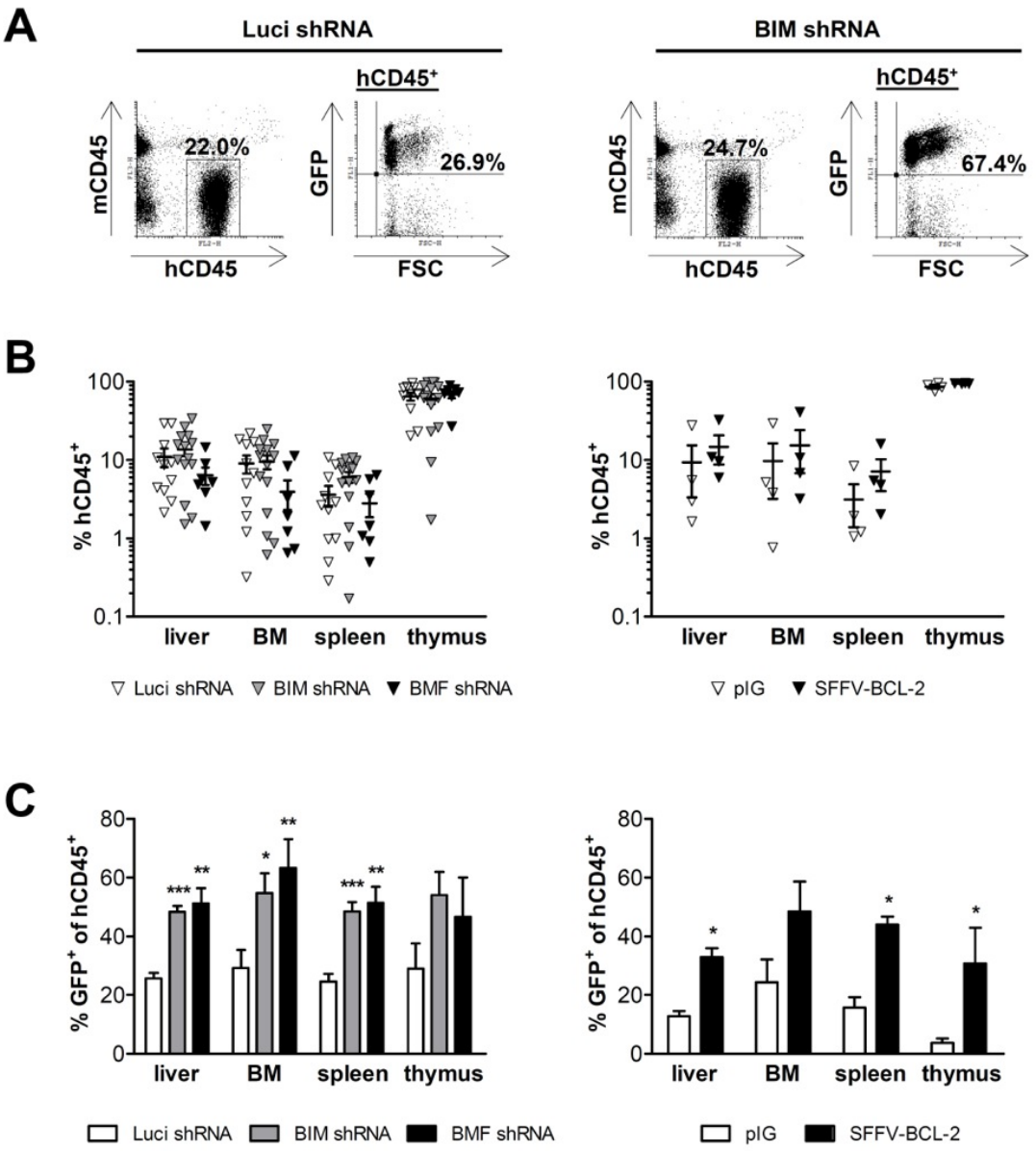

Figure 3.21: Knockdown of BIM or BMF improves reconstitution of human CD45⁺ haematopoietic cells - Lentivirally transduced human CD34⁺ cells were injected intrahepatically into newborn *rag2*$^{-/-}\gamma c^{-/-}$ mice. After 8 weeks animals were sacrificed and single cell suspensions of haematological organs were stained with the indicated antibodies and analyzed by flow cytometry. (A) Dot blots of representative experiments are shown (BM). (B) Total human engraftment was determined by the percentage of hCD45⁺ cells. (C) Percentage of GFP⁺ cells within the human CD45⁺ cell population is shown. Data represent mean values +/-SEM of n=7-14 mice from four to six independent experiments (left panel) and of n=4 mice from two independent experiments (right panel). Significant p-values (Mann-Whitney-test): %GFP⁺ of hCD45⁺ cells: Luci shRNA versus BIM shRNA: liver $p<0.0001$, BM p=0.02, spleen p=0.0002, thymus p=0.052; Luci shRNA versus BMF shRNA: liver p=0.002, BM p=0.009, spleen p=0.004; pIG versus BCL-2: p=0.03 in liver, spleen and thymus.

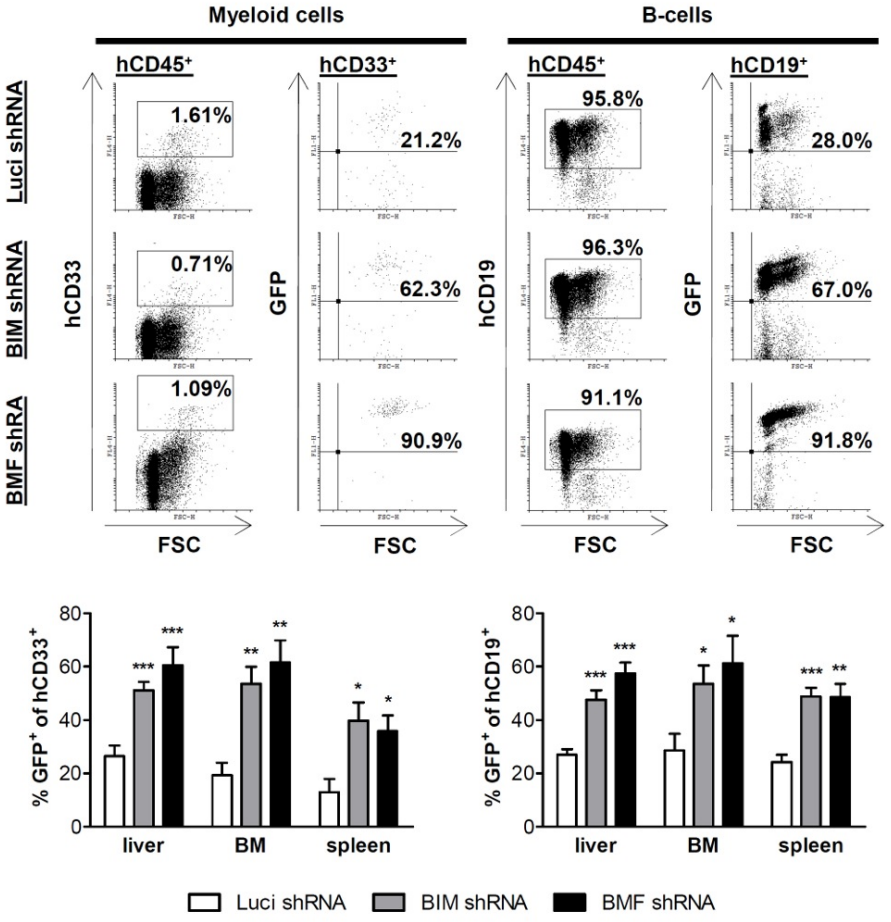

Figure 3.22: Reconstitution advantage of GFP⁺ cells expressing BIM or BMF shRNAs affects differentiated B cells and myeloid cells - Lentivirally transduced human CD34⁺ cells were injected intrahepatically into newborn *rag2*$^{-/-}\gamma c^{-/-}$ mice. After 8 weeks animals were sacrificed. Single cell suspensions of haematological organs were stained with antibodies against human CD45, human CD19 or human CD33 and murine CD45 and analyzed by flow cytometry. The percentage of GFP⁺CD19⁺ B-cells or GFP⁺CD33⁺ myeloid cells within the human CD45⁺ population, as shown in the representative dot plots of the BM, was determined. Data represent mean values +/-SEM of n=7-14 mice from four to six independent experiments (left panel) and of n=4 mice from two independent experiments (right panel). Significant p-values (Mann-Whitney-test): %GFP⁺ of hCD33⁺ cells: Luci shRNA versus BIM shRNA: liver p=0.0001, BM p=0.002, spleen p=0.02; Luci shRNA versus BMF shRNA: liver p=0.001, BM p=0.002, spleen p=0.04; %GFP⁺ of hCD19⁺ cells: Luci shRNA versus BIM shRNA: liver p=0.001, BM p=0.02, spleen p=0.0002; Luci shRNA versus BMF shRNA: liver p=0.001, BM p=0.02, spleen p=0.002.

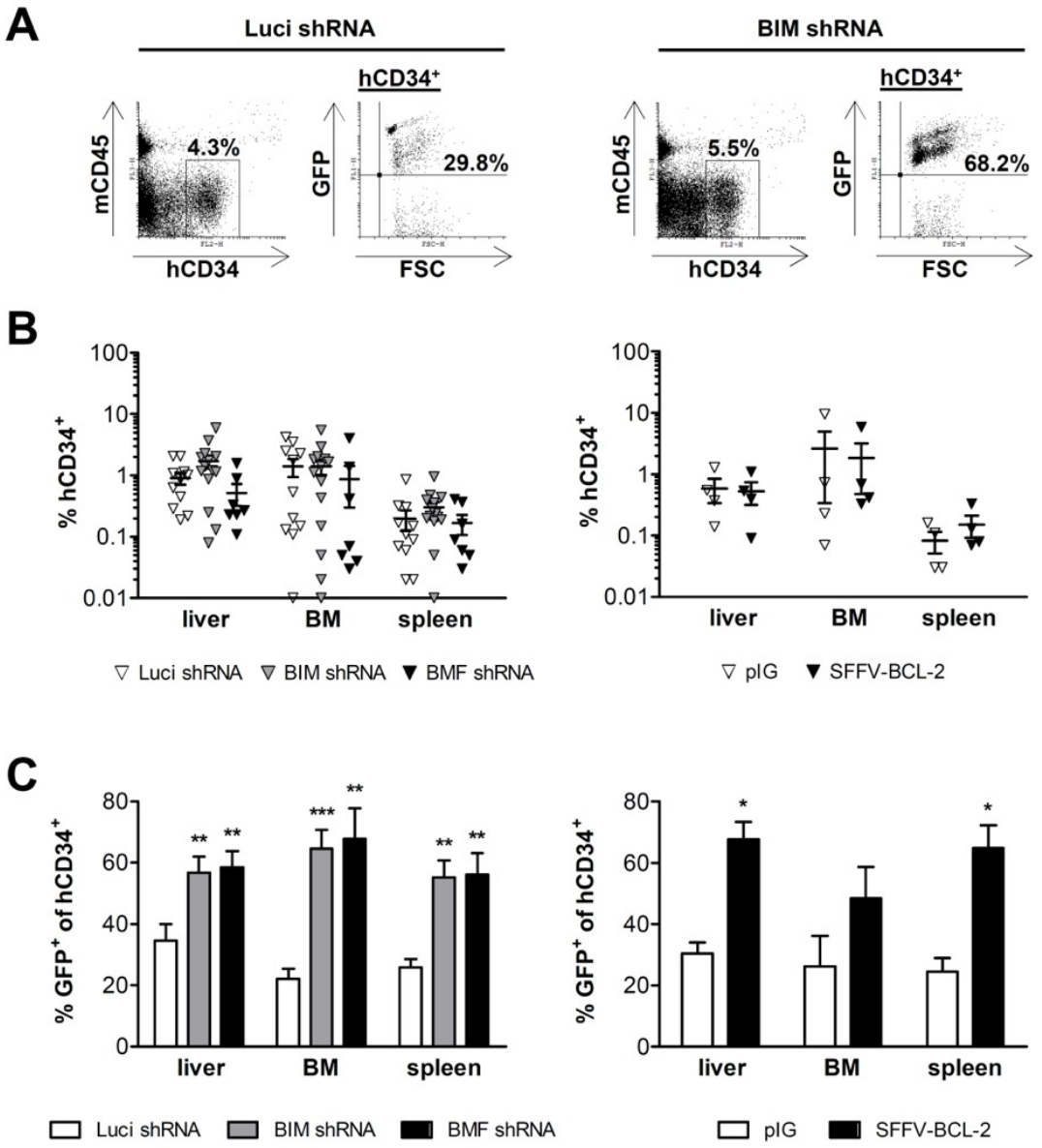

Figure 3.23: Engraftment advantage conferred by BIM or BMF knockdown is already seen in immature human CD34⁺ cells - Lentivirally transduced human CD34⁺ cells were injected intrahepatically into newborn *rag2*$^{-/-}\gamma c^{-/-}$ mice. After 8 weeks animals were sacrificed. Single cell suspensions of haematological organs were stained with the indicated antibodies and analyzed by flow cytometry. (A) Dot blots of representative experiments are shown (BM). The percentage of hCD34⁺ cells (B) as well as the percentage of GFP⁺ cells within the human CD34⁺ cell population (C) is shown. Data represent mean values +/-SEM of n=7-14 mice from four to six independent experiments (left panel) and of n=4 mice from two independent experiments (right panel). Significant p-values (Mann-Whitney-test): %GFP⁺ of hCD34⁺ cells: Luci shRNA versus BIM shRNA: liver p=0.006, BM p=0.0001, spleen p=0.001; Luci shRNA versus BMF shRNA: liver p=0.009, BM p=0.002, spleen 0.005; pIG versus BCL-2: p=0.03 in liver and spleen.

3.4.5 Apoptotic cell death mediated by BIM limits HSPC engraftment already early after transplantation

The next question was whether reduced levels of BIM or BMF promoted engraftment of CD34$^+$ cells early after transplantation or whether the advantageous effect observed was only due to accumulation of cells over time. To address this, transplantation experiments were performed as described before, but mice were sacrificed already 2.5 weeks after transplantation. Prior to transplantation the transduction efficiency was determined and found to be almost comparable, except a slightly increased level of GFP$^+$ BIM shRNA and BCL-XL expressing cells (Figure 3.24).

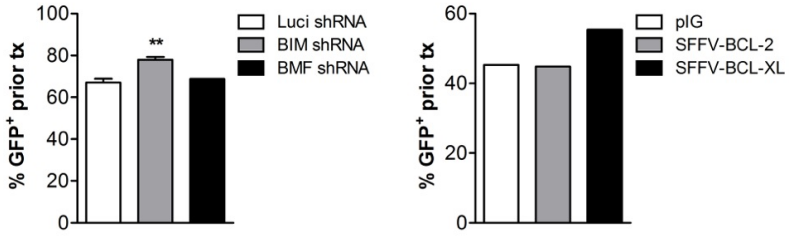

Figure 3.24: Comparable transduction efficiency before transplantation - Following one day of culture CB isolated human CD34$^+$ cells were transduced twice within 48 h with the indicated lentiviruses (2x MOI=10). After 2nd infection the percentage of GFP$^+$ cells was analyzed by flow cytometry. Bars represent mean values +/-SEM of n=3-9 mice from two independent experiments for BIM and 1 experiment for BMF (left panel); n=2-3 mice from 1 experiment (right panel). Significant differences were observed for Luci shRNA versus Bim shRNA p=0.004 (Mann-Whitney-test).

Surprisingly, already 2.5 weeks after transplantation the percentage of hCD45$^+$ cells expressing BIM shRNA was significantly increased in the liver and the BM (Figure 3.25C left panel). Similar effects were observed in the respective cells overexpressing BCL-XL and to a minor extent those overexpressing BCL-2 (Figure 3.25C right panel). Furthermore, a significant engraftment advantage of GFP$^+$ cells with reduced levels of BIM was already present in immature CD34$^+$ and even in the more immature CD34$^+$38$^-$ cells (Figure 3.26). Although BMF shRNA expressing HSPCs did not perform better than Luci shRNA expressing HSPCs at this early time point, analysis of the immature CD34$^+$38$^-$ cells in the liver revealed a significant increase of GFP$^+$ cells with reduced levels of BMF (compare Figure 3.25 with Figure 3.26).

Thus, these results indicate that in contrast to murine HSPCs, where BMF seems to be very important during initial reconstitution, the role of BMF in human HSPCs might rather be essential later during reconstitution. In contrast, BIM seems to be important throughout the entire reconstitution of the haematopoietic system.

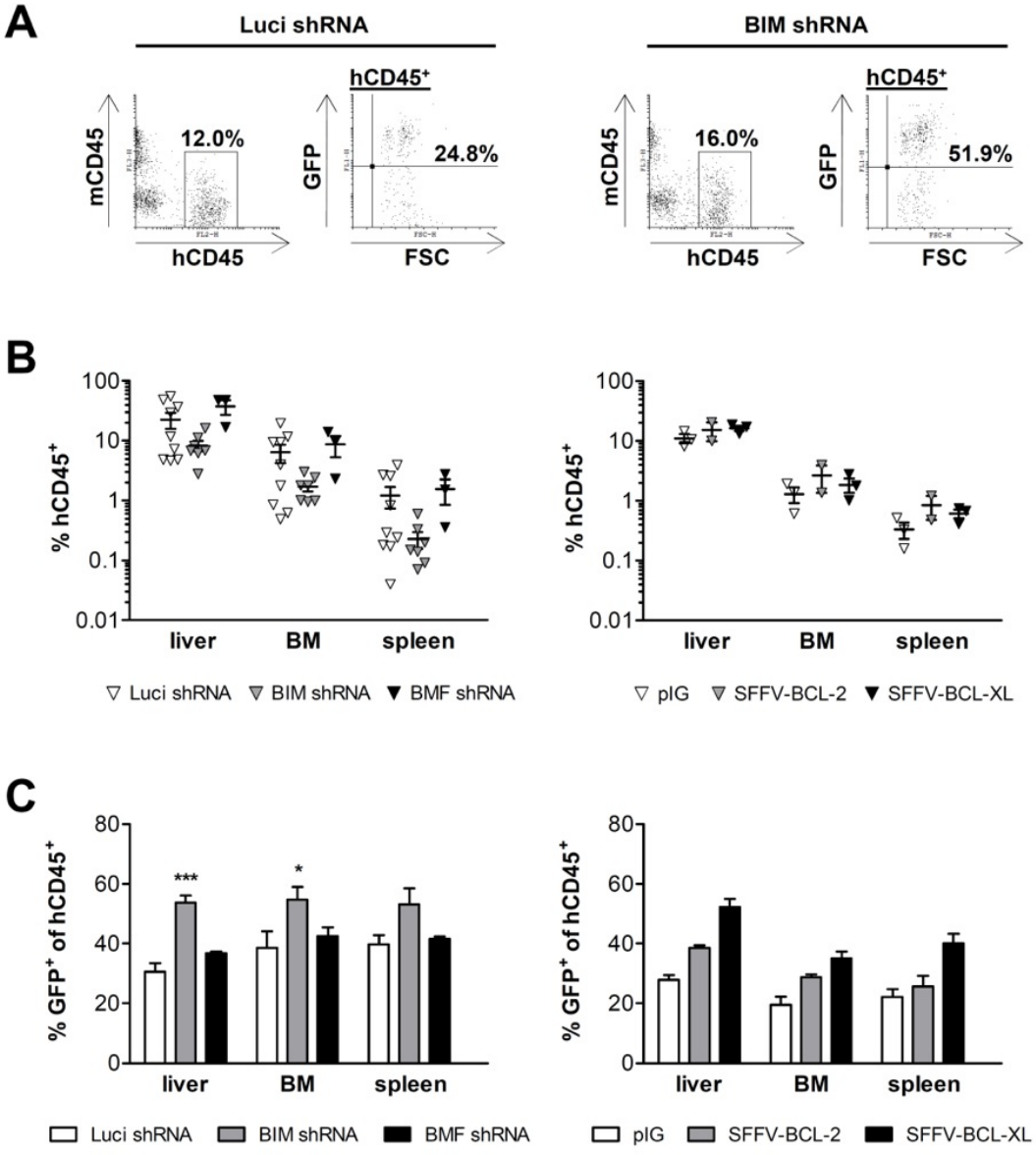

Figure 3.25: Knockdown of BIM improves reconstitution of human CD45⁺ haematopietic cells already early after transplantation - Lentivirally transduced human CD34⁺ cells were injected intrahepatically into newborn *rag2*$^{-/-}\gamma c^{-/-}$ mice. 2.5 weeks later animals were sacrificed and single cell suspensions of haematological organs were stained with the indicated antibodies and analyzed by flow cytometry. (A) Dot blots of representative experiments are shown (liver). (B) Total human engraftment was determined by the percentage of hCD45⁺ cells. (C) Percentage of GFP⁺ cells within the human CD45⁺ cell population is shown. Data represent mean values +/-SEM of n=3-9 mice from two independent experiments for BIM and 1 experiment for BMF (left panel) and of n=2-3 mice from 1 experiment (right panel). Significant p-values (Mann-Whitney-test): Luci shRNA versus BIM shRNA: p=0.001 in liver and p=0.03 in BM.

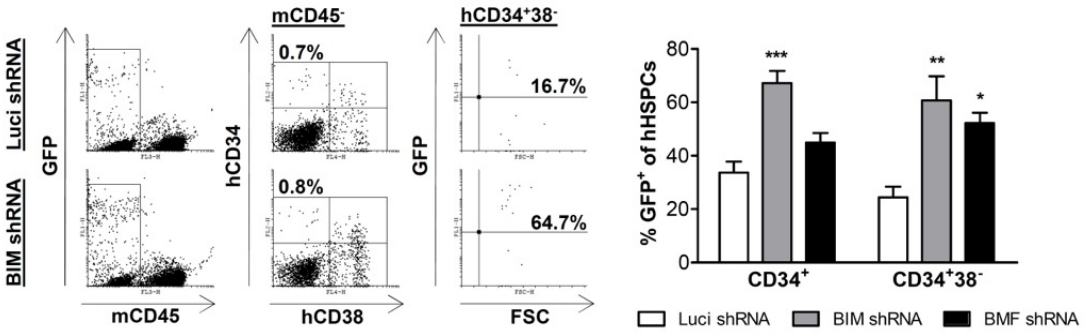

Figure 3.26: Early engraftment advantage of GFP⁺ cells expressing BIM or BMF shRNAs already in immature human CD34⁺ cells and CD34⁺38⁻ cells - Lentivirally transduced human CD34⁺ cells were injected intrahepatically into newborn *rag2*$^{-/-}\gamma c^{-/-}$ mice. 2.5 weeks later animals were sacrificed and single cell suspension of the liver was stained with the indicated antibodies and analyzed by flow cytometry. The percentage of GFP⁺ cells was determined within the human CD34⁺ cell population (hCD34⁺ versus mCD45⁺ cells as shown in Figure 3.23A) and within the more immature CD34⁺38⁻ cell population as shown by the representative dot blots. Data represent mean values +/-SEM of n=3-9 mice from two independent experiments for BIM and 1 experiment for BMF. Significant p-values (Mann-Whitney-test): Luci shRNA versusBim shRNA: p=0.0003 in CD34⁺ cells and p= 0.002 in CD34⁺38⁻ cells; Luci shRNA versus BMF shRNA: p=0.02 in CD34⁺38⁻ cells.

3.4.6 Apoptotic cell death mediated by BIM limits the reconstitution potential of intravenously injected HSPCs

To mimic the clinical procedure of HSCT, relying on intravenous injection and subsequent intraosseous engraftment more preciously, human CD34$^+$ cells were next injected intravenously into adult sublethally irradiated *rag2*$^{-/-}\gamma c^{-/-}$ mice. In line with the intrahepatic transplantation experiments there was no difference observed between BIM and Luci shRNA expressing cells concerning the overall human engraftment, the percentages of differentiated cell as well as the proportion of the immature CD34$^+$ cells (Figure 3.27A). However, the amount of BIM shRNA expressing cells was again highly increased in all cell populations analyzed (Figure 3.27B).

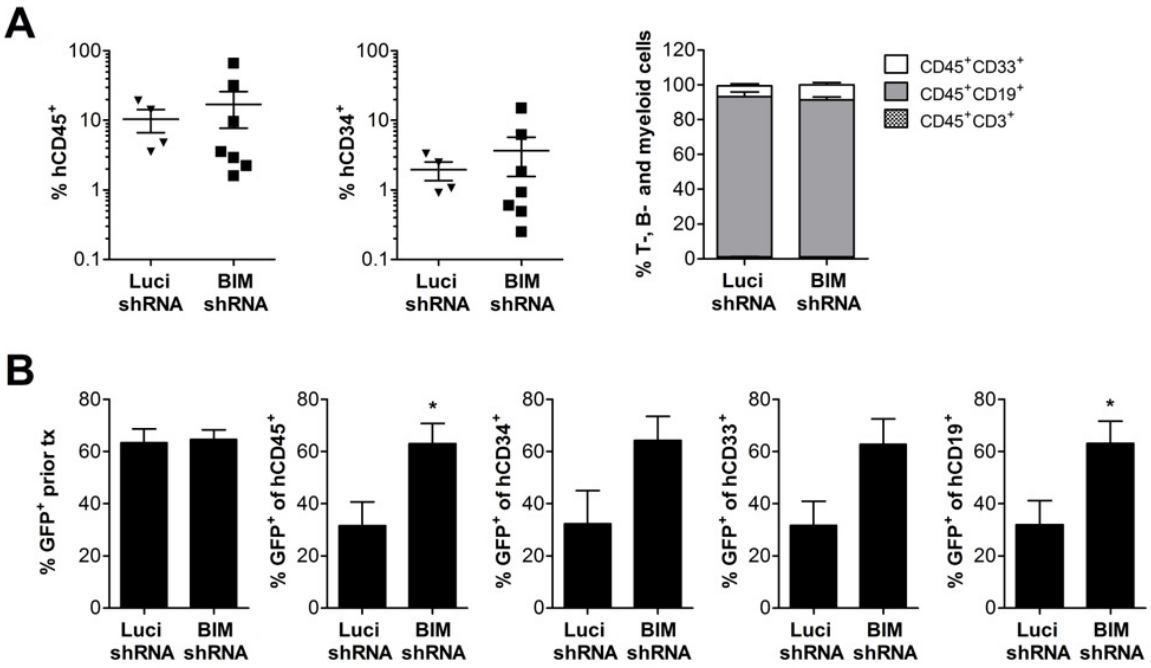

Figure 3.27: Reconstitution advantage of BIM shRNA expressing HSPCs upon intravenous injection - Human CD34$^+$ cells were transduced with lentiviruses expressing shRNA against Luciferase or BIM and injected intravenously into 7 weeks old *rag2*$^{-/-}\gamma c^{-/-}$ mice. After 8 weeks mice were sacrificed and BM was stained with the indicated antibodies. (A) Total human engraftment, indicated by the percentage of CD45$^+$ cells (left), percentage of immature CD34$^+$ cells (middle) and mature cell populations (right) is shown. (B) Transduction efficacy of CD34$^+$ cells before transplantation (left) as well as the percentages of GFP$^+$ cells in different cell populations was analyzed. Data represent mean values +/-SEM of n=4-7 mice form three independent experiments. Significant differences were observed for (Mann-Whitney-test) CD45$^+$ cells p=0.04 and for CD19$^+$ cells p=0.02.

3.4.7 Increased reconstitution potential of human HSPCs expressing BIM shRNA is not due to increased proliferation

The xenograft experiments demonstrate that inhibition of apoptosis mediated by knockdown of BIM highly increases transplantation efficacy of human HSPCs. However, it still has to be clarified whether this beneficial effect can be ascribed only to apoptosis resistance or whether proliferation is also increased.

To exclude the contribution of proliferation to the engraftment advantage of BIM knockdown $CD34^+$ cells, the proliferation capacity was analyzed in lentivirally transduced $CD34^+$ cells 8 weeks after transplantation. As shown in Figure 3.28 this property was comparable between BIM knockdown and control cells. Additionally, the proliferation potential was analyzed in freshly CB isolated human $CD34^+$ cells, in lentivirally transduced $CD34^+$ cells (3 days of culture in the presence of the cytokines 50 ng/ml TPO, 100 ng/ml SCF, Flt3L and 20 ng/ml IL3) as well as in lentivirally transduced $CD34^+$ cells cultured for 6 days in total. Freshly isolated $CD34^+$ cells were predominantly found to be in G_0 and G_1 phase, while *ex vivo* cultivation with cytokines strongly activated their cell cycle entry and progression. Interestingly, the strong proliferation observed after 3 days of culture (S-G_2-M phase: Luci shRNA 44.5%, Bim shRNA 45.9%) was again reduced after 6 days of culture (S-G_2-M phase: Luci shRNA 36.2%, Bim shRNA 34.5%), suggesting that stem cells reentered the G_0 phase. In any case, BIM and Luci shRNA expressing cells entered the cell cycle simultaneously *in vitro* as well as in *in vivo*.

In conclusion, our proliferation experiments confirmed that engraftment advantage of human HSPCs with reduced levels of BIM is due to apoptosis inhibiton and not due to increased proliferation.

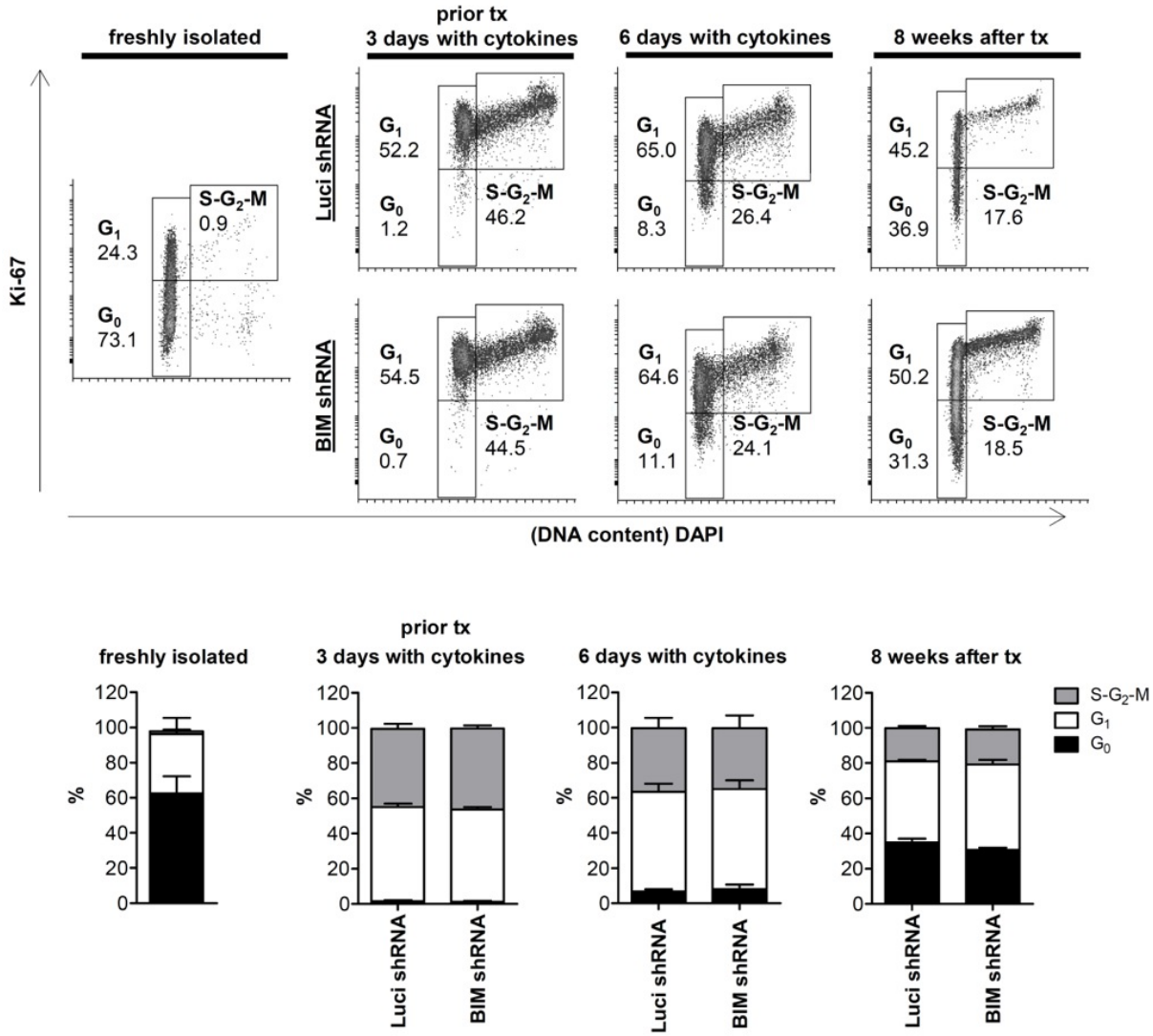

Figure 3.28: Knockdown of BIM does not modify the proliferation potential of human CD34⁺ cells - CB isolated human CD34⁺ cells were analyzed immediately after isolation (n=5) or after culture in the presence of cytokines for 1 day followed by lentiviral transduction performed twice within 2 days. Afterwards, lentivirally transduced CD34⁺ cells were sorted for GFP expression and analyzed directly or after culture for another 3 days (n=3). Lentivirally transduced cells were additionally transplanted intravenously into 7 week old *rag2*$^{-/-}\gamma c^{-/-}$ mice (n=4). 8 weeks later mice were sacrificed and cell cycle state of GFP⁺ cells was determined. Cell cycle state was analyzed by flow cytometry of DAPI and Ki-67 stained nuclei. Representative dot blots are shown (upper panel). Data represent mean values +/-SEM of three independent experiment (lower panel). No significant differences were observed (Mann-Whitney-test).

3.5 Transient modulation of the BCL-2 rheostat

Our findings so far suggested, that inhibition of the intrinsic apoptosis pathway in HSPCs could serve as a therapeutic approach to improve efficacy of HSCT by increasing the numbers of viable donor cells. However, permanent apoptosis inhibition and random lentiviral integration into the host genome may lead to malignant transformation of HSPCs and/or their arising progeny over time. To utilize apoptosis inhibition for therapy without having the potential risk of tumor formation, this study was extended to adenoviral transduction of HSPCs. Unlike lentiviruses, adenoviruses are not integrated into the host genome and mediate transient gene expression (Järås *et al.*, 2007). Therefore apoptosis of HSPCs may be inhibited only transiently during the stress-associated transplantation phase and therefore overcome the limitations of the lentiviral proof-of-principal approach.

Unfortunately, HSPCs lack expression of the coxsackie and adenovirus receptor (CAR) which is required for uptake of conventional adenoviruses (adenovirus serotype 5 = Ad5). We therefore used the modified Ad5-based vector (Ad5/F35), which was constructed by Xiaolong Fan and colleagues by exchanging the Ad5 fiber gene against the Ad35 fiber gene (Nilsson *et al.*, 2004b). Ad35 utilizes the ubiquitously expressed CD46 as a cellular receptor and thereby facilitates gene transfer into human primitive haematopoietic cells. Gene transfer mediated by Ad5/F35-viruses was shown to be efficient in both dividing and nondividing $CD34^+$ cells (Nilsson *et al.*, 2004a). The Ad5/F35 vector backbone was kindly provided by Xialong Fan from the Lund University.

3.5.1 Adenovirally mediated knockdown of BIM and BMF and overexpression of BCL-XL

As described in Material and Methods, Ad5/F35-viruses expressing shRNA against BIM or BMF under the control of a RNA polymerase III-dependent THT promoter or overexpressing BCL-XL under the control of a CMV promoter were generated using the AdEasy system (Luo *et al.*, 2007). Generated Ad5/F35-viruses were tested for RNAi efficacy or overexpression potential. To this end, HeLa cells were transduced with Ad5/F35-viruses, sorted for GFP expression and analyzed by Western blot.

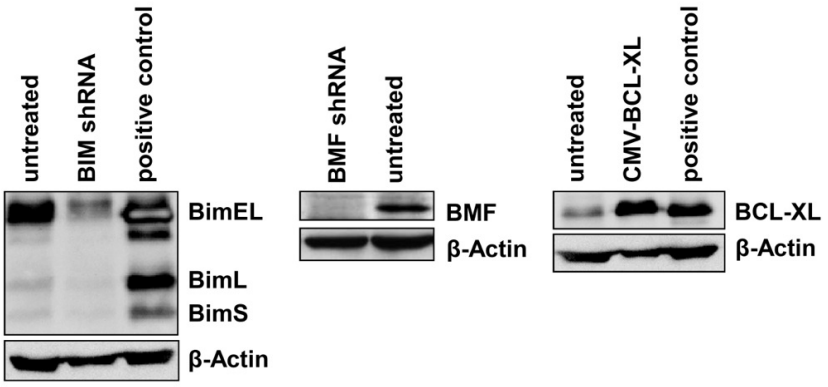

Figure 3.29: Knockdown of BIM or BMF and overexpression of BCL-XL mediated by Ad5/F35-viruses - HeLa cells were transduced with Ad5/F35-viruses expressing shRNA against BIM or BMF or overexpressing BCL-XL. After sorting for GFP^+ cells knockdown of BIM or BMF and overexpression of BCL-XL was determined on protein level using Western blot analysis. The Burkitt's lymphoma cell line BL40 was used as a positive control for BIM and BCL-XL expression. β-Actin served as a loading control.

As shown in Figure 3.29 shRNAs against BIM or BMF led to efficient downregulation of BIM or BMF on the protein level. Furthermore, BCL-XL was highly upregulated in cells transduced with Ad5/F35-CMV-GFP/CMV-BCL-XL-viruses.

3.5.2 Establishment of adenoviral transduction

In order to optimize transduction of $CD34^+$ cells with Ad5/F35-viruses, we evaluated the effects of $CD34^+$ purity, viral concentration, cultivation time and cytokine combinations on transduction efficiency. As depicted in Figure 3.30, the efficiency of Ad5/F35-virus transduction was highly dependent on CD34 purity. However, CD34 purity obtained by MACS-based sorting is strongly variable. Since maximal effects were already obtained with low amounts of Ad5/F35-viruses, a MOI of 10-20 was used for further experiments (Figure 3.30 right panel).

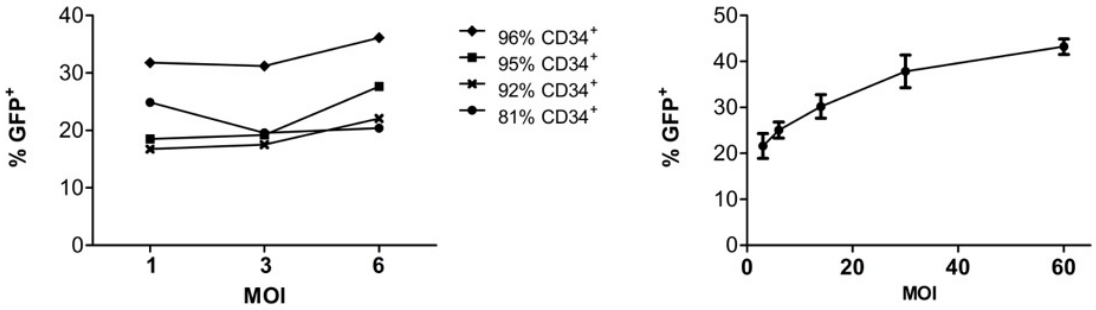

Figure 3.30: Ad5/F35-virus transduction depends on CD34 purity and less on viral concentration - CB isolated CD34+ cells were exposed to Ad5/F35-PGK-GFP at the indicated MOI. Percentage of GFP+ cells was determined 24 h after transduction by flow cytometry. Transduction efficiency depending on CD34 purity (left panel) and on viral concentration (right panel) is shown. Data represent mean values +/-SEM of n=2-8 from at least two independent experiments (except of MOI=60 1 experiment).

Next, we investigated whether the transduction efficacy of CD34+ cells was influenced by cell culture duration pre- or post-infection. As shown in Figure 3.31, this was highly dependent on cultivation length prior to infection, with shorter times being beneficial (Figure 3.31). Furthermore, GFP expression was increased during the first days after transduction and cells lost GFP-positivity from day 9 on. Hence the transient nature of adenoviral expression, caused by repeated cell divisions, could be confirmed.

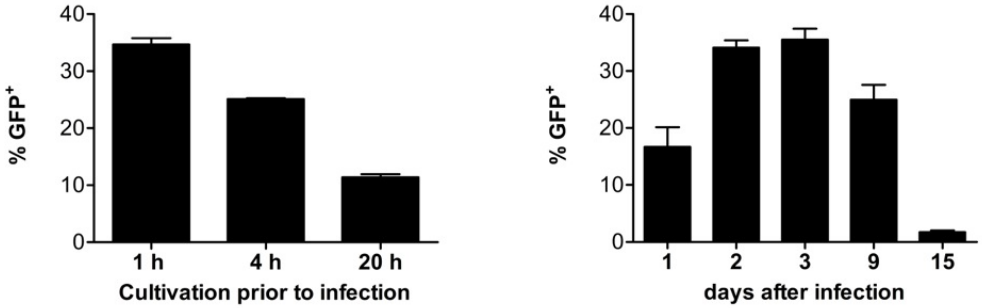

Figure 3.31: Effect of cultivation length pre- and post-infection on transduction efficiency - CD34+ cells were prestimulated with TPO (50 ng/ml), SCF and Flt3L (100 ng/ml each) for 1, 4 or 20 h followed by infection with Ad5/F35-PGK-GFP for 3 h. Percentage of GFP+ cells was determined 48 h after transduction by flow cytometry (left panel). GFP expression was additionally monitored for 15 days after adenoviral transduction of CD34+ cells (right panel). Data represent mean values of n=2-3 +/-SD from 1 experiment.

Although the cultivation length before and after infection seemed to affect GFP expression in CD34+ cells, the infection length had almost no effect on the transduction efficiency (Figure

3.32). The CMV promoter turned out to be less efficient than the PGK promoter (Figure 3.32). However, the former seemed to be slightly more active in the presence of TPO 50 ng/ml, SCF and Flt3L (100 ng/ml each) and IL3 20 ng/ml as shown in Figure 3.32 (right panel).

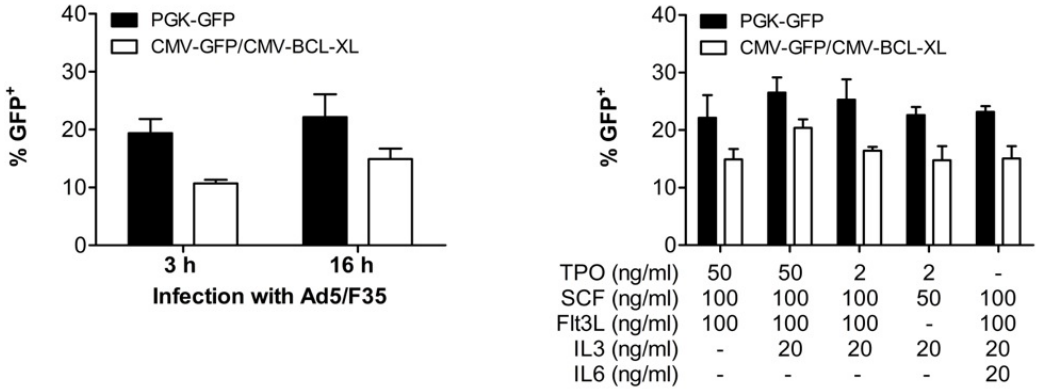

Figure 3.32: CMV promoter is less efficient than PGK promoter - CD34+ cells were prestimulated for 1 h with TPO (50 ng/ml), SCF and Flt3L (100 ng/ml each) and exposed to Ad5/F35-viruses for 3 or 16 h (left panel). CD34+ cells were prestimulated with the indicated cytokine combinations followed by infection with the Ad5/F35-viruses for 16 h (right panel). Percentage of GFP+ cells was determined 48 h after infection by flow cytometry. Data represent mean values of n=2 +/-SD of one experiment

To enhance CMV promoter activity the BoosterExpress™ reagent was used (Figure 3.33) as described by Lavazza and colleagues (Lavazza *et al.*, 2007). In brief, CD34+ cells were incubated with Ad5/F35-CMV-GFP/CMV-BCL-XL virus for 24 h in the presence of the BoosterExpress™ reagent for 24 h, 20 h or 4 h. GFP expression was analyzed 24 h after transduction using fluorescence microscopy and 48 h after transduction by flow cytometry. As shown in Figure 3.33 (upper panel), already 24 h after transduction GFP expression was markedly increased in the presence of the BoosterExpress™ reagent and correlated with the incubation length and concentration of BoosterExpress™ reagent. Flow cytometry analysis confirmed this increased GFP expression for both Ad5/F35-CMV-GFP/CMV-BCL-XL virus- and Ad5/F35-PGK-GFP virus-infected CD34+ cells. Since, the length of BoosterExpress™ exposure increased cytotoxicity (Figure 3.33 lower right panel), the reagent was used for maximal 4 h in further experiments.

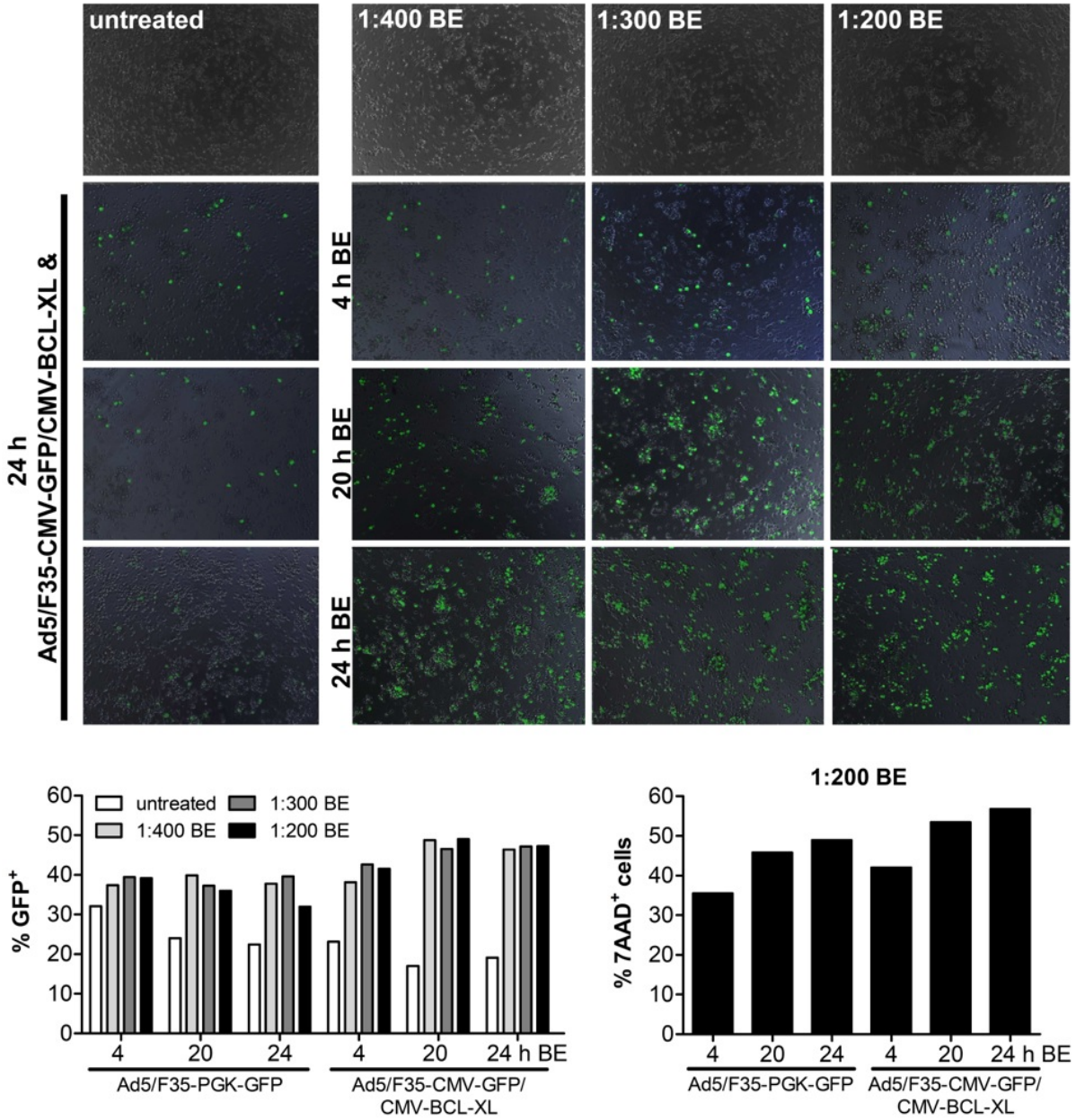

Figure 3.33: CMV activity is increased upon exposure to BoosterExpress™ reagent (BE) - CB isolated CD34+ cells were prestimulated with TPO (50 ng/ml), SCF, Flt3L (100 ng/ml each) and IL3 (20 ng/ml) for 1 h prior infection with adenoviruses for 24 h. BE was added simultaneously with Ad5/F35-viruses (24 h BE), 4 h later (20 h BE) or 20 h later (4 h BE). Afterwards medium was exchanged and GFP expression was determined after 24 h by fluorescence microscopy (upper panel) and after 48 h by flow cytometry together with the amount of dead cells (%7-AAD+) (lower panel). Data represent values of one experiment.

To confirm the survival function of the Ad5/F35-CMV-GFP/CMV-BCL-XL virus upon BoosterExpress™ reagent treatment, adenovirally transduced CD34+ cells were sorted for GFP expression and exposed to etoposide or taxol for 24 h. As depicted in Figure 3.34 CD34+ cells transduced with Ad5/F35-CMV-GFP/CMV-BCL-XL-virus were protected from apoptosis induced by etoposide or taxol.

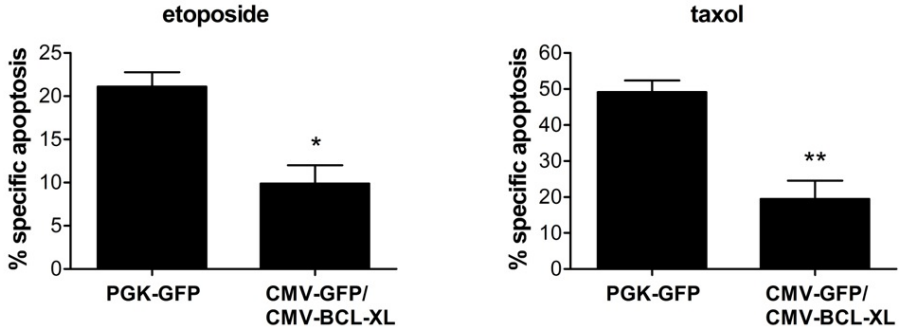

Figure 3.34: Transient overexpression of BCL-XL protects CD34+ cells from apoptosis induced by etoposide and taxol - CD34+ cells were prestimulated with TPO (50 ng/ml), SCF, Flt3L (100 ng/ml each) and IL3 (20 ng/ml) for 1 h prior to adenovirus infection for 24 h in the presence of BoosterExpress™ reagent for the last 4 h. 24 h after transduction GFP+ cells were sorted and cultured afterwards for 24 h in the presence of etoposide or taxol. Data represent mean values of n=3-8 from three independent experiments. Significant p-values (Mann-Whitney-test): etoposide p=0.02; taxol p=0.01.

3.5.3 Adenoviral transduction efficacy and CMV promoter activity are not sufficient for *in vivo* studies

Finally, we investigated whether transient overexpression of BCL-XL could confer resistance of CD34+ cells to stress signals during HSCT thereby enhancing engraftment. Thus, CD34+ cells were transduced with Ad5/F35-CMV-GFP/CMV-BCL-XL in the presence of BoosterExpress™ reagent and transplanted into the livers of *rag2*$^{-/-}\gamma c^{-/-}$ mice within their first week of life. However, transplantation of the cells pretreated with this reagent led to strong adverse effects such as joint edema and weight loss and prompted us to terminate these experiments. These side effects were not observed when cells were transduced with adenoviruses in the absence of BoosterExpress™ reagent. However, due to the inefficient gene expression mediated by adenoviruses under control of the CMV promoter, we did not further pursue *in vivo* experiments. In contrast, we think that other and more efficient methods for transient gene transfer are required to enable apoptosis inhibition during HSCT for therapeutical usage.

4

Discussion

Although allogeneic HSCT has been successfully used to cure many haematological diseases, this therapy is still limited by transplantation-related mortality due to graft failure and delayed haematopoietic and immune reconstitution. Increasing the number of HSPCs during transplantation is a very attractive strategy to improve and accelerate haematopoietic regeneration (Mavroudis *et al.*, 1996) and can be achieved for example by *ex vivo* (Hofmeister *et al.*, 2007) or *in vivo* expansion of HSPCs (Wadhwa *et al.*, 2003).

Inhibition of HSPC apoptosis might be a new strategy to increase donor cell numbers, since HSPCs are exposed to several potentially lethal cell stress situations during transplantation. These include lack of pro-survival signals such as cytokines or extracellular matrix proteins, which are normally provided by the stem cell niche, but also cell stress due to cryopreservation or the transplantation procedure itself (Greco *et al.*, 2006). Cytokine deprivation triggers apoptosis mainly via the intrinsic apoptosis pathway, which is regulated by Bcl-2 family members (Cory *et al.*, 2003). The anti-apoptotic Bcl-2 family members Bcl-x_L (Motoyama *et al.*, 1995) and Mcl-1 (Opferman *et al.*, 2005) are crucial for survival of murine HSPCs, and overexpression of Bcl-2 increases their ability to reconstitute the haematopoietic system of lethally irradiated mice (Domen *et al.*, 2000). However, so far it is unclear whether their antagonists, the pro-apoptotic BH3-only proteins, are equally important for regulation of HSPC survival and death. Previous studies of Verena Labi and Miriam Erlacher demonstrated that the absence of Bim or Bmf in murine HSPCs (LSK cells) dramatically increases their long-term haematopoietic reconstitution potential (Labi *et al.*, 2012). While the first part of this study is focused on the question whether this effect is caused by an increased survival of HSPCs, the second part concentrates on the relevance of BH3-only proteins in human HSPCs during cytokine deprivation *in vitro* and transplantation-related stress *in vivo*.

4.1 The role of BH3-only proteins downstream of cytokine withdrawal

BH3-only proteins serve as upstream regulators of the intrinsic apoptosis pathway. They mediate apoptosis in response to certain cell stress signals dependent on the individual cell type (Bouillet *et al.*, 1999). During transplantation one such cell stress signal might be cytokine deprivation. Thus, in order to mimic the situation during HSCT *in vitro* we subjected HSPCs (lineage$^-$sca1$^+$c-kit$^+$ = LSK cells) isolated from murine wt BM to cytokine deprivation. Indeed, in the absence of cytokines LSK cells underwent rapid cell death accompanied by mRNA upregulation of the BH3-only proteins Bim, Bmf, Puma and Noxa. In contrast, neither Bad nor Bid were upregulated on mRNA level, and Bik and Hrk were not expressed at all. Moreover, we analyzed the transcriptional regulation of other Bcl-2 family members acting either as BH3-only antagonists (pro-survival proteins) or downstream thereof (Bax and Bak). While Bax and Bak were not upregulated in response to cytokine wihtdrawal, the anti-apoptotic Bcl-2 family members Bcl-2 and Bcl-x_L were significantly downregulated. Expression of other apoptosis-related genes remained largely unchanged. Thus, cytokine deprived LSK cells showed a disturbed balance between pro- and anti-apoptotic Bcl-2 proteins in favor of the pro-apoptotic state.

To clarify whether upregulation of Bim, Bmf, Noxa and Puma mRNA was indeed responsible for the rapid cell death observed in LSK cells after cytokine deprivation, we isolated LSK cells from mice deficient for various BH3-only proteins and subjected them to cytokine deprivation. Interestingly, only Bim-deficient and to a minor extent also Puma-deficient LSK cells were protected from cytokine deprivation-induced apoptosis. This might be due to distinct binding affinities of different BH3-only proteins to their pro-survival antagonists. While Bim and Puma bind to all pro-survival proteins with high affinity, Bmf and Bad bind with high affinity only to Bcl-2, Bcl-x_L and Bcl-w, and Noxa only binds to Mcl-1 and A1 (Chen *et al.*, 2005). Accordingly, only Bim and Puma may be able to sufficiently antagonize all anti-apoptotic proteins allowing for efficient Bax and Bak activation. The fact that deficiency of Bim but not Bmf protected HSPCs from cytokine deprivation-induced cell death may also be explained by the so called ”direct activation” model where only Bim is able to act as direct activator of Bax and Bak, whereas Bmf only neutralizes anti-apoptotic Bcl-2 family members thus freeing Bim and/or Bax/Bak without directly activating them (see 1.5) (Certo *et al.*, 2006). The observation that Bim is important for apoptosis induction in murine HSPCs in the absence of cytokine-mediated survival signaling is in line with its role in mature lymphocytes and granulocytes (Bouillet *et al.*, 1999; Villunger *et al.*, 2003a). Interestingly, Bim and Puma were found to cooperate in mediating cytokine deprivation-induced apoptosis in different lymphocyte subsets (Erlacher *et al.*, 2006; You *et al.*,

2006). Thus, the combined loss of Bim and Puma might protect LSK cells more efficiently from apoptosis in the absence of cytokine mediated survival signaling. Consistent with previously published data, overexpression of Bcl-2 almost completely inhibited apoptosis induced by cytokine deprivation in LSK cells (Domen *et al.*, 2000; Ogilvy *et al.*, 1999).

4.2 The role of Bim and Bmf during transplantation

Since Bim was critically involved in apoptosis induction of LSK cells in response to cytokine deprivation *in vitro*, it was conceivable to assume that it was also crucial for LSK cell apoptosis during transplantation, when cells are removed from their supportive stem cell niche. As a consequence, the number of transplanted cells in the engrafted recipients would be reduced. Indeed, haematopoietic reconstitution was dramatically increased if donor cells were deficient for Bim. 16 weeks after competitive transplantation of wt and *bim*$^{-/-}$ LSK cells (1:1 ratio) Bim-deficient cells accounted for all mature lymphatic and myeloid cells as shown previously by Verena Labi (see Figure 1.7). Our study now suggests that the displacement of the wt haematopoiesis starts within the HSPC pool, since Bim-deficient cells also accounted for the majority of LSK and more immature LSK CD150^{+} cells (Figure 3.4). Importantly, *bim*$^{-/-}$ LSK cells performed better already 10 days after transplantation, confirming that loss of Bim contributed primarily to HSPC survival. Noteworthy, the repopulation ability of *bim*$^{-/-}$ and *bcl-2 tg* HSPCs was comparable, indicating that Bim induction accounted for all cell death during reconstitution which could be blocked by overexpression of Bcl-2. In summary, our data indicate that HSPC apoptosis occurring during transplantation is relevant for the outcome of stem cell transplantations, and that apoptosis inhibition can increase LSK cell engraftment robustly. The superior performance of Bim-deficient LSK cells during transplantation could also be confirmed by limiting dilution experiments. While 10,000 wt BM cells were unable to successfully reconstitute lethally irradiated recipient mice, successful reconstitution was achieved upon transplantation of an equal amount of Bim-deficient BM cells.

Although loss of Bmf did not protect HSPCs from cytokine deprivation-induced apoptosis *in vitro*, the reconstitution potential of *bmf*$^{-/-}$ LSK cells was superior when compared to wt LSK cells. Similar to *bim*$^{-/-}$ LSK cells, first effects were observed already 10 days after competitive transplantation. One possible explanation for the better performance of *bmf*$^{-/-}$ LSK cells *in vivo* might be that Bmf is involved in cell death induction downstream of stress signals other than cytokine deprivation. In other cell types, Bmf has been described to be released from the actin cytoskeleton in response to cell detachment (Puthalakath *et al.*, 2001). Accordingly, Bmf could induce ”anoikis” (detachment-induced apoptosis) in HSPCs when they are removed from their

niche. However, this hypothesis could not be confirmed in an *in vitro* model since the presence of extracellular proteins (i.e. fibronectin) did not increase viability of HSPCs *in vitro* (data not shown).

Of note, Ooi and colleagues recently demonstrated that overexpression of miR-125b leads to an increased engraftment capability of HSPCs, both during primary and secondary transplantation (Ooi *et al.*, 2010). The authors ascribed these effects to the downregulation of the pro-apoptotic proteins Bmf and/or KLF13 without confirming their hypothesis. Our findings now nicely complete the work of Ooi by demonstrating that loss of Bmf is indeed capable of enhancing the reconstitution ability of HSPCs and that the effect observed upon overexpression of miR-125b is likely to be caused, at least in part, by an inhibition of Bmf.

While the definite Ly5.1:Ly5.2 ratio in wt:*bmf*$^{-/-}$ BM chimera was achieved within the first 10 days after transplantation (36%:64%), wt haematopoiesis was further displaced in wt:*bim*$^{-/-}$ and wt:*bcl-2 tg* chimera, and 16 weeks after transplantation almost no wt HSPCs could be found in the latter two groups (see Figure 3.4). This indicates that Bim but not Bmf additionally plays a crucial role during later stages of haematopoietic regeneration. Apoptosis might be important to suppress excessive HSPC expansion as soon as the peripheral haematological system is replenished, and this apoptosis could be dependent on Bim. However, this hypothesis has not been formally confirmed in this study. Alternatively, HSCs have been shown to continuously exit and resettle into stem cell niches during division or steady state condition (Bhattacharya *et al.*, 2009), implicating the absence of protective survival signals from time to time. Thus, increased survival of *bim*$^{-/-}$ or *bcl-2 tg* HSCs outside of the supportive niche might lead to an ongoing competitive advantage over wt LSK cells, finally resulting in the almost complete displacement of wt LSK cells.

Some Bcl-2 family members such as Bcl-2 itself are not only important for apoptosis regulation but have also been implicated in cell cycle control (Zinkel *et al.*, 2006). We therefore tested whether the strong and ongoing competitive advantage of Bim-deficient cells could be partially independent of their apoptosis resistance but caused by increased proliferation. Notably, our data demonstrated that the cell cycle state of wt and *bim*$^{-/-}$ LSK cells prior to transplantation or after *in vitro* stimulation with cytokines was comparable. In line with a recent publication, displaying an impaired cell cycle progression from G_1 to S phase *in vivo* in *bim*$^{-/-}$ LSK cells (Kozuma *et al.*, 2010), our data also showed a slightly increased amount of *bim*$^{-/-}$ cells in the G_1 phase 4 weeks after transplantation during stress haematopoiesis. At this time point, re-

generation of the haematopoietic system still is ongoing ("stress haematopoiesis") as shown by high amounts of cells in S-G_2-M phase. Thus, deficiency for Bim seems to delay cell cycle progression rather than to increase the proliferative potential of LSK cells. This is consistent with the previous finding that Bcl-2 overexpression prolongs the G_1 and delays entry into S phase of numerous different cell types (Borner, 1996). Taken together, our proliferation experiments strongly suggest that the significant engraftment advantage of *bim*$^{-/-}$ LSK cells can be ascribed uniquely to their apoptosis resistance and is not caused by increased proliferation of these cells. Moreover, Bim deficiency did not change the homing capacity of LSK cells, further confirming the importance of Bim for apoptosis induction during haematopoietic stem cell transplantation. As demonstrated by Verena Labi, *bim*$^{-/-}$ LSK cells also differentiate normally in all mature blood and immune cells (Labi *et al.*, 2012).

4.3 From mice to men

Our data clearly indicate that HSPC apoptosis is a limiting factor during stem cell transplantations, at least in the murine system. Could this finding be applied to humans so that apoptosis inhibition might be used for optimization of therapeutically applied stem cell transplantations? The central aim of this study was therefore to analyze whether the role of BIM and BMF is conserved between mouse and human cells.

In contrast to murine LSK cells, human CD34$^+$ cells were less sensitive to cytokine deprivation and showed a more restricted upregulation of BH3-only proteins with a notable induction of BIM and BMF. The anti-apoptotic Bcl-2 family member BCL-XL, which is able to inhibit both BIM and BMF, was simultaneously downregulated further shifting the balance towards pro-apoptotic proteins. While expression of other apoptosis-related genes upon cytokine withdrawal remained largely unchanged in murine LSK cells, the expression levels of BNIP-3L, NAIP and Survivin were altered in human CD34$^+$ cells. It would be highly interesting to determine how the observed changes in these other apoptosis-related genes contribute to the sensitivity of CD34$^+$ cells to growth factor deprivation. So far, Survivin has been shown to be important for HSPCs, however mainly for cell cycle regulation (Fukuda & Pelus, 2002). It is currently a matter of debate whether Survivin has anti-apoptotic functions at all, although it is a member of the IAP (inhibitor of apoptosis) family (Bourhis *et al.*, 2007). Notably, the exposure of CD34$^+$ cells to single cytokines revealed that they were efficiently protected from apoptosis *in vitro* by addition of SCF or Flt3L alone. This was accompanied by an almost complete repression of BIM by SCF and by repression of BMF by both SCF and Flt3L. This further suggested an involvement of BIM and BMF in cytokine deprivation-induced apoptosis in human HSPCs.

Aside from cytokine deprivation, diverse other cell death stimuli induced apoptotic cell death of $CD34^+$ cells via the activation of different BH3-only proteins. While DNA damage caused by γ-irradiation, etoposide or treosulfan resulted in the upregulation of PUMA mRNA, ER-stress induced by tunicamycin led to the induction of PUMA and BIM. The stimulus-specific induction of BH3-only proteins observed in $CD34^+$ cells is in line with previously published data in other cell types (reviewed in (Happo *et al.*, 2012)).

Although mRNA levels of BIM and BMF were significantly increased in human $CD34^+$ cells in the absence of cytokines only the knockdown of BIM but not that of BMF partially protected these cells from cytokine deprivation-induced apoptosis. This is consistent with the data obtained in murine cells, where the knockout of Bmf also failed to rescue LSK cells from cytokine deprivation-induced apoptosis *in vitro*. As discussed before, this is likely due to the distinct affinities of BIM and BMF to their pro-survival antagonists. shRNA-mediated knockdown of BIM protected human $CD34^+$ cells less efficiently from cytokine deprivation-induced apoptosis than complete loss of Bim did in murine LSK cells. This could be explained by the presence of residual BimEL protein, which might be activated in response to cytokine deprivation via inactivation of the ERK1/2 pathway leading to dephosphorylation of BimEL and thereby enabling binding to anti-apoptotic proteins (Ewings *et al.*, 2007; Ley *et al.*, 2003). Interestingly, the downregulation of BIM highly increased survival of $CD34^+$ cells during long-term cultivation in methylcellulose supplemented with cytokines. This indicates that the residual BIM protein in the knockdown cells was degraded over time and new production of BIM protein was inhibited by BIM shRNA. In addition, transcriptional regulation of BIM might be more important upon a slow decline of cytokines, whereas acute and complete cytokine deprivation might predominantly result in its posttranslational activation.

Notably, overexpression of BCL-2 or BCL-XL protected $CD34^+$ cells more efficiently from cytokine deprivation-induced apoptosis than downregulation of BIM, indicating that other BH3-only proteins may contribute to cell death induction. Thus, it would be interesting to analyze whether simultaneous knockdown of BIM and BMF is superior in protecting $CD34^+$ cells than the knockdown of BIM alone.

4.4 Apoptosis inhibition in human HSPCs

In vivo analysis of human haematopoiesis is restricted to humanized mice which are generated by engrafting immunodeficient mice with for example human cord blood derived $CD34^+$ cells. However, long-term maintenance of human stem cells and differentiation is restricted in these mice due to limited cross-reactivity of murine factors on human cells (Rongvaux *et al.*, 2011). Since we were interested in the survival of HSPCs under suboptimal conditions these restrictions were advantageous for our purpose. In addition, the impact of apoptosis inhibition during early engraftment rather than during late reconstitution events was of particular interest for our study.

In line with the data obtained from murine competitive transplantation experiments, the knockdown of BIM or BMF in human CB derived HSPCs significantly improved the reconstitution of human $CD45^+$ haematopoietic cells. Analysis of the different haematopoietic lineages showed that the engraftment advantage of cells with reduced levels of BIM or BMF was present both in B cells and myeloid cells. Consistent with previously published data, B cell reconstitution was robust, whereas reconstitution of myeloid cells was relatively poor, and almost no peripheral T cells were present (Traggiai *et al.*, 2004). The minor reconstitution of myeloid cells in humanized mice is likely due to missing human specific cytokines (Chen *et al.*, 2009). Human T cell differentiation and survival is restricted due to expression of mouse MHC components rather than human MHC (Manz, 2007). Highly important for our project was that the superior performance of cells expressing BIM or BMF shRNAs was already present at the level of $CD34^+$ cells and even in more immature $CD34^+38^-$ cells. Moreover, first advantageous effects could be observed as early as 2.5 weeks after transplantation. Although BIM and BMF shRNA expressing HSPCs efficiently displaced GFP-negative HSPCs they did not show an overall engraftment advantage compared to the control group. This might be explained by the growing animal tissues restricting expansion of human cells. Since overexpression of the antagonist Bcl-2 protected HSPCs similarly from transplantation-associated cell death as the expression of shRNAs against BIM or BMF after 8 weeks of transplantation, BIM and BMF seem to be the major BH3-only proteins involved in reconstitution-associated cell death.

The primary fetal haematopoietic site, the liver, contributes significantly to the expansion of HSPCs (Magnon & Frenette, 2008). Hence, intrahepatic injection of $CD34^+$ cells into newborn mice embeds HSPCs directly into a supportive niche and thereby provides a model in which engraftment can be analyzed independently of homing. However, clinical HSCT is based on intravenous injection and subsequent intraosseous engraftment. Therefore, as a second and better

comparable model adult recipient mice were injected intravenously with lentivirally transduced $CD34^+$ cells. Again, BIM shRNA expressing cells showed a much better engraftment than Luciferase shRNA expressing cells, corroborating the results obtained in the neonatal model. In line with previously published data, we also observed inferior engraftment of human HSPCs in adult mice (Brehm *et al.*, 2010). Engraftment can be increased by intraosseous transplantation indicating a reduced homing capacity of human cells into murine stem cell niches. Another explanation for the minor engraftment seen in adult mice is that less cells per gram body weight were used. Thus, higher numbers of $CD34^+$ cells might be required for adult *rag2*$^{-/-}\gamma c^{-/-}$ mice to reach an engraftment efficiency comparable to that obtained in newborn mice.

Importantly, the cell cycle status of GFP^+ cells expressing BIM shRNA or control shRNA was found to be comparable during reconstitution, excluding that altered cell cycling or proliferation potential caused the enhanced reconstitution potential. Additionally, the cell cycle state of control or BIM shRNA expressing $CD34^+$ cells was found to be similar prior to transplantation and in response to cytokine stimulation. Moreover, the distribution of human T, B and myeloid cells was comparable between Luci shRNA and BIM shRNA expressing cells (see Figure 3.27). Thus, downregulation of BIM did not interfere with HSPC differentitation, as also observed in colony-forming unit assays *in vitro*.

4.5 Apoptosis inhibition: a novel therapeutic approach?

Clinical experience has shown that low stem cell numbers delay engraftment and increase the risk of graft failure and, by consequence, infection-related mortality (Demirer *et al.*, 2009). Therefore, different approaches have been developed to enhance the number of donor cells. For example, stem cell mobilization into the PB has been greatly improved by using G-CSF in combination with plerixafor, an antagonist of the BM-homing receptor CXCR4 (Brave *et al.*, 2010). If allogeneic transplantation is required and a suitable donor is unavailable, umbilical cord blood (UCB) can be used as an alternative HSPC source. However, the use of UCB for transplantation is limited due to the relatively low amounts of HSPCs within one cord blood unit. Thus, new approaches to increase donor cell numbers have attracted considerable attention particularly in the context of UCB transplantations (reviewed in (Rocha & Broxmeyer, 2010)).

So far, the most successful advancement is simultaneous transplantation of two different cord blood samples (Barker *et al.*, 2005). This is however associated with the risk of mutual rejection of both samples (Gutman *et al.*, 2010). In addition, *ex vivo* expansion of cord blood HSPCs seems to be a very promising strategy to improve outcome and application of UCBT.

Most of the methods used for *ex vivo* expansion of HSPCs are however based on cytokines which induce differentiation and loss of stemness at the same time (Jaroscak *et al.*, 2003). Therefore in order to ensure long-term engraftment, only half of the cord blood (or one of two samples) is expanded prior transplantation, whereas the remaining part of the graft is transplanted without previous manipulation. Moreover, it has been shown that *ex vivo* expansion causes defective homing ability, cell cycle alterations and induction of apoptosis (Hofmeister *et al.*, 2007). Other and more recent attempts have aimed to support molecular pathways regulating stem cell maintenance during expansion. The most promising approach for *ex vivo* expansion of HSCs without concomitant loss of stemness is currently achieved by the aryl hydrocarbon receptor (AhR) antagonist StemReginin 1 (SR1) (Boitano *et al.*, 2010). First clinical trials have been initiated. In addition, mesenchymal stromal cell-based HSPC culture has been reported to support stem cell function during *ex vivo* expansion (de Lima *et al.*, 2012).

Here we demonstrate that HSPCs lacking Bim or Bmf are superior to wt HSPCs during reconstitution of the haematopoietic system. This indicates that apoptosis inhibition during transplantation might be a novel and promising therapeutic approach to increase numbers of HSPCs homing to the BM. Thereby, haematopoietic regeneration could be accelerated and risk of graft failure reduced. We are convinced that apoptosis inhibition might also be beneficial during the *ex vivo* expansion of HSPCs. To this end, stem cell expansion in combination with technologies supporting maintenance of stemness and increasing their viability will ultimately permit a more frequent use of cord blood for adult patients and will even make HSCT accessible to patients lacking a suitable HLA-matched donor.

4.6 Clinical translation: transient modulation of the Bcl-2 rheostat

To translate our promising results into a clinical setting, many concerns regarding safe HSPC modification and prevention of possible tumor formation need to be addressed. Since both Bim and Bmf are critically involved in lymphocyte homeostasis and development, their inhibition could result in the development of tumors or autoimmune diseases (Bouillet *et al.*, 1999; Labi *et al.*, 2008; Strasser, 2005). Although *bim*$^{-/-}$ mice develop tumors in the presence of myc or other oncogenes and autoimmune glomerulonephritis on a mixed (129SVxC57BL/6) genetic background, loss of Bim by itself only rarely promotes tumor formation, and fatal autoimmune pathology was not observed on an inbred C57BL/6 background (Bouillet *et al.*, 1999, 2001; Egle *et al.*, 2004; Erlacher *et al.*, 2006). Accordingly, an increased incidence of tumors was not shown in *bmf*$^{-/-}$ mice (Labi *et al.*, 2008). Also recipient mice transplanted with *bim*$^{-/-}$ or *bmf*$^{-/-}$ donor cells did not develop tumors up to 8 month after transplantation (Labi *et al.*, 2012).

Despite the obviously rare incidence of tumor formation upon loss of Bim or Bmf in mice, this does not exclude the possibility of malignant transformation upon stable knockdown of BIM or BMF in human haematopoietic cells over time. Even more importantly, the use of lentiviral vectors may increase the risk of malignant transformation due to random integration (see introduction). Therefore, inhibition of BIM or BMF has to be transient if used therapeutically. One possible transduction system for transient cell manipulation is given by adenoviral vectors. Recently, the fiber-retargeted Ad5/F35 adenoviral vector has been demonstrated to efficiently transduce $CD34^+$ cells by utilizing the ubiquitously expressed CD46 receptor (Nilsson *et al.*, 2004a). As adenoviruses do not integrate into the genome of the host cell (Järås *et al.*, 2007), Ad5/F35 mediated downregulation of Bim or Bmf, or overexpression of their antagonists Bcl-2 or Bcl-x_L should only transiently inhibit apoptosis in $CD34^+$ cells and therefore minimize the risk of tumor formation following reconstitution. Since the transduction efficiency of human $CD34^+$ cells with the Ad5/F35 virus turned out to be very low, Ad5/F35 viruses overexpressing BCL-XL rather than downregulating BIM or BMF were used for our experimental approach.

Gene expression from adenoviral vectors in $CD34^+$ cells strongly depends on the promoter used (Sakurai *et al.*, 2005). As published by different groups and also shown in our studies the PGK promoter is superior to the CMV promoter but still rather inefficient for transgene expression in cord blood derived $CD34^+$ cells. BoosterExpress^{TM} reagent seems to be a very promising chemical cocktail to increase adenoviral mediated gene expression (Lavazza *et al.*, 2007). Indeed, the presence of BoosterExpress^{TM} reagent highly increased the activity of the CMV promoter in $CD34^+$ cells. However, we observed strong adverse effects in recipient mice including joint swelling and weight loss and therefore had to stop our experiments immediately. Clearly, other strategies are needed to overcome inefficient adenoviral mediated gene transfer. One possibility might be the use of other promoters such as the SFFV promoter, shown in our study to mediate gene expression with high efficiency.

Of note, whereas adenoviral vectors are important for proof-of-principle experiments showing that transient apoptosis inhibition is sufficient to increase transplantation efficiency, the use of viral vectors in general will not find a way into clinical application. In contrast, several recent strategies developed to transiently modify target cells without the need of viral vectors, appear to be more promising for therapeutic use. The cationic liposome DOTAP was successfully used to deliver siRNA into $CD34^+$ cells with an efficiency comparable to lentiviral mediated gene transfer, and mRNA can be delivered successfully by nucleofection (Martino *et al.*, 2009; Wiehe *et al.*, 2007). Moreover, cell penetrating peptides are promising and could be used for

intracellular delivery of Bcl-x_L. Delivery of Bcl-x_L by fusion to the protein transduction domain of HIV TAT has recently been reported to inhibit cell death of neuronal cells (Dietz *et al.*, 2002).

In summary, our data suggest that cell death occurring during transplantation leads to a relevant loss of stem cells, and that in both murine and human HSPCs apoptosis depends critically on Bim and Bmf. By demonstrating that human HSPCs with reduced levels of BIM or BMF performed superior in engrafting immunodeficient recipient mice, this study identified inhibition of the intrinsic apoptosis pathway as a promising novel approach to increase HSCT efficiency. However, to overcome the risk of tumor formation associated with permanent apoptosis inhibition further studies are required, and safer and more transient methods of apoptosis inhibition have to be developed.

References

Adolfsson, J., Borge, O.J., Bryder, D., Theilgaard-Mönch, K., Åstrand-Grundström, I., Sitnicka, E., Sasaki, Y., & Jacobsen, S.E.W. 2001. Upregulation of Flt3 Expression within the Bone Marrow Lin$^-$Sca1$^+$c-kit$^+$ Stem Cell Compartment Is Accompanied by Loss of Self-Renewal Capacity. *Immunity*, **15**(4), 659–669. 3

Adolfsson, J., Månsson, R., Buza-Vidas, N., Hultquist, A., Liuba, K., Jensen, C.T., Bryder, D., Yang, L., Borge, O.J., Thoren, L.A.M., *et al.* 2005. Identification of Flt3$^+$ Lympho-Myeloid Stem Cells Lacking Erythro-Megakaryocytic Potential: A Revised Road Map for Adult Blood Lineage Commitment. *Cell*, **121**(2), 295–306. 5

Aguila, H.L., & Weissman, IL. 1996. Hematopoietic stem cells are not direct cytotoxic targets of natural killer cells. *Blood*, **87**(4), 1225–1231. 22

Akala, O.O., Park, I.K., Qian, D., Pihalja, M., Becker, M.W., & Clarke, M.F. 2008. Long-term haematopoietic reconstitution by Trp53-/-p16Ink4a-/-p19Arf-/-multipotent progenitors. *Nature*, **453**(7192), 228–232. 37

Akashi, K., Traver, D., Miyamoto, T., Weissman, I.L., *et al.* 2000. A clonogenic common myeloid progenitor that gives rise to all myelold lineages. *Nature*, **404**(6774), 193–196. 5

Ballen, K.K., Spitzer, T.R., Yeap, B.Y., McAfee, S., Dey, B.R., Attar, E., Haspel, R., Kao, G., Liney, D., Alyea, E., *et al.* 2007. Double unrelated reduced-intensity umbilical cord blood transplantation in adults. *Biology of Blood and Marrow Transplantation*, **13**(1), 82–89. 8

Barker, J.N., Weisdorf, D.J., DeFor, T.E., Blazar, B.R., McGlave, P.B., Miller, J.S., Verfaillie, C.M., & Wagner, J.E. 2005. Transplantation of 2 partially HLA-matched umbilical cord blood units to enhance engraftment in adults with hematologic malignancy. *Blood*, **105**(3), 1343–1347. 8, 102

Basañez, G., Soane, L., & Hardwick, J.M. 2012. A New View of the Lethal Apoptotic Pore. *PLoS Biology*, **10**(9), e1001399. 16

Baum, C.M., Weissman, I.L., Tsukamoto, A.S., Buckle, A.M., & Peault, B. 1992. Isolation of a candidate human hematopoietic stem-cell population. *Proceedings of the National Academy of Sciences*, **89**(7), 2804–2808. 3

Bautista, G., Cabrera, JR, Regidor, C., Forés, R., García-Marco, JA, Ojeda, E., Sanjuán, I., Ruiz, E., Krsnik, I., Navarro, B., *et al.* 2008. Cord blood transplants supported by co-infusion of mobilized hematopoietic stem cells from a third-party donor. *Bone marrow transplantation*, **43**(5), 365–373. 8

Benveniste, P., Frelin, C., Janmohamed, S., Barbara, M., Herrington, R., Hyam, D., & Iscove, N.N. 2010. Intermediate-term hematopoietic stem cells with extended but time-limited reconstitution potential. *Cell Stem Cell*, **6**(1), 48–58. 3

Bergelson, J.M., Cunningham, J.A., Droguett, G., Kurt-Jones, E.A., Krithivas, A., Hong, J.S., Horwitz, M.S., Crowell, R.L., & Finberg, R.W. 1997. Isolation of a common receptor for Coxsackie B viruses and adenoviruses 2 and 5. *Science*, **275**(5304), 1320–1323. 24

Bhattacharya, D., Czechowicz, A., Ooi, A.G.L., Rossi, D.J., Bryder, D., & Weissman, I.L. 2009. Niche recycling through division-independent egress of hematopoietic stem cells. *The Journal of experimental medicine*, **206**(12), 2837–2850. 98

Blank, U., Karlsson, G., & Karlsson, S. 2008. Signaling pathways governing stem-cell fate. *Blood*, **111**(2), 492–503. 1, 2

Boitano, A.E., Wang, J., Romeo, R., Bouchez, L.C., Parker, A.E., Sutton, S.E., Walker, J.R., Flaveny, C.A., Perdew, G.H., Denison, M.S., *et al.* 2010. Aryl hydrocarbon receptor antagonists promote the expansion of human hematopoietic stem cells. *Science Signalling*, **329**(5997), 1345. 9, 103

Borner, Christoph. 1996. Diminished cell proliferation associated with the death-protective activity of Bcl-2. *Journal of Biological Chemistry*, **271**(22), 12695–12698. 99

Bosma, G.C., Custer, R.P., & Bosma, M.J. 1983. A severe combined immunodeficiency mutation in the mouse. 6

Bouillet, P., Metcalf, D., Huang, D.C.S., Tarlinton, D.M., Kay, T.W.H., Köntgen, F., Adams, J.M., & Strasser, A. 1999. Proapoptotic Bcl-2 relative Bim required for certain apoptotic responses, leukocyte homeostasis, and to preclude autoimmunity. *Science*, **286**(5445), 1735–1738. 17, 96, 103

Bouillet, P., Cory, S., Zhang, L.C., Strasser, A., & Adams, J.M. 2001. Degenerative disorders caused by Bcl-2 deficiency prevented by loss of its BH3-only antagonist Bim. *Developmental cell*, **1**(5), 645–653. 103

Bouillet, P., Purton, J.F., Godfrey, D.I., Zhang, L.C., Coultas, L., Puthalakath, H., Pellegrini, M., Cory, S., Adams, J.M., & Strasser, A. 2002. BH3-only Bcl-2 family member Bim is required for apoptosis of autoreactive thymocytes. *Nature*, **415**(6874), 922–926. 17

Bourhis, E., Hymowitz, S.G., & Cochran, A.G. 2007. The mitotic regulator Survivin binds as a monomer to its functional interactor Borealin. *Journal of Biological Chemistry*, **282**(48), 35018–35023. 99

Boztug, K., Schmidt, M., Schwarzer, A., Banerjee, P.P., Díez, I.A., Dewey, R.A., Böhm, M., Nowrouzi, A., Ball, C.R., Glimm, H., *et al.* 2010. Stem-cell gene therapy for the Wiskott–Aldrich syndrome. *New England Journal of Medicine*, **363**(20), 1918–1927. 23

Brave, M., Farrell, A., Ching Lin, S., Ocheltree, T., Pope Miksinski, S., Lee, S.L., Saber, H., Fourie, J., Tornoe, C., Booth, B., *et al.* 2010. FDA review summary: Mozobil in combination with granulocyte colony-stimulating factor to mobilize hematopoietic stem cells to the peripheral blood for collection and subsequent autologous transplantation. *Oncology*, **78**(3-4), 282–288. 8, 102

Brehm, M.A., Cuthbert, A., Yang, C., Miller, D.M., Dilorio, P., Laning, J., Burzenski, L., Gott, B., Foreman, O., Kavirayani, A., *et al.* 2010. Parameters for establishing humanized mouse models to study human immunity: Analysis of human hematopoietic stem cell engraftment in three immunodeficient strains of mice bearing the IL2rγnull mutation. *Clinical immunology (Orlando, Fla.)*, **135**(1), 84. 102

Brehm, M.A., Racki, W.J., Leif, J., Burzenski, L., Hosur, V., Wetmore, A., Gott, B., Herlihy, M., Ignotz, R., Dunn, R., *et al.* 2012. Engraftment of human HSCs in nonirradiated newborn NOD-scid IL2rγnull mice is enhanced by transgenic expression of membrane-bound human SCF. *Blood*, **119**(12), 2778–2788. 8

Broudy, V.C. 1997. Stem cell factor and hematopoiesis. *Blood*, **90**(4), 1345–1364. 7

Broxmeyer, H.E., Kohli, L., Kim, C.H., Lee, Y., Mantel, C., Cooper, S., Hangoc, G., Shaheen, M., Li, X., & Clapp, D.W. 2003. Stromal cell-derived factor-1/CXCL12 directly enhances survival/antiapoptosis of myeloid progenitor cells through CXCR4 and Gαi proteins and enhances engraftment of competitive, repopulating stem cells. *Journal of leukocyte biology*, **73**(5), 630–638. 9

Broxmeyer, H.E., Hoggatt, J., O'Leary, H.A., Mantel, C., Chitteti, B.R., Cooper, S., Messina-Graham, S., Hangoc, G., Farag, S., Rohrabaugh, S.L., *et al.* 2012. Dipeptidylpeptidase 4 negatively regulates colony-stimulating factor activity and stress hematopoiesis. *Nature Medicine*. 9

Bryder, D., Ramsfjell, V., Dybedal, I., Theilgaard-Mönch, K., Högerkorp, C.M., Adolfsson, J., Borge, O.J., & Jacobsen, S.E.W. 2001. Self-renewal of multipotent long-term repopulating hematopoietic stem cells is negatively regulated by Fas and tumor necrosis factor receptor activation. *The Journal of experimental medicine*, **194**(7), 941–952. 22

Calvi, LM, Adams, GB, Weibrecht, KW, Weber, JM, Olson, DP, Knight, MC, Martin, RP, Schipani, E., Divieti, P., Bringhurst, FR, *et al.* 2003. Osteoblastic cells regulate the haematopoietic stem cell niche. *Nature*, **425**(6960), 841–846. 1

Campbell, C.J.V., Lee, J.B., Levadoux-Martin, M., Wynder, T., Xenocostas, A., Leber, B., & Bhatia, M. 2010a. The human stem cell hierarchy is defined by a functional dependence on Mcl-1 for self-renewal capacity. *Blood*, **116**(9), 1433–1442. 20

Campbell, K.J., Bath, M.L., Turner, M.L., Vandenberg, C.J., Bouillet, P., Metcalf, D., Scott, C.L., & Cory, S. 2010b. Elevated Mcl-1 perturbs lymphopoiesis, promotes transformation of hematopoietic stem/progenitor cells, and enhances drug resistance. *Blood*, **116**(17), 3197–3207. 20

Campbell, T.B., Hangoc, G., Liu, Y., Pollok, K., & Broxmeyer, H.E. 2007. Inhibition of CD26 in human cord blood $CD34^+$ cells enhances their engraftment of nonobese diabetic/severe combined immunodeficiency mice. *Stem cells and development*, **16**(3), 347–354. 9

Cartron, P.F., Gallenne, T., Bougras, G., Gautier, F., Manero, F., Vusio, P., Meflah, K., Vallette, F.M., & Juin, P. 2004. The first α helix of Bax plays a necessary role in its ligand-induced activation by the BH3-only proteins Bid and PUMA. *Molecular cell*, **16**(5), 807–818. 15

Certo, M., Del Gaizo Moore, V., Nishino, M., Wei, G., Korsmeyer, S., Armstrong, S.A., & Letai, A. 2006. Mitochondria primed by death signals determine cellular addiction to antiapoptotic BCL-2 family members. *Cancer cell*, **9**(5), 351–365. 96

Chaudhary, P.M., Eby, M., Jasmin, A., Bookwalter, A., Murray, J., & Hood, L. 1997. Death receptor 5, a new member of the TNFR family, and DR4 induce FADD-dependent apoptosis and activate the NF-κB pathway. *Immunity*, **7**(6), 821–830. 11

Chen, L., Willis, S.N., Wei, A., Smith, B.J., Fletcher, J.I., Hinds, M.G., Colman, P.M., Day, C.L., Adams, J.M., & Huang, D. 2005. Differential targeting of prosurvival Bcl-2 proteins by their BH3-only ligands allows complementary apoptotic function. *Molecular cell*, **17**(3), 393–403. 15, 96

Chen, Q., Khoury, M., & Chen, J. 2009. Expression of human cytokines dramatically improves reconstitution of specific human-blood lineage cells in humanized mice. *Proceedings of the National Academy of Sciences*, **106**(51), 21783–21788. 101

Chinnaiyan, A.M., O'Rourke, K., Tewari, M., Dixit, V.M., *et al.* 1995. FADD, a novel death domain-containing protein, interacts with the death domain of Fas and initiates apoptosis. *Cell*, **81**(4), 505–512. 11

Chipuk, J.E., Moldoveanu, T., Llambi, F., Parsons, M.J., & Green, D.R. 2010. The BCL-2 family reunion. *Molecular cell*, **37**(3), 299–310. 15

Choi, BK, Joo, SY, Moon, C., Park, KS, Kim, SH, Park, JB, Jung, GO, Choi, GS, Kwon, CH, Chun, JM, *et al.* 2008. Reconstitution of Human Lymphocytes Following Ex Vivo Expansion of Human Umbilical Cord Blood $CD34^+$ Cells and Transplantation in $Rag2^{-/-}\gamma c^{-/-}$ Mice Model. *Pages 2655–2660 of: Transplantation proceedings*, vol. 40. Elsevier. 77

Choy, E.Y.W., Siu, K.L., Kok, K.H., Lung, R.W.M., Tsang, C.M., To, K.F., Kwong, D.L.W., Tsao, S.W., & Jin, D.Y. 2008. An Epstein-Barr virus–encoded microRNA targets PUMA to promote host cell survival. *The Journal of experimental medicine*, **205**(11), 2551–2560. 18

Christensen, J.L., & Weissman, I.L. 2001. Flk-2 is a marker in hematopoietic stem cell differentiation: a simple method to isolate long-term stem cells. *Proceedings of the National Academy of Sciences*, **98**(25), 14541–14546. 3

Christopherson II, K.W., Hangoc, G., & Broxmeyer, H.E. 2002. Cell surface peptidase CD26/dipeptidylpeptidase IV regulates CXCL12/stromal cell-derived factor-1α-mediated chemotaxis of human cord blood $CD34^+$ progenitor cells. *The Journal of Immunology*, **169**(12), 7000–7008. 9

Coffer, P.J., *et al.* 2000. Expression of the pro-apoptotic Bcl-2 family member Bim is regulated by the forkhead transcription factor FKHR-L1. *Current Biology*, **10**(19), 1201–1204. 18, 55

Cory, S., Huang, D.C.S., & Adams, J.M. 2003. The Bcl-2 family: roles in cell survival and oncogenesis. *Oncogene*, **22**(53), 8590–8607. 95

Coultas, L., Bouillet, P., Loveland, K.L., Meachem, S., Perlman, H., Adams, J.M., & Strasser, A. 2005. Concomitant loss of proapoptotic BH3-only Bcl-2 antagonists Bik and Bim arrests spermatogenesis. *The EMBO journal*, **24**(22), 3963–3973. 17

Coultas, L., Terzano, S., Thomas, T., Voss, A., Reid, K., Stanley, E.G., Scott, C.L., Bouillet, P., Bartlett, P., Ham, J., *et al.* 2007. Hrk/DP5 contributes to the apoptosis of select neuronal populations but is dispensable for haematopoietic cell apoptosis. *Journal of cell science*, **120**(12), 2044–2052. 17

Czabotar, Peter E, Westphal, Dana, Dewson, Grant, Ma, Stephen, Hockings, Colin, Fairlie, W Douglas, Lee, Erinna F, Yao, Shenggen, Robin, Adeline Y, Smith, Brian J, *et al.* 2013. Bax Crystal Structures Reveal How BH3 Domains Activate Bax and Nucleate Its Oligomerization to Induce Apoptosis. *Cell*, **152**(3), 519–531. 16

De Lima, M., McMannis, J., Gee, A., Komanduri, K., Couriel, D., Andersson, BS, Hosing, C., Khouri, I., Jones, R., Champlin, R., *et al.* 2008. Transplantation of ex vivo expanded cord blood cells using the copper chelator tetraethylenepentamine: a phase I/II clinical trial. *Bone marrow transplantation*, **41**(9), 771–778. 9

de Lima, M., McNiece, I., Robinson, S.N., Munsell, M., Eapen, M., Horowitz, M., Alousi, A., Saliba, R., McMannis, J.D., Kaur, I., *et al.* 2012. Cord-Blood Engraftment with Ex Vivo Mesenchymal-Cell Coculture. *New England Journal of Medicine*, **367**(24), 2305–2315. 103

Degterev, A., Huang, Z., Boyce, M., Li, Y., Jagtap, P., Mizushima, N., Cuny, G.D., Mitchison, T.J., Moskowitz, M.A., & Yuan, J. 2005. Chemical inhibitor of nonapoptotic cell death with therapeutic potential for ischemic brain injury. *Nature chemical biology*, **1**(2), 112–119. 10

Delaney, C., Varnum-Finney, B., Aoyama, K., Brashem-Stein, C., & Bernstein, I.D. 2005. Dose-dependent effects of the Notch ligand Delta1 on ex vivo differentiation and in vivo marrow repopulating ability of cord blood cells. *Blood*, **106**(8), 2693–2699. 9

Demirer, T., Buckner, C.D., & Bensinger, W.I. 2009. Optimization of peripheral blood stem cell mobilization. *Stem Cells*, **14**(1), 106–116. 25, 55, 102

Dewson, G., Kratina, T., Sim, H.W., Puthalakath, H., Adams, J.M., Colman, P.M., & Kluck, R.M. 2008. To trigger apoptosis, Bak exposes its BH3 domain and homodimerizes via BH3: groove interactions. *Molecular cell*, **30**(3), 369–380. 16

Dewson, G., Kratina, T., Czabotar, P., Day, C.L., Adams, J.M., & Kluck, R.M. 2009. Bak activation for apoptosis involves oligomerization of dimers via their α6 helices. *Molecular cell*, **36**(4), 696–703. 16

Dietz, G.P.H., Kilic, E., & Bähr, M. 2002. Inhibition of Neuronal Apoptosis *in Vitro* and *in Vivo* Using TAT-Mediated Protein Transduction. *Molecular and Cellular Neuroscience*, **21**(1), 29–37. 105

Dohlman, W., Caroti, M., Leflowitz, R., Nathans, J., Kubo, T., Bonner, T., Buckley, N., Young, A., Brann, M., Julius, D., *et al.* 1988. Bcl-2 gene promotes haemopoietic cell survival and cooperates with c-myc to immortalize pre-B cells. *Nature*, **335**, 440–442. 13

Domen, J., & Weissman, I.L. 2000. Hematopoietic stem cells need two signals to prevent apoptosis; BCL-2 can provide one of these, Kitl/c-Kit signaling the other. *The Journal of experimental medicine*, **192**(12), 1707–1718. 20, 58

Domen, J., & Weissman, I.L. 2003. Hematopoietic stem cells and other hematopoietic cells show broad resistance to chemotherapeutic agents in vivo when overexpressing *bcl*-2. *Experimental hematology*, **31**(7), 631–639. 20

Domen, J., Gandy, K.L., & Weissman, I.L. 1998. Systemic overexpression of BCL-2 in the hematopoietic system protects transgenic mice from the consequences of lethal irradiation. *Blood*, **91**(7), 2272–2282. 20

Domen, J., Cheshier, S.H., & Weissman, I.L. 2000. The role of apoptosis in the regulation of hematopoietic stem cells Overexpression of Bcl-2 increases both their number and repopulation potential. *The Journal of experimental medicine*, **191**(2), 253–264. 1, 20, 95, 97

Doulatov, S., Notta, F., Eppert, K., Nguyen, L.T., Ohashi, P.S., & Dick, J.E. 2010. Revised map of the human progenitor hierarchy shows the origin of macrophages and dendritic cells in early lymphoid development. *Nature immunology*, **11**(7), 585–593. 5

Doulatov, S., Notta, F., Laurenti, E., & Dick, J.E. 2012. Hematopoiesis: a human perspective. *Cell stem cell*, **10**(2), 120–136. 4

Eckelman, B.P., Salvesen, G.S., & Scott, F.L. 2006. Human inhibitor of apoptosis proteins: why XIAP is the black sheep of the family. *EMBO reports*, **7**(10), 988–994. 13

Egle, A., Harris, A.W., Bouillet, P., & Cory, S. 2004. Bim is a suppressor of Myc-induced mouse B cell leukemia. *Proceedings of the National Academy of Sciences of the United States of America*, **101**(16), 6164–6169. 18, 103

Eldering, E., Spek, C.A., Aberson, H.L., Grummels, A., Derks, I.A., De Vos, A.F., McElgunn, C.J., & Schouten, J.P. 2003. Expression profiling via novel multiplex assay allows rapid assessment of gene regulation in defined signalling pathways. *Nucleic acids research*, **31**(23), e153–e153. 48, 56

Enari, M., Sakahira, H., Yokoyama, H., Okawa, K., Iwamatsu, A., & Nagata, S. 1998. A caspase-activated DNase that degrades DNA during apoptosis, and its inhibitor ICAD. *Nature*, **391**(6662), 43–50. 11

Enders, A., Bouillet, P., Puthalakath, H., Xu, Y., Tarlinton, D.M., & Strasser, A. 2003. Loss of the pro-apoptotic BH3-only Bcl-2 family member Bim inhibits BCR stimulation–induced apoptosis and deletion of autoreactive B cells. *The Journal of experimental medicine*, **198**(7), 1119–1126. 17

Erlacher, M., Michalak, E.M., Kelly, P.N., Labi, V., Niederegger, H., Coultas, L., Adams, J.M., Strasser, A., & Villunger, A. 2005. BH3-only proteins Puma and Bim are rate-limiting for γ-radiation–and glucocorticoid-induced apoptosis of lymphoid cells in vivo. *Blood*, **106**(13), 4131–4138. 17, 19, 68

Erlacher, M., Labi, V., Manzl, C., Böck, G., Tzankov, A., Häcker, G., Michalak, E., Strasser, A., & Villunger, A. 2006. Puma cooperates with Bim, the rate-limiting BH3-only protein in cell death during lymphocyte development, in apoptosis induction. *The Journal of experimental medicine*, **203**(13), 2939–2951. 17, 71, 96, 103

Ewings, K.E., Hadfield-Moorhouse, K., Wiggins, C.M., Wickenden, J.A., Balmanno, K., Gilley, R., Degenhardt, K., White, E., & Cook, S.J. 2007. ERK1/2-dependent phosphorylation of BimEL promotes its rapid dissociation from Mcl-1 and Bcl-xL. *The EMBO journal*, **26**(12), 2856–2867. 18, 100

Fleming, H.E., Janzen, V., Lo Celso, C., Guo, J., Leahy, K.M., Kronenberg, H.M., & Scadden, D.T. 2008. Wnt signaling in the niche enforces hematopoietic stem cell quiescence and is necessary to preserve self-renewal in vivo. *Cell Stem Cell*, **2**(3), 274–283. 2

Frassoni, F., Gualandi, F., Podestà, M., Raiola, A.M., Ibatici, A., Piaggio, G., Sessarego, M., Sessarego, N., Gobbi, M., Sacchi, N., *et al.* 2008. Direct intrabone transplant of unrelated cord-blood cells in acute leukaemia: a phase I/II study. *The lancet oncology*, **9**(9), 831–839. 9

Fukuda, S., & Pelus, L.M. 2002. Elevation of Survivin levels by hematopoietic growth factors occurs in quiescent CD34+ hematopoietic stem and progenitor cells before cell cycle entry. *Cell Cycle*, **1**(5), 323–324. 99

Gaggar, A., Shayakhmetov, D.M., & Lieber, A. 2003. CD46 is a cellular receptor for group B adenoviruses. *Nature medicine*, **9**(11), 1408–1412. 24

Gazitt, Y., *et al.* 1999. TRAIL is a potent inducer of apoptosis in myeloma cells derived from multiple myeloma patients and is not cytotoxic to hematopoietic stem cells. *Leukemia: official journal of the Leukemia Society of America, Leukemia Research Fund, UK*, **13**(11), 1817. 22

Godfrey, W.R., Spoden, D.J., Ying, G.G., Baker, S.R., Liu, B., Levine, B.L., June, C.H., Blazar, B.R., & Porter, S.B. 2005. Cord blood CD4+ CD25+-derived T regulatory cell lines express FoxP3 protein and manifest potent suppressor function. *Blood*, **105**(2), 750–758. 5

Golks, A., Brenner, D., Fritsch, C., Krammer, P.H., & Lavrik, I.N. 2005. c-FLIPR, a new regulator of death receptor-induced apoptosis. *Journal of Biological Chemistry*, **280**(15), 14507–14513. 11

Greco, N.J., Seetharaman, S., Kurtz, J., Lee, W.R., & Moroff, G. 2006. Evaluation of the reactivity of apoptosis markers before and after cryopreservation in cord blood $CD34^+$ cells. *Stem cells and development*, **15**(1), 124–135. 95

Grespi, F., Soratroi, C., Krumschnabel, G., Sohm, B., Ploner, C., Geley, S., Hengst, L., Häcker, G., & Villunger, A. 2010. BH3-only protein Bmf mediates apoptosis upon inhibition of CAP-dependent protein synthesis. *Cell Death & Differentiation*, **17**(11), 1672–1683. 19

Gutman, J.A., Turtle, C.J., Manley, T.J., Heimfeld, S., Bernstein, I.D., Riddell, S.R., & Delaney, C. 2010. Single-unit dominance after double-unit umbilical cord blood transplantation coincides with a specific CD8+ T-cell response against the nonengrafted unit. *Blood*, **115**(4), 757–765. 8, 102

Han, J., Flemington, C., Houghton, A.B., Gu, Z., Zambetti, G.P., Lutz, R.J., Zhu, L., & Chittenden, T. 2001. Expression of bbc3, a pro-apoptotic BH3-only gene, is regulated by diverse cell death and survival signals. *Proceedings of the National Academy of Sciences*, **98**(20), 11318–11323. 19

Han, P., Hodge, G., Story, C., & Xu, X. 2008. Phenotypic analysis of functional T-lymphocyte subtypes and natural killer cells in human cord blood: relevance to umbilical cord blood transplantation. *British journal of haematology*, **89**(4), 733–740. 5

Hande, KR, *et al.* 1998. Etoposide: four decades of development of a topoisomerase II inhibitor. *European journal of cancer (Oxford, England: 1990)*, **34**(10), 1514. 68

Hao, Q.L., Shah, A.J., Thiemann, F.T., Smogorzewska, E.M., & Crooks, GM. 1995. A functional comparison of $CD34^+CD38^-$ cells in cord blood and bone marrow. *Blood*, **86**(10), 3745–3753. 3

Happo, L., Strasser, A., & Cory, S. 2012. BH3-only proteins in apoptosis at a glance. *Journal of Cell Science*, **125**(5), 1081–1087. 15, 16, 17, 18, 100

Haspel, RL, Kao, G., Yeap, BY, Cutler, C., Soiffer, RJ, Alyea, EP, Ho, VT, Koreth, J., Dey, BR, McAfee, SL, *et al.* 2007. Preinfusion variables predict the predominant unit in the setting of reduced-intensity double cord blood transplantation. *Bone marrow transplantation*, **41**(6), 523–529. 8

Hematti, P., Hong, B.K., Ferguson, C., Adler, R., Hanawa, H., Sellers, S., Holt, I.E., Eckfeldt, C.E., Sharma, Y., Schmidt, M., *et al.* 2004. Distinct genomic integration of MLV and SIV vectors in primate hematopoietic stem and progenitor cells. *PLoS biology*, **2**(12), e423. 24

Hershko, T., & Ginsberg, D. 2004. Up-regulation of Bcl-2 homology 3 (BH3)-only proteins by E2F1 mediates apoptosis. *Journal of Biological Chemistry*, **279**(10), 8627–8634. 18

Hofmeister, CC, Zhang, J., Knight, KL, Le, P., & Stiff, PJ. 2007. Ex vivo expansion of umbilical cord blood stem cells for transplantation: growing knowledge from the hematopoietic niche. *Bone marrow transplantation*, **39**(1), 11–23. 95, 103

Holt, N., Wang, J., Kim, K., Friedman, G., Wang, X., Taupin, V., Crooks, G.M., Kohn, D.B., Gregory, P.D., Holmes, M.C., *et al.* 2010. Zinc finger nuclease-mediated CCR5 knockout hematopoietic stem cell transplantation controls HIV-1 in vivo. *Nature biotechnology*, **28**(8), 839. 24

Hughes, P.D., Belz, G.T., Fortner, K.A., Budd, R.C., Strasser, A., & Bouillet, P. 2008. Apoptosis regulators Fas and Bim cooperate in shutdown of chronic immune responses and prevention of autoimmunity. *Immunity*, **28**(2), 197–205. 17

Ikuta, K., & Weissman, I.L. 1992. Evidence that hematopoietic stem cells express mouse c-kit but do not depend on steel factor for their generation. *Proceedings of the National Academy of Sciences*, **89**(4), 1502–1506. 3

Imaizumi, K., Benito, A., Kiryu-Seo, S., Gonzalez, V., Inohara, N., Leiberman, A.P., Kiyama, H., & Nuñez, G. 2004. Critical role for DP5/Harakiri, a Bcl-2 homology domain 3-only Bcl-2 family member, in axotomy-induced neuronal cell death. *The Journal of neuroscience*, **24**(15), 3721–3725. 17

Irmler, M., Thome, M., Hahne, M., Schneider, P., Hofmann, K., Steiner, V., Bodmer, J.L., Schroter, M., Burns, K., Mattmann, C., *et al.* 1997. Inhibition of death receptor signals by cellular FLIP. *Nature*, **388**(6638), 190–194. 11

Ito, M., Hiramatsu, H., Kobayashi, K., Suzue, K., Kawahata, M., Hioki, K., Ueyama, Y., Koyanagi, Y., Sugamura, K., Tsuji, K., *et al.* 2002. NOD/SCID/γ mouse: an excellent recipient mouse model for engraftment of human cells. *Blood*, **100**(9), 3175–3182. 7

Järås, M., Brun, A., Karlsson, S., & Fan, X. 2007. Adenoviral vectors for transient gene expression in human primitive hematopoietic cells: applications and prospects. *Experimental hematology*, **35**(3), 343–349. 24, 89, 104

Jaroscak, J., Goltry, K., Smith, A., Waters-Pick, B., Martin, P.L., Driscoll, T.A., Howrey, R., Chao, N., Douville, J., Burhop, S., *et al.* 2003. Augmentation of umbilical cord blood (UCB) transplantation with ex vivo–expanded UCB cells: results of a phase 1 trial using the AastromReplicell System. *Blood*, **101**(12), 5061–5067. 103

Jeffers, J.R., Parganas, E., Lee, Y., Yang, C., Wang, J.L., Brennan, J., MacLean, K.H., Han, J., Chittenden, T., Ihle, J.N., *et al.* 2003. Puma is an essential mediator of p53-dependent and-independent apoptotic pathways. *Cancer cell*, **4**(4), 321–328. 17, 19

Kater, A.P., Evers, L.M., Remmerswaal, E., Jaspers, A., Oosterwijk, M.F., Lier, R.A.W., Oers, M.H.J., & Eldering, E. 2004. CD40 stimulation of B-cell chronic lymphocytic leukaemia cells enhances the anti-apoptotic profile, but also Bid expression and cells remain susceptible to autologous cytotoxic T-lymphocyte attack. *British journal of haematology*, **127**(4), 404–415. 48

Kaufmann, T., Tai, L., Ekert, P.G., Huang, D., Norris, F., Lindemann, R.K., Johnstone, R.W., Dixit, V.M., & Strasser, A. 2007. The BH3-only protein bid is dispensable for DNA damage-and replicative stress-induced apoptosis or cell-cycle arrest. *Cell*, **129**(2), 423–433. 17

Kerr, J.F.R., Wyllie, A.H., & Currie, A.R. 1972. Apoptosis: a basic biological phenomenon with wide-ranging implications in tissue kinetics. *British journal of cancer*, **26**(4), 239. 10

Kiel, M.J., Yilmaz, Ö.H., Iwashita, T., Yilmaz, O.H., Terhorst, C., & Morrison, S.J. 2005. SLAM family receptors distinguish hematopoietic stem and progenitor cells and reveal endothelial niches for stem cells. *Cell*, **121**(7), 1109–1121. 1, 3

Kim, H., Whartenby, K.A., Georgantas, R.W., Wingard, J., & Civin, C.I. 2002. Human CD34$^+$ Hematopoietic Stem/Progenitor Cells Express High Levels of FLIP and Are Resistant to Fas-Mediated Apoptosis. *Stem Cells*, **20**(2), 174–182. 22

Kim, J.Y., Ahn, H.J., Ryu, J.H., Suk, K., & Park, J.H. 2004. BH3-only protein Noxa is a mediator of hypoxic cell death induced by hypoxia-inducible factor 1α. *The Journal of experimental medicine*, **199**(1), 113–124. 18

Kohn, D.B. 2010. Update on gene therapy for immunodeficiencies. *Clinical Immunology*, **135**(2), 247–254. 23

Kolb, H.J. 2008. Graft-versus-leukemia effects of transplantation and donor lymphocytes. *Blood*, **112**(12), 4371–4383. 5

Komuro, K., Itakura, K., Boyse, EA, & John, M. 1974. Ly-5: a new T-lymphocyte antigen system. *Immunogenetics*, **1**(1), 452–456. 6

Kondo, M., Weissman, I.L., & Akashi, K. 1997. Identification of clonogenic common lymphoid progenitors in mouse bone marrow. *Cell*, **91**(5), 661–672. 5

Kozak, M., *et al.* 1987. At least six nucleotides preceding the AUG initiator codon enhance translation in mammalian cells. *Journal of molecular biology*, **196**(4), 947. 40

Kozuma, Y., Ninomiya, H., Murata, S., Kono, T., Mukai, HY, & Kojima, H. 2010. The pro-apoptotic BH3-only protein Bim regulates cell cycle progression of hematopoietic progenitors during megakaryopoiesis. *Journal of Thrombosis and Haemostasis*, **8**(5), 1088–1097. 98

Kraunus, J., Schaumann, DHS, Meyer, J., Modlich, U., Fehse, B., Brandenburg, G., Von Laer, D., Klump, H., Schambach, A., Bohne, J., *et al.* 2004. Self-inactivating retroviral vectors with improved RNA processing. *Gene therapy*, **11**(21), 1568–1578. 23

Krueger, A., Schmitz, I., Baumann, S., Krammer, P.H., & Kirchhoff, S. 2001. Cellular FLICE-inhibitory protein splice variants inhibit different steps of caspase-8 activation at the CD95 death-inducing signaling complex. *Journal of Biological Chemistry*, **276**(23), 20633–20640. 11

Kushnareva, Y., Andreyev, A.Y., Kuwana, T., & Newmeyer, D.D. 2012. Bax Activation Initiates the Assembly of a Multimeric Catalyst that Facilitates Bax Pore Formation in Mitochondrial Outer Membranes. *PLoS Biology*, **10**(9), e1001394. 16

Kuwana, T., Bouchier-Hayes, L., Chipuk, J.E., Bonzon, C., Sullivan, B.A., Green, D.R., Newmeyer, D.D., *et al.* 2005. BH3 domains of BH3-only proteins differentially regulate Bax-mediated mitochondrial membrane permeabilization both directly and indirectly. *Molecular cell*, **17**(4), 525–536. 15

Labi, V., Erlacher, M., Kiessling, S., & Villunger, A. 2006. BH3-only proteins in cell death initiation, malignant disease and anticancer therapy. *Cell Death & Differentiation*, **13**(8), 1325–1338. 17

Labi, V., Erlacher, M., Kiessling, S., Manzl, C., Frenzel, A., O'Reilly, L., Strasser, A., & Villunger, A. 2008. Loss of the BH3-only protein Bmf impairs B cell homeostasis and accelerates γ irradiation–induced thymic lymphoma development. *The Journal of experimental medicine*, **205**(3), 641–655. 17, 19, 103

Labi, V., Bertele, D., Woess, C., Tischner, D., Bock, F.J., Schwemmers, S., Pahl, H.L., Geley, S., Kunze, M., Niemeyer, C.M., Villunger, A., & Erlacher, M. 2012. Haematopoietic stem cell survival and transplantation efficacy is limited by the BH3-only proteins Bim and Bmf. *EMBO Molecular Medicine*. 21, 95, 99, 103

Lanvers-Kaminsky, C., Bremer, A., Dirksen, U., Jürgens, H., & Boos, J. 2006. Cytotoxicity of treosulfan and busulfan on pediatric tumor cell lines. *Anti-cancer drugs*, **17**(6), 657–662. 68

Lapidot, T., Dar, A., & Kollet, O. 2005. How do stem cells find their way home? *Blood*, **106**(6), 1901–1910. 38

Laurenti, E., Varnum-Finney, B., Wilson, A., Ferrero, I., Blanco-Bose, W.E., Ehninger, A., Knoepfler, P.S., Cheng, P.F., MacDonald, H.R., Eisenman, R.N., *et al.* 2008. Hematopoietic stem cell function and survival depend on c-Myc and N-Myc activity. *Cell Stem Cell*, **3**(6), 611–624. 22, 23

Lavazza, C., Carlo-Stella, C., Di Nicola, M., Longoni, P., Milanesi, M., Magni, M., & Gianni, A.M. 2007. Highly efficient gene transfer into mobilized CD34$^+$ hematopoietic cells using serotype-5 adenoviral vectors and BoosterExpress Reagent. *Experimental hematology*, **35**(6), 888–897. 92, 104

Lavrik, I., Krueger, A., Schmitz, I., Baumann, S., Weyd, H., Krammer, PH, & Kirchhoff, S. 2003. The active caspase-8 heterotetramer is formed at the CD95 DISC. *Cell Death & Differentiation*, **10**(1), 144–145. 11

Legrand, N., Huntington, N.D., Nagasawa, M., Bakker, A.Q., Schotte, R., Strick-Marchand, H., de Geus, S.J., Pouw, S.M., Böhne, M., Voordouw, A., *et al.* 2011. Functional CD47/signal regulatory protein alpha (SIRPα) interaction is required for optimal human T-and natural killer-(NK) cell homeostasis in vivo. *Proceedings of the National Academy of Sciences*, **108**(32), 13224–13229. 8

Lei, K., & Davis, R.J. 2003. JNK phosphorylation of Bim-related members of the Bcl2 family induces Bax-dependent apoptosis. *Proceedings of the National Academy of Sciences*, **100**(5), 2432–2437. 18

Lepus, C.M., Gibson, T.F., Gerber, S.A., Kawikova, I., Szczepanik, M., Hossain, J., Ablamunits, V., Kirkiles-Smith, N., Herold, K.C., Donis, R.O., *et al.* 2009. Comparison of human fetal liver, umbilical cord blood, and adult blood hematopoietic stem cell engraftment in NOD-*scid*/γc$^{-/-}$, Balb/c-*Rag1*$^{-/-}\gamma$c$^{-/-}$, and C.B-17-*scid*/bg immunodeficient mice. *Human immunology*, **70**(10), 790–802. 7

Letai, A., Bassik, M.C., Walensky, L.D., Sorcinelli, M.D., Weiler, S., & Korsmeyer, S.J. 2002. Distinct BH3 domains either sensitize or activate mitochondrial apoptosis, serving as prototype cancer therapeutics. *Cancer cell*, **2**(3), 183–192. 15

Levine, B., Yuan, J., *et al.* 2005. Autophagy in cell death: an innocent convict? *Journal of Clinical Investigation*, **115**(10), 2679. 10

Lewis, Paul F, & Emerman, Michael. 1994. Passage through mitosis is required for oncoretroviruses but not for the human immunodeficiency virus. *Journal of virology*, **68**(1), 510–516. 24

Ley, R., Balmanno, K., Hadfield, K., Weston, C., & Cook, S.J. 2003. Activation of the ERK1/2 signaling pathway promotes phosphorylation and proteasome-dependent degradation of the BH3-only protein, Bim. *Journal of Biological Chemistry*, **278**(21), 18811–18816. 18, 100

Li, H., Zhu, H., Xu, CJ, Yuan, J., *et al.* 1998. Cleavage of BID by caspase 8 mediates the mitochondrial damage in the Fas pathway of apoptosis. *Cell*, **94**(4), 491–502. 11

Li, J., & Yuan, J. 2008. Caspases in apoptosis and beyond. *Oncogene*, **27**(48), 6194–6206. 10, 11

Li, L.Y., Luo, X., & Wang, X. 2001. Endonuclease G is an apoptotic DNase when released from mitochondria. *Nature*, **412**(6842), 95–99. 13

Li, P., Nijhawan, D., Budihardjo, I., Srinivasula, S.M., Ahmad, M., Alnemri, E.S., Wang, X., *et al.* 1997. Cytochrome c and dATP-dependent formation of Apaf-1/caspase-9 complex initiates an apoptotic protease cascade. *Cell*, **91**(4), 479–490. 13

Limanni, A., Baker, WH, Chang, CM, Seemann, R., Williams, DE, & Patchen, ML. 1995. c-kit ligand gene expression in normal and sublethally irradiated mice. *Blood*, **85**(9), 2377–2384. 7

Lockshin, R.A., & Zakeri, Z. 2004. Apoptosis, autophagy, and more. *The international journal of biochemistry & cell biology*, **36**(12), 2405–2419. 10

Locksley, R.M., Killeen, N., & Lenardo, M.J. 2001. The TNF and TNF receptor superfamilies: integrating mammalian biology. *Cell*, **104**(4), 487. 11

Lombardo, A., Genovese, P., Beausejour, C.M., Colleoni, S., Lee, Y.L., Kim, K.A., Ando, D., Urnov, F.D., Galli, C., Gregory, P.D., *et al.* 2007. Gene editing in human stem cells using zinc finger nucleases and integrase-defective lentiviral vector delivery. *Nature biotechnology*, **25**(11), 1298–1306. 24

Loris, R., Dao-Thi, M.H., Bahassi, E.M., Van Melderen, L., Poortmans, F., Liddington, R., Couturier, M., & Wyns, L. 1999. Crystal structure of CcdB, a topoisomerase poison from *E. coli*. *Journal of molecular biology*, **285**(4), 1667–1677. 42

Lowman, X.H., McDonnell, M.A., Kosloske, A., Odumade, O.A., Jenness, C., Karim, C.B., Jemmerson, R., & Kelekar, A. 2010. The proapoptotic function of Noxa in human leukemia cells is regulated by the kinase Cdk5 and by glucose. *Molecular cell*, **40**(5), 823–833. 18

Luo, J., Deng, Z.L., Luo, X., Tang, N., Song, W.X., Chen, J., Sharff, K.A., Luu, H.H., Haydon, R.C., Kinzler, K.W., *et al.* 2007. A protocol for rapid generation of recombinant adenoviruses using the AdEasy system. *Nature protocols*, **2**(5), 1236–1247. 41, 42, 50, 90

Maciejewski, J., Selleri, C., Anderson, S., & Young, NS. 1995. Fas antigen expression on $CD34^+$ human marrow cells is induced by interferon gamma and tumor necrosis factor alpha and potentiates cytokine-mediated hematopoietic suppression in vitro. *Blood*, **85**(11), 3183–3190. 22

MacMillan, M.L., Weisdorf, D.J., Brunstein, C.G., Cao, Q., DeFor, T.E., Verneris, M.R., Blazar, B.R., & Wagner, J.E. 2009. Acute graft-versus-host disease after unrelated donor umbilical cord blood transplantation: analysis of risk factors. *Blood*, **113**(11), 2410–2415. 8

Magnon, C., & Frenette, P.S. 2008. Hematopoietic stem cell trafficking. 101

Mailleux, A.A., Overholtzer, M., Schmelzle, T., Bouillet, P., Strasser, A., & Brugge, J.S. 2007. BIM regulates apoptosis during mammary ductal morphogenesis, and its absence reveals alternative cell death mechanisms. *Developmental cell*, **12**(2), 221–234. 19

Majeti, R., Park, C.Y., & Weissman, I.L. 2007. Identification of a hierarchy of multipotent hematopoietic progenitors in human cord blood. *Cell Stem Cell*, **1**(6), 635–645. 3

Manz, M.G. 2007. Human-hemato-lymphoid-system mice: opportunities and challenges. *Immunity*, **26**(5), 537–541. 101

Martino, S., Di Girolamo, I., Tiribuzi, R., D'Angelo, F., Datti, A., & Orlacchio, A. 2009. Efficient siRNA delivery by the cationic liposome DOTAP in human hematopoietic stem cells differentiating into dendritic cells. *Journal of biomedicine and biotechnology*, **2009**. 104

Matsuzaki, Y., Nakayama, K., Nakayama, K., Tomita, T., Isoda, M., Loh, D.Y., & Nakauchi, H. 1997. Role of bcl-2 in the development of lymphoid cells from the hematopoietic stem cell. *Blood*, **89**(3), 853–862. 20

Mavroudis, D., Read, E., Cottler-Fox, M., Couriel, D., Molldrem, J., Carter, C., Yu, M., Dunbar, C., & Barrett, J. 1996. $CD34^+$ cell dose predicts survival, posttransplant morbidity, and rate of hematologic recovery after allogeneic marrow transplants for hematologic malignancies. *Blood*, **88**(8), 3223–3229. 55, 95

Mayani, H., Dragowska, W., & Lansdorp, PM. 1993. Characterization of functionally distinct subpopulations of $CD34^+$ cord blood cells in serum-free long-term cultures supplemented with hematopoietic cytokines. *Blood*, **82**(9), 2664–2672. 3

Mazurier, F., Gan, O.I., McKenzie, J.L., Doedens, M., & Dick, J.E. 2004. Lentivector-mediated clonal tracking reveals intrinsic heterogeneity in the human hematopoietic stem cell compartment and culture-induced stem cell impairment. *Blood*, **103**(2), 545–552. 24

McDermott, S.P., Eppert, K., Lechman, E.R., Doedens, M., & Dick, J.E. 2010. Comparison of human cord blood engraftment between immunocompromised mouse strains. *Blood*, **116**(2), 193–200. 7

Mérino, D., Giam, M., Hughes, P.D., Siggs, O.M., Heger, K., O'Reilly, L.A., Adams, J.M., Strasser, A., Lee, E.F., Fairlie, W.D., *et al.* 2009. The role of BH3-only protein Bim extends beyond inhibiting Bcl-2–like prosurvival proteins. *The Journal of cell biology*, **186**(3), 355–362. 15

Michalak, EM, Villunger, A., Adams, JM, & Strasser, A. 2008. In several cell types tumour suppressor p53 induces apoptosis largely via Puma but Noxa can contribute. *Cell Death & Differentiation*, **15**(6), 1019–1029. 17, 19

Mohr, A., Zwacka, R.M., Jarmy, G., Büneker, C., Schrezenmeier, H., Döhner, K., Beltinger, C., Wiesneth, M., Debatin, K.M., & Stahnke, K. 2005. Caspase-8L expression protects CD34+ hematopoietic progenitor cells and leukemic cells from CD95-mediated apoptosis. *Oncogene*, **24**(14), 2421–2429. 22

Morishima, Y., Sasazuki, T., Inoko, H., Juji, T., Akaza, T., Yamamoto, K., Ishikawa, Y., Kato, S., Sao, H., Sakamaki, H., *et al.* 2002. The clinical significance of human leukocyte antigen (HLA) allele compatibility in patients receiving a marrow transplant from serologically HLA-A, HLA-B, and HLA-DR matched unrelated donors. *Blood*, **99**(11), 4200–4206. 5

Motoyama, N., Wang, F., Roth, K.A., Sawa, H., Nakayama, K., Negishi, I., Senju, S., Zhang, Q., Fujii, S., *et al.* 1995. Massive cell death of immature hematopoietic cells and neurons in Bcl-x-deficient mice. *Science (New York, NY)*, **267**(5203), 1506. 20, 95

Murphy, M.J., Wilson, A., & Trumpp, A. 2005. More than just proliferation: Myc function in stem cells. *Trends in cell biology*, **15**(3), 128–137. 23

Muzio, M., Chinnaiyan, A.M., Kischkel, F.C., O'Rourke, K., Shevchenko, A., Ni, J., Scaffidi, C., Bretz, J.D., Zhang, M., Gentz, R., *et al.* 1996. FLICE, a novel FADD-homologous ICE/CED-3-like protease, is recruited to the CD95 (Fas/APO-1) death-inducing signaling complex. *Cell*, **85**(6), 817. 11

Naik, E., Michalak, E.M., Villunger, A., Adams, J.M., & Strasser, A. 2007. Ultraviolet radiation triggers apoptosis of fibroblasts and skin keratinocytes mainly via the BH3-only protein Noxa. *The Journal of cell biology*, **176**(4), 415–424. 19

Nakajima, H., Shores, E.W., Noguchi, M., & Leonard, W.J. 1997. The common cytokine receptor γ chain plays an essential role in regulating lymphoid homeostasis. *The Journal of experimental medicine*, **185**(2), 189–196. 7

Nakamura, Y., Arai, F., Iwasaki, H., Hosokawa, K., Kobayashi, I., Gomei, Y., Matsumoto, Y., Yoshihara, H., & Suda, T. 2010. Isolation and characterization of endosteal niche cell populations that regulate hematopoietic stem cells. *Blood*, **116**(9), 1422–1432. 1

Nakano, K., Vousden, K.H., *et al.* 2001. PUMA, a novel proapoptotic gene, is induced by p53. *Molecular cell*, **7**(3), 683. 18, 19

Naldini, L. 2011. Ex vivo gene transfer and correction for cell-based therapies. *Nature Reviews Genetics*, **12**(5), 301–315. 23

Nilsson, M., Karlsson, S., & Fan, X. 2004a. Functionally distinct subpopulations of cord blood $CD34^+$ cells are transduced by adenoviral vectors with serotype 5 or 35 tropism. *Molecular Therapy*, **9**(3), 377–388. 24, 89, 104

Nilsson, Marcus, Ljungberg, Johan, Richter, Johan, Kiefer, Thomas, Magnusson, Mattias, Lieber, André, Widegren, Bengt, Karlsson, Stefan, & Fan, Xiaolong. 2004b. Development of an adenoviral vector system with adenovirus serotype 35 tropism; efficient transient gene transfer into primary malignant hematopoietic cells. *The journal of gene medicine*, **6**(6), 631–641. 89

Notta, F., Doulatov, S., Laurenti, E., Poeppl, A., Jurisica, I., & Dick, J.E. 2011. Isolation of single human hematopoietic stem cells capable of long-term multilineage engraftment. *Science*, **333**(6039), 218–221. 3

O'Connor, L., Strasser, A., O'Reilly, L.A., Hausmann, G., Adams, J.M., Cory, S., & Huang, D.C.S. 1998. Bim: a novel member of the Bcl-2 family that promotes apoptosis. *The EMBO journal*, **17**(2), 384–395. 17

Oda, E., Ohki, R., Murasawa, H., Nemoto, J., Shibue, T., Yamashita, T., Tokino, T., Taniguchi, T., & Tanaka, N. 2000. Noxa, a BH3-only member of the Bcl-2 family and candidate mediator of p53-induced apoptosis. *Science Signalling*, **288**(5468), 1053. 18, 19

Oehm, A., Behrmann, I., Falk, W., Pawlita, M., Maier, G., Klas, C., Li-Weber, M., Richards, S., Dhein, J., & Trauth, BC. 1992. Purification and molecular cloning of the APO-1 cell surface antigen, a member of the tumor necrosis factor/nerve growth factor receptor superfamily. Sequence identity with the Fas antigen. *Journal of Biological Chemistry*, **267**(15), 10709–10715. 11

Oettinger, M.A., Schatz, D.G., Gorka, C., Baltimore, D., *et al.* 1990. RAG-1 and RAG-2, adjacent genes that synergistically activate V (D) J recombination. *Science*, **248**(4962), 1517–1523. 7

Ogilvy, S., Metcalf, D., Bath, M.L., Harris, A.W., Adams, J.M., *et al.* 1999. Constitutive Bcl-2 expression throughout the hematopoietic compartment affects multiple lineages and enhances progenitor cell survival. *Proceedings of the National Academy of Sciences*, **96**(26), 14943–14948. 20, 58, 97

Ooi, A.G.L., Sahoo, D., Adorno, M., Wang, Y., Weissman, I.L., & Park, C.Y. 2010. MicroRNA-125b expands hematopoietic stem cells and enriches for the lymphoid-balanced and lymphoid-biased subsets. *Proceedings of the National Academy of Sciences*, **107**(50), 21505–21510. 98

Opferman, J.T., Iwasaki, H., Ong, C.C., Suh, H., Mizuno, S., Akashi, K., & Korsmeyer, S.J. 2005. Obligate role of anti-apoptotic MCL-1 in the survival of hematopoietic stem cells. *Science Signalling*, **307**(5712), 1101. 20, 95

OReilly, L.A., Cullen, L., Visvader, J., Lindeman, G.J., Bath, M.L., Huang, D., Strasser, A., *et al.* 2000. The proapoptotic BH3-only protein bim is expressed in hematopoietic, epithelial, neuronal, and germ cells. *The American journal of pathology*, **157**(2), 449–461. 17

Orelio, C., Harvey, K.N., Miles, C., Oostendorp, R.A.J., van der Horn, K., & Dzierzak, E. 2004. The role of apoptosis in the development of AGM hematopoietic stem cells revealed by Bcl-2 overexpression. *Blood*, **103**(11), 4084–4092. 20

Osawa, M., Hanada, K., Hamada, H., Nakauchi, H., *et al.* 1996. Long-term lymphohematopoietic reconstitution by a single CD34-low/negative hematopoietic stem cell. *Science-AAAS-Weekly Paper Edition*, **273**(5272), 242–244. 3

Pan, G., O'Rourke, K., Chinnaiyan, A.M., Gentz, R., Ebner, R., Ni, J., & Dixit, V.M. 1997. The receptor for the cytotoxic ligand TRAIL. *Science*, **276**(5309), 111–113. 11

Park, I., Qian, D., Kiel, M., Becker, M.W., Pihalja, M., Weissman, I.L., Morrison, S.J., & Clarke, M.F. 2003. Bmi-1 is required for maintenance of adult self-renewing haematopoietic stem cells. *Nature*, **423**(6937), 302–305. 1

Pearl-Yafe, M., Yolcu, E.S., Stein, J., Kaplan, O., Shirwan, H., Yaniv, I., & Askenasy, N. 2007. Expression of Fas and Fas-ligand in donor hematopoietic stem and progenitor cells is dissociated from the sensitivity to apoptosis. *Experimental hematology*, **35**(10), 1601–1612. 22

Peled, T., Glukhman, E., Hasson, N., Adi, S., Assor, H., Yudin, D., Landor, C., Mandel, J., Landau, E., Prus, E., *et al.* 2005. Chelatable cellular copper modulates differentiation and self-renewal of cord blood–derived hematopoietic progenitor cells. *Experimental hematology*, **33**(10), 1092–1100. 9

Pellegrini, M., Belz, G., Bouillet, P., & Strasser, A. 2003. Shutdown of an acute T cell immune response to viral infection is mediated by the proapoptotic Bcl-2 homology 3-only protein Bim. *Proceedings of the National Academy of Sciences*, **100**(24), 14175–14180. 17

Petit, I., Szyper-Kravitz, M., Nagler, A., Lahav, M., Peled, A., Habler, L., Ponomaryov, T., Taichman, R.S., Arenzana-Seisdedos, F., Fujii, N., *et al.* 2002. G-CSF induces stem cell mobilization by decreasing bone marrow SDF-1 and up-regulating CXCR 4. *Nature immunology*, **3**(7), 687–694. 5

Pillay, J., den Braber, I., Vrisekoop, N., Kwast, L.M., de Boer, R.J., Borghans, J.A.M., Tesselaar, K., & Koenderman, L. 2010. In vivo labeling with 2H2O reveals a human neutrophil lifespan of 5.4 days. *Blood*, **116**(4), 625–627. 22

Porteus, M.H., & Carroll, D. 2005. Gene targeting using zinc finger nucleases. *Nature biotechnology*, **23**(8), 967–973. 24

Putcha, G.V., Le, S., Frank, S., Besirli, C.G., Clark, K., Chu, B., Alix, S., Youle, R.J., LaMarche, A., Maroney, A.C., *et al.* 2003. JNK-mediated BIM phosphorylation potentiates BAX-dependent apoptosis. *Neuron*, **38**(6), 899–914. 17, 18

Puthalakath, H., Huang, DC, O'Reilly, L.A., King, S.M., Strasser, A., *et al.* 1999. The proapoptotic activity of the Bcl-2 family member Bim is regulated by interaction with the dynein motor complex. *Molecular cell*, **3**(3), 287. 17, 18

Puthalakath, H., Villunger, A., O'Reilly, L.A., Beaumont, J.G., Coultas, L., Cheney, R.E., Huang, D., & Strasser, A. 2001. Bmf: a proapoptotic BH3-only protein regulated by interaction with the myosin V actin motor complex, activated by anoikis. *Science Signalling*, **293**(5536), 1829. 18, 19, 97

Puthalakath, H., Strasser, A., *et al.* 2002. Keeping killers on a tight leash: transcriptional and post-translational control of the pro-apoptotic activity of BH3-only proteins. *Cell death and differentiation*, **9**(5), 505. 17

Puthalakath, H., O'Reilly, L.A., Gunn, P., Lee, L., Kelly, P.N., Huntington, N.D., Hughes, P.D., Michalak, E.M., McKimm-Breschkin, J., Motoyama, N., *et al.* 2007. ER stress triggers apoptosis by activating BH3-only protein Bim. *Cell*, **129**(7), 1337–1349. 18

Ranger, A.M., Zha, J., Harada, H., Datta, S.R., Danial, N.N., Gilmore, A.P., Kutok, J.L., Le Beau, M.M., Greenberg, M.E., & Korsmeyer, S.J. 2003. Bad-deficient mice develop diffuse large B cell lymphoma. *Proceedings of the National Academy of Sciences*, **100**(16), 9324–9329. 17

Rebel, V.I., Hartnett, S., Denham, J., Chan, M., Finberg, R., & Sieff, C.A. 2000. Maturation and Lineage-Specific Expression of the Coxsackie and Adenovirus Receptor in Hematopoietic Cells. *Stem Cells*, **18**(3), 176–182. 24

Rocha, V., & Broxmeyer, H.E. 2010. New approaches for improving engraftment after cord blood transplantation. *Biology of Blood and Marrow Transplantation*, **16**(1), S126–S132. 6, 102

Roelz, R., Pilz, I.H., Mutschler, M., & Pahl, H.L. 2010. Of mice and men: Human RNA polymerase III promoter U6 is more efficient than its murine homologue for shRNA expression from a lentiviral vector in both human and murine progenitor cells. *Experimental hematology*, **38**(9), 792–797. 40, 41

Rong, Y., & Distelhorst, C.W. 2008. Bcl-2 protein family members: versatile regulators of calcium signaling in cell survival and apoptosis. *Annu. Rev. Physiol.*, **70**, 73–91. 15

Rongvaux, A., Willinger, T., Takizawa, H., Rathinam, C., Auerbach, W., Murphy, A.J., Valenzuela, D.M., Yancopoulos, G.D., Eynon, E.E., Stevens, S., *et al.* 2011. Human thrombopoietin knockin mice efficiently support human hematopoiesis in vivo. *Proceedings of the National Academy of Sciences*, **108**(6), 2378–2383. 8, 101

Rubinstein, P., Carrier, C., Scaradavou, A., Kurtzberg, J., Adamson, J., Migliaccio, A.R., Berkowitz, R.L., Cabbad, M., Dobrila, N.L., Taylor, P.E., *et al.* 1998. Outcomes among 562 recipients of placental-blood transplants from unrelated donors. *New England Journal of Medicine*, **339**(22), 1565–1577. 6

Saelens, X., Festjens, N., Walle, L.V., Van Gurp, M., Van Loo, G., & Vandenabeele, P. 2004. Toxic proteins released from mitochondria in cell death. *Oncogene*, **23**(16), 2861–2874. 13

Sakurai, F., Kawabata, K., Yamaguchi, T., Hayakawa, T., & Mizuguchi, H. 2005. Optimization of adenovirus serotype 35 vectors for efficient transduction in human hematopoietic progenitors: comparison of promoter activities. *Gene therapy*, **12**(19), 1424–1433. 104

Samavedi, V., Sacher, R.A., Efiom-Ekaha, D., Patel, AG, Kuku, A., & Ladapo, A. 2009. Hematopoietic stem cell transplantation. *Emedicine. com. http://emedicine. medscape. com/article/208954-overview (Accessed March 23, 2010)*. 5

Sansonetti, P.J., Phalipon, A., Arondel, J., Thirumalai, K., Banerjee, S., Akira, S., Takeda, K., & Zychlinsky, A. 2000. Caspase-1 Activation of IL-1β and IL-18 Are Essential for *Shigella flexneri*-Induced Inflammation. *Immunity*, **12**(5), 581–590. 11

Sattler, M., Liang, H., Nettesheim, D., Meadows, R.P., Harlan, J.E., Eberstadt, M., Yoon, H.S., Shuker, S.B., Chang, B.S., Minn, A.J., *et al.* 1997. Structure of Bcl-xL-Bak peptide complex: recognition between regulators of apoptosis. *Science*, **275**(5302), 983–986. 15

Scaffidi, C., Fulda, S., Srinivasan, A., Friesen, C., Li, F., Tomaselli, K.J., Debatin, K.M., Krammer, P.H., & Peter, M.E. 1998. Two CD95 (APO-1/Fas) signaling pathways. *The EMBO Journal*, **17**(6), 1675–1687. 11

Schneider, E., Moreau, G., Arnould, A., Vasseur, F., Khodabaccus, N., Dy, M., & Ezine, S. 1999. Increased fetal and extramedullary hematopoiesis in Fas-deficient C57BL/6-lpr/lpr mice. *Blood*, **94**(8), 2613–2621. 22

Shamas-Din, A., Brahmbhatt, H., Leber, B., & Andrews, D.W. 2011. BH3-only proteins: Orchestrators of apoptosis. *Biochimica et Biophysica Acta (BBA)-Molecular Cell Research*, **1813**(4), 508–520. 16

Shibue, T., Takeda, K., Oda, E., Tanaka, H., Murasawa, H., Takaoka, A., Morishita, Y., Akira, S., Taniguchi, T., & Tanaka, N. 2003. Integral role of Noxa in p53-mediated apoptotic response. *Genes & development*, **17**(18), 2233–2238. 19

Shultz, L.D., Schweitzer, P.A., Christianson, S.W., Gott, B., Schweitzer, I.B., Tennent, B., McKenna, S., Mobraaten, L., Rajan, TV, & Greiner, D.L. 1995. Multiple defects in innate and adaptive immunologic function in NOD/LtSz-scid mice. *The Journal of Immunology*, **154**(1), 180–191. 7

Shultz, Leonard D, Ishikawa, Fumihiko, & Greiner, Dale L. 2007. Humanized mice in translational biomedical research. *Nature Reviews Immunology*, **7**(2), 118–130. 7

Shultz, Leonard D, Brehm, Michael A, Garcia-Martinez, J Victor, & Greiner, Dale L. 2012. Humanized mice for immune system investigation: progress, promise and challenges. *Nature Reviews Immunology*. 6

Sieburg, H.B., Cho, R.H., & Müller-Sieburg, C.E. 2002. Limiting dilution analysis for estimating the frequency of hematopoietic stem cells: uncertainty and significance. *Experimental hematology*, **30**(12), 1436–1443. 6

Spangrude, G.J., Heimfeld, S., Weissman, I.L., *et al.* 1988. Purification and characterization of mouse hematopoietic stem cells. *Science*, **241**(4861), 58–62. 3

Stier, S., Cheng, T., Dombkowski, D., Carlesso, N., & Scadden, D.T. 2002. Notch1 activation increases hematopoietic stem cell self-renewal in vivo and favors lymphoid over myeloid lineage outcome. *Blood*, **99**(7), 2369–2378. 2

Strasser, A. 2005. The role of BH3-only proteins in the immune system. *Nature Reviews Immunology*, **5**(3), 189–200. 22, 103

Strasser, A., Cory, S., & Adams, J.M. 2011. Deciphering the rules of programmed cell death to improve therapy of cancer and other diseases. *The EMBO journal*, **30**(18), 3667–3683. 15, 16, 17

Strowig, T., Rongvaux, A., Rathinam, C., Takizawa, H., Borsotti, C., Philbrick, W., Eynon, E.E., Manz, M.G., & Flavell, R.A. 2011. Transgenic expression of human signal regulatory protein alpha in Rag2-/- γc-/- mice improves engraftment of human hematopoietic cells in humanized mice. *Proceedings of the National Academy of Sciences*, **108**(32), 13218–13223. 8

Sugamura, K., Asao, H., Kondo, M., Tanaka, N., Ishii, N., Ohbo, K., Nakamura, M., & Takeshita, T. 1996. The interleukin-2 receptor γ chain: its role in the multiple cytokine receptor complexes and T cell development in XSCID. *Annual review of immunology*, **14**(1), 179–205. 7

Sugiyama, T., Kohara, H., Noda, M., & Nagasawa, T. 2006. Maintenance of the hematopoietic stem cell pool by CXCL12-CXCR4 chemokine signaling in bone marrow stromal cell niches. *Immunity*, **25**(6), 977–988. 1

Susin, S.A., Lorenzo, H.K., Zamzami, N., Marzo, I., Snow, B.E., Brothers, G.M., Mangion, J., Jacotot, E., Costantini, P., Loeffler, M., *et al.* 1999. Molecular characterization of mitochondrial apoptosis-inducing factor. *Nature*, **397**(6718), 441–446. 13

Tait, S.W.G., & Green, D.R. 2010. Mitochondria and cell death: outer membrane permeabilization and beyond. *Nature Reviews Molecular Cell Biology*, **11**(9), 621–632. 10, 11, 12, 16

Takenaka, K., Nagafuji, K., Harada, M., Mizuno, S., Miyamoto, T., Makino, S., Gondo, H., Okamura, T., & Niho, Y. 1996. In vitro expansion of hematopoietic progenitor cells induces functional expression of Fas antigen (CD95). *Blood*, **88**(8), 2871–2877. 22

Till, J.E., McCulloch, E.A., & Siminovitch, L. 1964. A stochastic model of stem cell proliferation, based on the growth of spleen colony-forming cells. *Proceedings of the National Academy of Sciences of the United States of America*, **51**(1), 29. 1

Traggiai, E., Chicha, L., Mazzucchelli, L., Bronz, L., Piffaretti, J.C., Lanzavecchia, A., & Manz, M.G. 2004. Development of a human adaptive immune system in cord blood cell-transplanted mice. *Science*, **304**(5667), 104–107. 7, 37, 77, 101

Tsujimoto, Y., Cossman, J., Jaffe, E., Croce, C.M., *et al.* 1985. Involvement of the bcl-2 gene in human follicular lymphoma. *Science (New York, NY)*, **228**(4706), 1440. 13

Ulukaya, E., Acilan, C., & Yilmaz, Y. 2011. Apoptosis: why and how does it occur in biology? *Cell Biochemistry and Function*, **29**(6), 468–480. 10

Uren, R.T., Dewson, G., Chen, L., Coyne, S.C., Huang, D.C.S., Adams, J.M., & Kluck, R.M. 2007. Mitochondrial permeabilization relies on BH3 ligands engaging multiple prosurvival Bcl-2 relatives, not Bak. *The Journal of cell biology*, **177**(2), 277–287. 15

Veis, D.J., Sorenson, C.M., Shutter, J.R., Korsmeyer, S.J., *et al.* 1993. Bcl-2-deficient mice demonstrate fulminant lymphoid apoptosis, polycystic kidneys, and hypopigmented hair. *Cell*, **75**(2), 229. 20

Ventura, A., Young, A.G., Winslow, M.M., Lintault, L., Meissner, A., Erkeland, S.J., Newman, J., Bronson, R.T., Crowley, D., Stone, J.R., *et al.* 2008. Targeted Deletion Reveals Essential and Overlapping Functions of the *miR-17∼92* Family of miRNA Clusters. *Cell*, **132**(5), 875–886. 18

Villunger, A., Scott, C., Bouillet, P., & Strasser, A. 2003a. Essential role for the BH3-only protein Bim but redundant roles for Bax, Bcl-2, and Bcl-w in the control of granulocyte survival. *Blood*, **101**(6), 2393–2400. 19, 96

Villunger, A., Michalak, E.M., Coultas, L., Mullauer, F., Bock, G., Ausserlechner, M.J., Adams, J.M., & Strasser, A. 2003b. p53-and drug-induced apoptotic responses mediated by BH3-only proteins puma and noxa. *Science Signalling*, **302**(5647), 1036. 17, 19, 68

Wadhwa, P.D., Lazarus, H.M., Koc, O.N., Jaroscak, J., Woo, D., Stevens, C.E., Rubinstein, P., & Laughlin, M.J. 2003. Hematopoietic recovery after unrelated umbilical cord-blood allogeneic transplantation in adults treated with in vivo stem cell factor (R-MetHuSCF) and filgrastim administration. *Leukemia research*, **27**(3), 215–220. 95

Wagner, J.E., Rosenthal, J., Sweetman, R., Shu, X.O., Davies, S.M., Ramsay, NK, McGlave, PB, Sender, L., & Cairo, MS. 1996. Successful transplantation of HLA-matched and HLA-mismatched umbilical cord blood from unrelated donors: analysis of engraftment and acute graft-versus-host disease. *Blood*, **88**(3), 795–802. 5

Wang, J.C.Y., Doedens, M., & Dick, J.E. 1997. Primitive human hematopoietic cells are enriched in cord blood compared with adult bone marrow or mobilized peripheral blood as measured by the quantitative in vivo SCID-repopulating cell assay. *Blood*, **89**(11), 3919–3924. 3

Warr, M.R., Pietras, E.M., & Passegué, E. 2011. Mechanisms controlling hematopoietic stem cell functions during normal hematopoiesis and hematological malignancies. *Wiley Interdisciplinary Reviews: Systems Biology and Medicine*, **3**(6), 681–701. 1, 2

Weber, K., Bartsch, U., Stocking, C., & Fehse, B. 2008. A multicolor panel of novel lentiviral gene ontology(LeGO) vectors for functional gene analysis. *Molecular Therapy*, **16**(4), 698–706. 41

Westphal, D., Dewson, G., Czabotar, P.E., & Kluck, R.M. 2011. Molecular biology of Bax and Bak activation and action. *Biochimica et Biophysica Acta (BBA)-Molecular Cell Research*, **1813**(4), 521–531. 16

Wiehe, J.M., Ponsaerts, P., Rojewski, M.T., Homann, J.M., Greiner, J., Kronawitter, D., Schrezenmeier, H., Hombach, V., Wiesneth, M., Zimmermann, O., *et al.* 2007. mRNA-Mediated Gene Delivery Into Human Progenitor Cells Promotes Highly Efficient Protein Expression. *Journal of Cellular and Molecular Medicine*, **11**(3), 521–530. 104

Williams, B., Nilsson, S.K., *et al.* 2009. Investigating the interactions between haemopoietic stem cells and their niche: methods for the analysis of stem cell homing and distribution within the marrow following transplantation. *Methods in molecular biology (Clifton, NJ)*, **482**, 93. 38

Willis, S.N., Chen, L., Dewson, G., Wei, A., Naik, E., Fletcher, J.I., Adams, J.M., & Huang, D.C.S. 2005. Proapoptotic Bak is sequestered by Mcl-1 and Bcl-xL, but not Bcl-2, until displaced by BH3-only proteins. *Genes & development*, **19**(11), 1294–1305. 15

Willis, S.N., Fletcher, J.I., Kaufmann, T., van Delft, M.F., Chen, L., Czabotar, P.E., Ierino, H., Lee, E.F., Fairlie, W.D., Bouillet, P., *et al.* 2007. Apoptosis initiated when BH3 ligands engage multiple Bcl-2 homologs, not Bax or Bak. *Science Signalling*, **315**(5813), 856. 15

Xiao, H., Verdier-Pinard, P., Fernandez-Fuentes, N., Burd, B., Angeletti, R., Fiser, A., Horwitz, S.B., & Orr, G.A. 2006. Insights into the mechanism of microtubule stabilization by Taxol. *Proceedings of the National Academy of Sciences*, **103**(27), 10166–10173. 68

Xiao, Y., Li, H., Zhang, J., Volk, A., Zhang, S., Wei, W., Zhang, S., Breslin, P., & Zhang, J. 2011. TNF-α/Fas-RIP-1–induced cell death signaling separates murine hematopoietic stem cells/progenitors into 2 distinct populations. *Blood*, **118**(23), 6057–6067. 23

Yee, J.K., Moores, J.C., Jolly, D.J., Wolff, J.A., Respess, J.G., & Friedmann, T. 1987. Gene expression from transcriptionally disabled retroviral vectors. *Proceedings of the National Academy of Sciences*, **84**(15), 5197–5201. 23

Yin, T., Li, L., *et al.* 2006. The stem cell niches in bone. *Journal of Clinical Investigation*, **116**(5), 1195. 2

Yin, X.M., Wang, K., Gross, A., Zhao, Y., Zinkel, S., Klocke, B., Roth, K.A., & Korsmeyer, S.J. 1999. Bid-deficient mice are resistant to Fas-induced hepatocellular apoptosis. *Nature*, **400**(6747), 886–891. 17

Yoshihara, H., Arai, F., Hosokawa, K., Hagiwara, T., Takubo, K., Nakamura, Y., Gomei, Y., Iwasaki, H., Matsuoka, S., Miyamoto, K., *et al.* 2007. Thrombopoietin/MPL signaling regulates hematopoietic stem cell quiescence and interaction with the osteoblastic niche. *Cell stem cell*, **1**(6), 685–697. 1

You, H., Pellegrini, M., Tsuchihara, K., Yamamoto, K., Hacker, G., Erlacher, M., Villunger, A., & Mak, T.W. 2006. FOXO3a-dependent regulation of Puma in response to cytokine/growth factor withdrawal. *The Journal of experimental medicine*, **203**(7), 1657–1663. 19, 96

Youle, R.J., & Strasser, A. 2008. The BCL-2 protein family: opposing activities that mediate cell death. *Nature Reviews Molecular Cell Biology*, **9**(1), 47–59. 13, 14, 17

Yu, J., Zhang, L., Hwang, P.M., Kinzler, K.W., Vogelstein, B., *et al.* 2001. PUMA induces the rapid apoptosis of colorectal cancer cells. *Mol cell*, **7**(3), 673–682. 18

Yu, S.F., Von Rüden, T., Kantoff, P.W., Garber, C., Seiberg, M., Rüther, U., Anderson, W.F., Wagner, E.F., & Gilboa, E. 1986. Self-inactivating retroviral vectors designed for transfer of whole genes into mammalian cells. *Proceedings of the National Academy of Sciences*, **83**(10), 3194–3198. 23

Yuan, J., & Kroemer, G. 2010. Alternative cell death mechanisms in development and beyond. *Genes & development*, **24**(23), 2592–2602. 10

Yuan, S., Yu, X., Topf, M., Ludtke, S.J., Wang, X., & Akey, C.W. 2010. Structure of an apoptosome-procaspase-9 CARD complex. *Structure*, **18**(5), 571–583. 13

Zhang, J., Niu, C., Ye, L., Huang, H., He, X., Tong, W.G., Ross, J., Haug, J., Johnson, T., Feng, J.Q., *et al.* 2003. Identification of the haematopoietic stem cell niche and control of the niche size. *Nature*, **425**(6960), 836–841. 1

Zhao, C., Chen, A., Jamieson, C.H., Fereshteh, M., Abrahamsson, A., Blum, J., Kwon, H.Y., Kim, J., Chute, J.P., Rizzieri, D., *et al.* 2009. Hedgehog signalling is essential for maintenance of cancer stem cells in myeloid leukaemia. *Nature*, **458**(7239), 776–779. 2

Zinkel, S., Gross, A., & Yang, E. 2006. BCL2 family in DNA damage and cell cycle control. *Cell Death & Differentiation*, **13**(8), 1351–1359. 98

Zou, C.G., Cao, X.Z., Zhao, Y.S., Gao, S.Y., Liu, X.Y., Zhang, Y., Zhang, K.Q., *et al.* 2009. The molecular mechanism of endoplasmic reticulum stress-induced apoptosis in PC-12 neuronal cells: the protective effect of insulin-like growth factor I. *Endocrinology*, **150**(1), 277–285. 68

Zychlinski, D., Schambach, A., Modlich, U., Maetzig, T., Meyer, J., Grassman, E., Mishra, A., & Baum, C. 2008. Physiological promoters reduce the genotoxic risk of integrating gene vectors. *Molecular Therapy*, **16**(4), 718–725. 23